DOE/NETL-2003/1200

A Review of Carbon Dioxide Selective Membranes

A Topical Report

Dushyant Shekhawat[1], David R. Luebke[2], and Henry W. Pennline[2]

National Energy Technology Laboratory
United States Department of Energy
[1]P.O. Box 880, Morgantown, WV 26507-0880
[2]P. O. Box 10940, Pittsburgh, PA 15236-0940

December 1, 2003

Acknowledgements

Dushyant Shekhawat wishes to thank the Oak Ridge Institute for Science and Education (ORISE) for its support of the review. The authors would like to thank Drs. Curt White, Kurt Rothenberger, Michael Ciocco, and Robert Enick for their review of the report, and Eileen Fitzpatrick, who provided editorial support.

Disclaimer

Abstract

The atmospheric concentration of anthropogenic carbon dioxide (CO_2) has been increasing since the start of industrialization in the mid 19th century, and the rate is increasing. It is highly unlikely that fossil fuel combustion, the main contributor to anthropogenic CO_2, will be replaced in the foreseeable future. Therefore, CO_2 capture and storage offer a new set of options for reducing greenhouse gas emissions, in addition to the current strategies of improving energy efficiency and increasing the use of renewable energy resources. Carbon dioxide selective membranes provide a viable energy-saving alternative for CO_2 separation, since membranes do not require any phase transformation. This review examines various CO_2 selective membranes for the separation of CO_2 and N_2, CO_2 and CH_4, and CO_2 and H_2 from flue or fuel gas. This review attempts to summarize recent significant advances reported in the literature about various CO_2 selective membranes, their stability, the effect of different parameters on the performance of the membrane, the structure and permeation properties relationships, and the transport mechanism applied in different CO_2 selective membranes. Finally, the future direction for CO_2 selective membranes is proposed. Hybrid organic-inorganic membranes have become an expanding field of research, as the introduction of organic molecules can improve the characteristics of a matrix. Hydrotalcite-type materials, perovskite-type oxides, lithium zirconate, and lithium silicate are also suggested as candidate materials for high temperature CO_2 selective membranes.

Keywords: carbon dioxide; inorganic membranes; ceramic membranes; polymeric membranes; composite membranes; carbon dioxide selective membranes, mixed matrix membranes, hydrotalcites, perovskite-type oxides, lithium zirconate, lithium silicate.

Table of Contents

Introduction

Atmospheric concentrations of several greenhouse gases (CO_2, CH_4, nitrous oxide, and chlorofluorocarbons) have increased by about 25 percent collectively since the industrial revolution began in the mid 19th century. In particular, anthropogenic CO_2 emissions have increased dramatically since the beginning of the industrial age, due largely to the burning of fossil fuels, such as coal or natural gas for the production of electricity, and petroleum or diesel for transportation. Increasing concentrations of greenhouse gases are likely to accelerate the rate of climate change. Unless significant controls are implemented, a continued rise in the atmospheric concentration of CO_2 is projected in the foreseeable future, due to increases in the consumption of and demand for fossil fuels. Several options exist to abate CO_2 emissions from fossil fuel utilization, including increasing the efficiency of fossil fuel combustion systems, or replacing fossil fuels with renewable energy sources. These alternatives are very attractive in controlling CO_2 emissions in the environment, but each has its limitation. Another viable option to manage CO_2 emissions is carbon sequestration, that is, capturing and securely storing the CO_2 emitted from large point sources, such as fossil-fuel-fired power plants. Carbon dioxide separation and capture may be achieved by several existing techniques [1, 2]: absorption using physical or chemical wet scrubbing; adsorption using solids in a pressure swing or temperature swing operational mode; cryogenic distillation; CO_2 selective membranes (polymeric or ceramic); or mineralization processes.

Membrane separation processes provide several advantages over other conventional separation techniques [3]. First, the membrane process is a viable energy-saving alternate for CO_2 separation, since it does not require any phase transformation. Second, the necessary process equipment is very simple with no moving parts, compact, relatively easy to operate and control, and also easy to scale-up.

Membranes have been widely used in various industrial separation applications for the last two decades. It is estimated that the annual revenue of the worldwide membrane industry is over a billion dollars, and an annual growth rate of about 10 percent has been forecasted for this industry [4]. Currently, the industry is dominated by polymeric membranes that have been used in a variety of applications ranging from food and beverage processing, desalination of seawater, and gas separations, to medical devices. Recently, research directed at the development and application of inorganic membranes is gaining momentum because of their high demand in the new application fields, such as fuel cells, membrane reactors, and other high-temperature separations. The annual growth rate of inorganic membranes is expected to be about 30 percent with almost 15 percent share of the total market volume [4].

It is envisioned that membranes can be effectively used to separate CO_2 from the gases of power generation point sources. Key considerations are the type of power generation and the location along the path of the process where the membrane separation is attempted [2]. For conventional pulverized coal combustion, the produced flue gas is in an oxidized state. Combusting a low sulfur eastern bituminous coal may result in a typical flue gas of about 15 percent CO_2, 7 percent water, 3 percent O_2, 74 percent N_2, and less than 1 percent other gases, including SO_2 and NO_x. In contrast, in integrated gasification combined cycle (IGCC), coal is reacted to produce reducing conditions. In oxygen-blown gasification and depending on the coal, type of gasifier, and operating conditions, the non-shifted fuel gas produced may consist of 33 percent H_2, 44

percent CO, 10 percent CO_2, 13 percent H_2O with small amounts of other gases (H_2S, CH_4, etc.).

The main goal of this report is to present an overview of recent accomplishments in the area of CO_2 selective membranes, and to provide recommendations for further direction of the research in this area. An enormous amount of work has been reported in the last 15 to 20 years on gas separations using membranes. Theoretical and experimental studies are included in the discussion. An excellent review by Stern [3] about polymeric membranes for gas separation should be consulted for the pre-1994 period. Koros et al. [5] and Pandey et al. [6] have also provided excellent reviews about membrane-based gas separation.

Fundamental Background

General Principles of Gas Separation Membranes

The permeability of a membrane toward gases is a function of membrane properties (physical and chemical structure), the nature of the permeant species (size, shape, and polarity), and the interaction between membrane and permeant species [3, 7, 8]. The first two, membrane properties and the nature of the permeant species, determines the diffusional characteristics of a particular gas through a given membrane. The third property, interaction between membrane and permeant, refers to the sorptivity or solubility of the gas in the membrane. The permeability coefficient (or permeability), P_1, of a penetrant 1 is the product of the solubility coefficient or the sorptivity (thermodynamic parameter), S_1, and the diffusion coefficient (kinetic parameter), D_1:

$$P_1 = S_1 D_1 \tag{I}$$

The permeability coefficient denotes the rate at which a penetrant traverses a membrane. The solubility/sorptivity coefficient is a measurement of the amount of gas sorbed by the membrane when equilibrated with a given pressure of gas at a given temperature. The diffusion coefficient indicates how fast a penetrant is transported through the membrane in the absence of obstructive sorption.

Membranes utilized in separations need to possess both high selectivity and high permeation. The selectivity of the membrane to specific gas or liquid molecules is subject to the ability of the molecules to diffuse through the membrane. The permselectivity or ideal separation factor (pure gas permeation), α, is simply the ratio of two gases, 1 and 2, being separated:

$$\alpha_{1,2} = \left(\frac{P_1}{P_2} \right) \tag{II}$$

From equation I and II

$$\alpha_{1,2} = \left(\frac{S_1}{S_2}\right)\left(\frac{D_1}{D_2}\right) \quad \text{(III)}$$

Or

$$\alpha_{1,2} = \alpha_S \alpha_D \quad \text{(IV)}$$

Therefore, permselectivity is the product of solubility (or sorptivity) selectivity (α_S) and the diffusion selectivity (α_D).

The real separation factor (mixed gas permeation) can be defined as:

$$\alpha_{1,2} = \frac{y_1 x_2}{y_2 x_1} \quad \text{(V)}$$

where y_1 and y_2 are the mole fraction of species 1 and 2, respectively in the feed, and x_1 and x_2 are the mole fraction of species 1 and 2, respectively, in the permeate.

Temperature dependence of permeability of a gaseous penetrant in a membrane is described by the Arrhenius expression:

$$P = P_0 \exp\left(\frac{-E_p}{RT}\right) \quad \text{(VI)}$$

where P_0 is a pre-exponential factor and E_p is the apparent activation energy for permeation. Similar expressions are used to describe the temperature dependence of diffusivity and solubility/sorptivity. Thus, the permeability may be expressed as follows:

$$P = S_0 D_0 \exp\left(\frac{-(H_s + E_D)}{RT}\right) \quad \text{(VII)}$$

Therefore, the apparent activation energy for permeation can be assumed to be the sum of the apparent heat of sorption (solubility), H_s, and the apparent activation energy of diffusion, E_D.

The gas flux (J) through the membrane is defined by the following expression:

$$J = \frac{\Delta V}{At} \tag{VIII}$$

where ΔV is the volume of the permeated gas, A is the membrane area, and t is the time.

The permeance (π) through the membrane is defined in equation (IX) and is related to the permeability (P) by equation (X):

$$\pi = \frac{J}{\Delta p} \tag{IX}$$

$$\pi = \frac{P}{L} \tag{X}$$

where, Δp is the partial pressure difference between the upstream and downstream side of the membrane, and L is the membrane thickness.

The solubility coefficient of a polymer depends on the free volume content in the polymer matrix, condensability of the penetrants in the polymer matrix, and the affinity of the penetrants for the polymer matrix. Similarly, the diffusion coefficient depends on the polymer chain mobility or flexibility, size of the penetrant, and also the free volume content of the polymer matrix.

The diffusion coefficient can be calculated from the equation

$$D = \frac{L^2}{6\tau} \tag{XI}$$

where τ is the time lag.

Gas diffusion through rubbery polymers is related by the free volumes of polymer [9]:

$$D = A\exp(-B/V_f) \tag{XII}$$

where A and B are characteristic parameters, depending only on the type of gas. The fractional free volume of polymers, V_f, can be calculated by:

$$V_f = \frac{(V - V_0)}{V} \qquad \text{(XIII)}$$

where V and V_0 are specific molar volumes at a temperature and 0° K, respectively. V_0 is estimated as 1.3 times the van der Walls volume of the polymer obtained by a group contribution method [10].

Permeability can be defined as a reciprocal resistance against mass transport through a porous medium [11]. Since a multilayer system can be considered as a resistance in series, the overall permeability, P, of the membrane is related to the permeabilities of different layers of the membrane and the support permeability in the following way:

$$\frac{1}{P} = \frac{1}{P(support)} + \frac{1}{P(layer1)} + \frac{1}{P(layer2)} + ... \qquad \text{(XIV)}$$

The permeability data of a two-layer system can be corrected using equation XIV for the influence of the support. Table 1 presents units and unit conversion related to membranes.

Table 1. Units Used in Membrane Science

	SI	Others
Permeance	mol m^{-2} s^{-1} Pa^{-1}	GPU (Gas Permeation Unit)[a]
Permeability	mol m^{-1} s^{-1} Pa^{-1}	Barrer[b]

[a] *GPU = 10^{-6} cm^3 (STP) cm^{-2} (membrane) s^{-1} $cmHg^{-1}$*

[b] *Barrer = 10^{-10} cm^3 (STP) cm^{-1} s^{-1} $cmHg^{-1}$ = 3.4 x 10^{-16} mol m^{-1} s^{-1} Pa^{-1}*

Classification

Inorganic Membranes

Inorganic membranes can be classified into two categories based on structure: porous and dense [7]. In porous inorganic membranes, a porous thin top layer is supported on a porous metal or ceramic support, which provides mechanical strength but offers minimum mass-transfer resistance. Alumina, carbon, glass, silicon carbide, titania, zeolite, and zirconia membranes are mainly used as porous inorganic membranes supported on different substrates, such as α-alumina, γ-alumina, zirconia, zeolite, or porous stainless steel. The porous inorganic membranes can be further classified, based on their pore size (microporous (<2 nm) or mesoporous (>2 nm to <50 nm) or macroporous (>50 nm)), or symmetry (symmetric, homogeneous structure throughout the membrane, or asymmetric, gradual change in structure throughout the membrane). Lange et al. [12] classified the microporous inorganic membranes based on synthesis route and material. According to them, the main types of microporous inorganic

membranes are: (1) sol-gel derived ceramic membranes, (2) chemical vapor deposition (CVD) modified (glass or ceramic) membranes, (3) leached hollow glass fibers (phase separation technique), (4) carbon molecular sieve membranes, and (5) zeolite membranes.

The dense inorganic membranes (nonporous material) consist of a thin layer of metal, such as palladium and its alloys (metallic membrane), or solid electrolytes, such as zirconia. These membranes are highly selective for hydrogen or oxygen separation: transport occurs via solution-diffusion method or charged particles in dense membranes. The low permeability across the dense inorganic membranes limits its intended applications, compared to porous inorganic membranes.

Another form of inorganic membrane is the liquid-immobilized membrane, where the pores of a membrane are completely filled with a liquid, which is permselective for certain compounds. The liquid reacts with the permeating component on the feed side to form a complex. The complex diffuses across the membrane and then releases the permeant on the product side, and at the same time converts the liquid back to the feed side.

Polymeric Membranes

Permselective polymeric membranes can be divided into two basic categories: glassy and rubbery [3]. Glassy polymers have low chain intrasegmental mobility and long relaxation times, while rubbery polymers exhibit the opposite characteristics, namely high intrasegmental mobility and short relaxation times. Almost all industrial permselective membrane processes for gas separation utilize glassy polymeric membranes because of their high gas selectivity and good mechanical properties.

Transport Mechanism for Inorganic Membranes

There are four main transport mechanisms by which gas separation using porous inorganic membranes can be described. See Figure 1 [13]. The basis of these transport mechanism are the molecular weight (Knudsen diffusion), surface interactions (surface diffusion and capillary condensation), and the size of molecules (molecular sieving) to be separated.

Pores in gas separation membranes can be classified as follows [14]: micropores equivalent to molecular dimensions, meso and macropores of the Knudsen diffusion regime; and pinholes of the Poiseuille flow regime. Knudsen diffusion occurs in the gas phase through the pores in the membrane layer having diameters (d) smaller than the mean free path dimensions of the molecules (λ) in the gas mixture (i.e. the Knudsen number (λ/d)), is much greater than one. As a result, the movement of molecules inside the narrow pore channels takes place through collisions of the diffusing molecules with the surface (wall) rather than with each other. Since the driving force for transport is the partial pressure of the gas species, Knudsen transport can occur either by concentration or by pressure gradients. The relative permeation rate of each component is inversely proportional to the square root of its molecular weight. According to Knudsen diffusion, N_2 molecules preferentially permeate in the case of CO_2/N_2 separation. The selectivities of CO_2 with respect to N_2, CH_4, and H_2 by Knudsen diffusion will be 0.8, 0.6, and 4.7, respectively. Hence, the selectivity of CO_2 achievable by the Knudsen mechanism is very low and not attractive in this particular gas mixture.

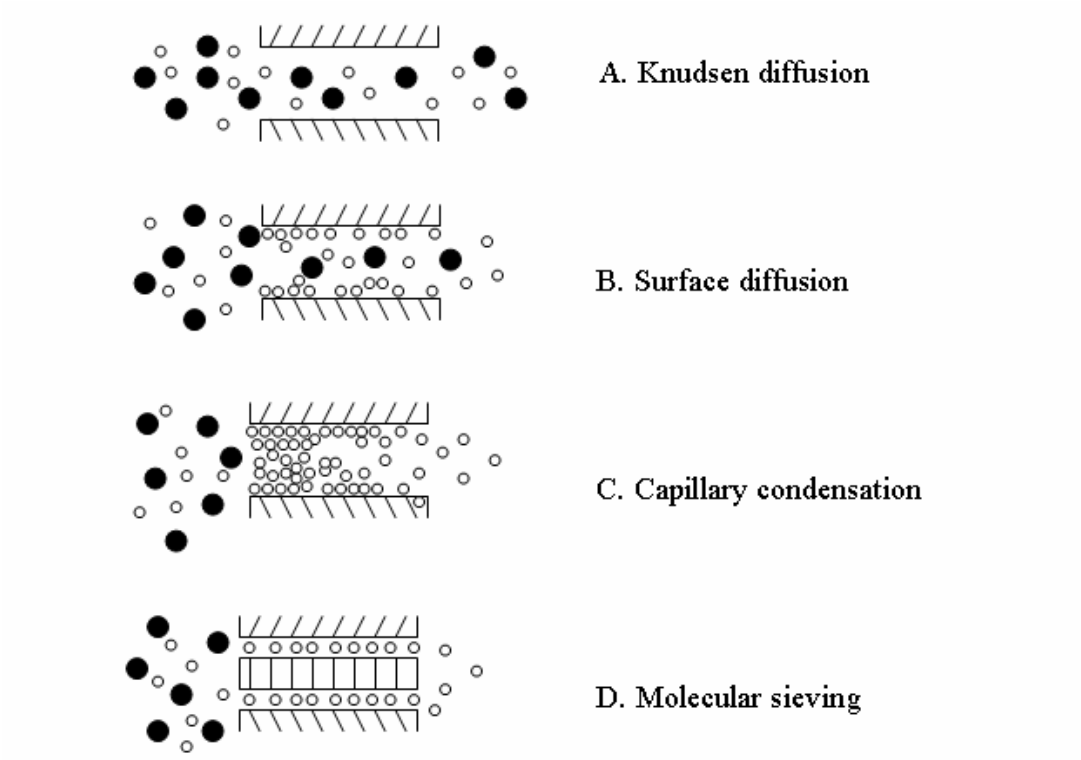

Figure 1. Transport Mechanism Through Microporous Membranes

In the surface diffusion mechanism, the diffusing species adsorb on the walls of the pore, and then readily transport across the surface in the direction of decreasing surface concentration. Rao et al. [15] called them Selective Surface Flow™ membranes, and mentioned several advantages for separation of gas mixtures using them. Typically, the molecules with larger molecular weight and with larger polarity and polarizability are selectively adsorbed on the membrane surface [16]. The adsorbed species on the membrane pores can also drastically reduce or eliminate the transport of non-selectively adsorbed molecules across the pore by reducing the size of accessible void space through the pore [16]. This hindrance effect introduces a non-adsorptive separation selectivity for the adsorbed species when the pore size is between 2 to 3 molecular diameters of the adsorbed species. The concentration of adsorbed species, depends upon the temperature, pressure, and the nature of the surface. The interaction between a gas and the pore can also be introduced by modification of adsorbent layers.

Multilayer diffusion occurs when species adsorb in several layers. A gas/vapor mixture permeates through pores of porous inorganic membranes; vapor species condense in the pores at a pressure lower than the saturation pressure at a given temperature. The multilayer diffusional flux is much larger than the gas phase flux (e.g., up to 20 times larger in the case of Freon on Vycor glass) [17]. The second important aspect is that by capillary condensation a pore is blocked by condensate, preventing gas transport of other components of the gas/vapor mixture. Both aspects can result in increased selectivities. The condensation pressure depends on the pore size and shape and also the strength of the interaction between the fluid and pore walls.

According to the molecular sieving mechanism, the separation is caused by passage of smaller molecules of a gas mixture through the pores of porous inorganic membranes, while the larger molecules cannot enter into these pores and a selective separation, based upon size exclusion is thus observed. High selectivity and permeability for the small gas molecules in a mixture can be obtained from molecular sieving membranes, but a very fine-tuning of the membrane pore sizes is required to achieve the desired separation efficiency [15].

Several models have been used to describe the transport mechanism in dense membranes, such as the solution-diffusion model [3, 18], the pore flow model [19], and the irreversible-thermodynamic model [20]. Among them, the solution-diffusion model seems to be accepted by the majority of membrane researchers. In this model [21], the mass transport process consists of three consecutive steps; (1) sorption of the gas from the feed to the membrane; (2) molecular diffusion of the gas in the membrane; and (3) desorption of the gas from the membrane on the downstream side of the membrane. The solution-diffusion model is also widely used to describe the transport mechanism for the polymeric membranes.

Physical Properties of CO_2, CH_4, N_2, and H_2

Table 2 gives the physical properties of CO_2, CH_4, N_2, and H_2 [22]. Methane is a relatively large penetrant (kinetic diameter 3.8 A), and usually has a very low permeability.

Table 2. Physical Properties of CO_2, CH_4, N_2, and H_2

	CO_2	CH_4	N_2	H_2
Molecular weight	44.01	16.04	28.01	2.02
Kinetic diameter, A	3.30	3.80	3.64	2.89
Specific volume at 70 °F, 1 atm, ml/g	547	1479.5	861.5	11967
Sublimation point at 1 atm, °C	-78.5	-161.5	-195.8	
Triple point pressure, atm	5.11	0.115	0.121	0.0695
Triple point temperature, °C	-56.6	-182.5	-210.0	-259.3
Density, gas at 0 °C, 1 atm, g/l	1.977	0.72	1.250[a]	0.0899
Specific gravity, gas at 0 °C, 1 atm (Air = 1)	1.521	0.5549[b]		0.06952
Critical temperature, °C	31.0	-82.1	-147.1	-240.2
Critical pressure, atm	72.9	45.8	33.5	12.8
Critical density, g/ml	0.468	0.162	0.311	0.031
Viscosity, gas at 70 °F, 1 atm, cp	0.0148	0.0106[c] 0.0116[d]	0.0170[e] 0.0174[f]	0.0087[f]
Solubility in water at 25 °C, 1 atm, ml/l water	759		23	19

[a]At 20 °C; [b]60 °F; [c]4.4 °C; [d]37.8 °C; [e]0 °C; [f]15 °C.

Methane is not as soluble as CO_2 but is relatively polarizable. For polymeric membranes, the penetrant condensability is a very important parameter. Typically, penetrants with higher critical temperatures are more condensable and, therefore, more soluble in polymers. Diffusion

coefficients often vary less than solubility coefficients for penetrants in most polymeric membranes. Therefore, the relative gas permeability coefficients in these membranes are determined by the gas solubility rather than the gas diffusivity unless the penetrant is a very small molecule for which diffusivity is high enough to compensate for its lower solubility.

CO_2 Selective Membranes

Inorganic Membranes

The development of inorganic membranes started in the 1940s for the separation of uranium isotopes by the process of diffusion applied to UF_6. There are not many publications about the inorganic membranes from the nuclear period because they were mainly used for defense purposes. The scope of inorganic membrane applications over the past 20 to 25 years has extended considerably and, therefore, extensive work has been reported on the synthesis, characterization, properties, and application of inorganic membranes. Currently, industrial and academic laboratories are now engaged in the inorganic membrane area. The growth achieved in the rapidly growing field of inorganic membranes is reflected by a number of recent overviews [4, 23-28]. Caro et al. [4] listed various advantages and disadvantages of inorganic membranes in comparison with polymeric membranes. Inorganic membranes are highly stable at high temperatures and can be resistant to harsh conditions.

Alumina Membranes

The generally mesoporous structure of alumina dictates that transport within membranes fabricated from it will take place by a Knudsen diffusion mechanism [8]. Since selectivity in this regime is limited, and the rate of diffusion is controlled by molecular weight, alumina membranes are of limited use in the separation of gases. With mixtures such as CO_2/N_2, where the gases have similar mass, and CO_2/H_2, where selectivity toward the heavier component is required, alumina is undesirable as a membrane material.

Alumina finds its use in the separation of gases mainly as a support, where its sound structural properties, and chemical and hydrothermal stabilities beyond 1,000 ^oC make it very desirable. A few attempts have been made to modify alumina membranes to facilitate CO_2 surface diffusion with limited success.

In order to achieve high separation factors in systems like CO_2 and N_2, an interaction between one of the gases in the mixture and the membrane surface can be introduced by chemical modification of separation layers. Uhlhorn et al. [11] modified a γ-alumina membrane systems by impregnating magnesia to induce the surface diffusion of CO_2. They reported that the introduction of magnesia into γ-alumina creates stronger basic sites, which result in stronger bonding of CO_2 to the modified surface. Therefore, adsorption of CO_2 on the surface becomes partially irreversible. They concluded that the more strongly bonded CO_2 is less mobile, resulting in lower CO_2 permeability across the membrane.

Cho et al. [29] also modified γ-alumina with CaO in an attempt to enhance CO_2/N_2 separation by introducing interaction between CO_2 molecules and the pore wall. However, the CO_2/N_2 separation factor was not different from the Knudsen diffusion mechanism. They also prepared

silica-modified γ-alumina to increase the CO_2/N_2 separation factor. The CO_2/N_2 separation factor was 1.72 at 25 °C and decreased with increasing temperature. It was concluded that surface diffusion could be applied as a separation mechanism when the pore size is very small and the temperature is low.

Zeolite Membranes

Zeolites are crystalline aluminosilicates with a uniform pore structure and a minimum channel diameter range of 0.3 to 1.0 nm. The presence of molecular-sized cavities and pores make the zeolites effective as shape-selective materials for a wide range of separation applications. These cavities are interconnected by pore openings through which molecules can pass. The electrical charge or polarity of the zeolites also functions to attract or sort molecules. This ability to selectively adsorb molecules by size and polarity is the key to the unusual efficiency of synthetic zeolites as the basis for separation. By tailoring the chemistry and structure of the materials used to prepare them, synthetic zeolites can be modified to provide a wide range of desired adsorption characteristics or selectivities and can be used as a membrane for gas separation applications.

Zeolite membranes have usually been prepared by in situ hydrothermal synthesis on porous stainless steel, α-alumina, or γ-alumina support tubes or disks for the gas permeation studies. These supported zeolite membranes have a thin and continuing zeolite separation layer with the porous support providing mechanical strength to the membrane. Membranes of various zeolites, such as ZSM-5 [30-37], Y type [38-43], silicalite [44-50], A type [42, 51, 52], P type [53], modernite [33], and silicoaluminophosphate [54-56] have been synthesized on porous supports.

Separation occurs in zeolite membranes by both molecular sieving and surface diffusion methods because the pore sizes of zeolite membranes are of molecular dimensions. In zeolite membranes, both molecular sizes relative to the zeolite pore, and the relative adsorption strengths determine the faster permeating species in a binary mixture [55, 57]. Poshusta et al. [55] identified three separation regimes where both components are able to diffuse through the zeolite pores. The first regime covers differences in diffusivity, where there is a difference in the size of molecules, but both molecules have similar adsorption strengths. The higher membrane selectivity will be observed for the smaller molecule in this regime. If the sum of the diameters of both molecules is larger than the pore size, then the molecules cannot pass each other inside the molecular sieve. This will reduce the permeation of the molecule with higher diffusivity, because it is blocked by the molecule with lower diffusivity (or slow moving molecule). The second regime is competitive adsorption, in which both molecules have similar sizes, but differ in their adsorption strengths. The molecules will be competing for the same adsorption site within the zeolite pore. The strongly adsorbing molecule will not spare many adsorption sites for the weakly adsorbing molecule, and thus the higher membrane selectivity will be observed for the strongly adsorbed molecule in this regime. At higher temperatures, the adsorption capacity decreases, which results in reducing the ability of the molecule to block adsorption sites for weakly adsorbing molecules. Therefore, the separation factor induced by competitive adsorption decreases with temperature. The third regime is combined differences in diffusivity and competitive adsorption. The molecules have significantly different sizes and adsorbing strengths. In this regime, the effect of each mechanism may combine to enhance the separation factor, or compete to reduce the separation factor.

Typically, the heat of adsorption of gases on most zeolites increase in this order [55]: $H_2 < CH_4 < N_2 < CO_2$. This order is consistent with the electrostatic properties of each molecule. Carbon dioxide adsorbs the strongest because it has the strongest electrostatic quadrupolar moment of the four gases, which significantly contributes to its attraction to polar surfaces, like those found in zeolites containing cations. Carbon dioxide preferentially permeates in CO_2/N_2, CO_2/CH_4, and CO_2/H_2 mixtures at low temperatures, because CO_2 adsorbs more strongly on zeolites than the other gases. For the CO_2/N_2 and CO_2/CH_4 mixtures, CO_2 is smaller in size and thus permeates faster at elevated temperatures. However, the permselectivities and separation factors are the same for the CO_2/N_2 or CO_2/CH_4 systems at elevated temperatures due to the absence of competitive adsorption. The CO_2/N_2 or CO_2/CH_4 mixture is separated by the third regime at lower temperatures, where differences in diffusivity and competitive adsorption combine to enhance the separation factor. At higher temperatures, the CO_2/N_2 or CO_2/CH_4 mixture is separated by the first regime, due to only differences in diffusivity. For the H_2/CO_2 mixture, separation also occurs by the third regime, where diffusivity difference and competitive adsorption compete, because CO_2 is the larger and more strongly adsorbing molecule. At higher temperatures, the CO_2/H_2 selectivity inversion occurs, where H_2 permeates faster than CO_2 by the first regime in the absence of competitive adsorption.

Morooka and his research group [30, 38-40] have synthesized several different zeolite membranes by hydrothermal reaction on the surface of a porous α-alumina support tube. The tube characteristics were length of 30 or 200 mm, an outer diameter of 2.9 mm, an internal diameter of 1.9 mm, an average pore size of ~ 150 nm, and a void fraction of ~ 0.45.

Kusakabe et al. [30] formed the ZSM-5-type zeolite film for a membrane by mixing a fine silica powder in an aqueous solution of the template and then calcining it at 400 or 550 °C. The template was the mixture of tetrapropylammoniumhydroxide (TPAOH) and tetrapropyl-ammoniumbromide (TPABr). They observed three zones in the film formed on the support tube: a crystalline layer deposited on the support tube, α-alumina macropores partially filled with deposits, and an intermediate layer that was a mixture of deposits and α-alumina particles. They reported that the permeance of zeolite membranes increased with decreasing the thickness of the zeolite top layer, while no correlation was found between membrane morphology and CO_2/N_2 permselectivity. (See Table 3.)

Table 3. Effects of Various Parameters on Permeation Properties of ZSM-5 Membrane

Permeation Temperature (°C)	Calcination Temperature (°C)	CO_2 Permeance (mol m^{-2} s^{-1} Pa^{-1})	Permselectivity (CO_2/N_2)
30	400	5×10^{-8}	9.3
30	540	3×10^{-7}	9.4
100	400	6×10^{-8}	8.6
100	540	2.1×10^{-7}	5.3
100	540	$5 \times 10^{-8,a}$	2.5
100	540	$1.4 \times 10^{-8,b}$	1.8
100	540	$1.8 \times 10^{-7,c}$	5.1

20 ml solution (SiO_2 1 : TPAOH x : TPABr (1-x) : H_2O 100 in mol) was placed in the autoclave; reaction temperature = 180 °C; reaction time = 24 hrs; and x = 0.67.

[a]Solution volume = 30 ml; [b]Solution volume = 40 ml; [c]x = 0.5.

Kusakabe et al. [38] further synthesized a Y-type zeolite membrane to determine the permeation properties for single-component, as well as for the equimolar mixtures of gases. The CO_2 permeance was approximately the same for the single-component system and the mixed CO_2/N_2 or CO_2/CH_4 system. However, the N_2 or CH_4 permeances were significantly decreased for an equimolar feed at lower temperatures (Table 4). This selective permeation was due to competitive adsorption of CO_2 molecules in micropores of the Y-type zeolite membrane. It was concluded that the CO_2 molecules, adsorbed on the mouth of the micropores of the membrane, impeded the penetration of nonadsorptive molecules (N_2 or CH_4) from entering into the pores. It was also observed that the CO_2 and N_2 permeances increased initially due to water desorption from the membrane surface before it gradually decreased with time due to possible adsorption of impurities. Separation factors were obtained as high as 100 and 21 for CO_2/N_2 and CO_2/CH_4 mixtures, respectively, at 30 °C. They also observed a decrease in separation factors and in permselectivities with increasing permeation temperatures.

Table 4. Summary of Results from Ion-Exchanged Zeolites

Membrane	Permeation Temperature (°C)	CO_2 Permeance (mol m^{-2} s^{-1} Pa^{-1})	CO_2/N_2 System		CO_2/CH_4 System	
			PS	SF	PS	SF
Y-type	30	1.2×10^{-7}	5	18	2	21
	30[a]	4×10^{-8}	4	100	2	
	80	3×10^{-7}	9	12	4	15
	130	3×10^{-7}	11	9	6	8
LiY	40	2×10^{-6}		4		
NaY	40	1.2×10^{-6}	5	20		
KY	40	1.4×10^{-6}		30		
MgY	40	3×10^{-7}		21		
CaY	40	5×10^{-7}		12		
BaY	40	8×10^{-7}		24		
Si/Al = 1.22	40	5×10^{-7}		50		
Si/Al = 1.54	40	4×10^{-7}		45		
Si/Al = 2.18	40	2×10^{-6}		20		
Li(20%)Y	35	7×10^{-7}	3	10		
K(30%)Y	35	9×10^{-7}	9	48		
NaY	100	2×10^{-6}		7		
	200	1.4×10^{-6}		3		
	300	1×10^{-6}		2		
K(62%)Y	40	5×10^{-7}	6	39		
Rb(38%)Y	40	5×10^{-7}	3	40		
Cs(32%)Y	40	2×10^{-7}	2	34		

PS: Permselectivity, SF: Separation Factor

[a]Membrane B

Separation factors for mixed gas systems significantly depend upon interactions between permeants and pore surface and pore size. It was understood that the selectivities of the membrane could be improved by ion-exchanging a zeolite with cations, which possess different interaction with permeants. Kusakabe et al. [39, 40] prepared NaY-type zeolite membranes ion exchanged with various alkali and alkaline earth cations to study the effect of ion-exchanged cations in the zeolite membranes on the permeation of CO_2 and N_2 in the equimolar mixture. As opposed to their previous study [39], NaY type zeolite membranes prepared for this work were stable over time. They observed an increase in CO_2 permeance and a decrease in the CO_2/N_2 separation factor increasing the Si/Al ratios in the zeolite membranes. It was also observed that the CO_2 permeances and separation factors of zeolite ion exchanged with alkali cations were higher than those of the membranes ion-exchanged with alkaline earth cations.

Kusakabe et al. [41] applied a sorption-diffusion model to describe CO_2/N_2 permeation properties of Y-type zeolite membranes ion exchanged with Li^+, Na^+, and K^+ cations. It was suggested that the high CO_2/N_2 separation factors for the binary mixed feed were caused by an increase in the selective sorption of CO_2. (See Table 4.) It was concluded that the high CO_2/N_2 separation factors of the K-exchanged zeolite membranes were due to the decrease in N_2 sorptivity for the mixed feed. They reported the highest CO_2 permeance through NaY zeolite membrane at 100 °C, but observed a decrease in CO_2/N_2 separation factor with increasing temperature. Preferential transport of adsorptive molecules through the Y-type zeolite membrane was also confirmed for the CO_2/H_2 system, where CO_2/H_2 separation factor was 98 for an equimolar feed of CO_2 and H_2.

Aoki et al. [31] also studied ZSM-5 zeolite membranes (Si/Al = 25 and 600) ion-exchanged with various alkali and alkaline earth cations for gas permeation. They observed low gas permeances and permselectivities from ion-exchanged zeolite membranes. For example, the highest CO_2 permeance was 8.5 x 10^{-8} mol m^{-2} s^{-1} Pa^{-1} from H-ZSM-5 (Si/Al = 600) membrane with CO_2/N_2 permselectivity of 1.9. It was also observed that both Si/Al ratio and the size of cation affect the gas permeation performance. Single gas permeances were in this order for the ZSM-5 membrane with Si/Al = 25: $K^+ < Ba^{2+} \sim Ca^{2+} < Cs^+ < Na^+ \sim H^+$, which corresponds with the decrease in cation size except Cs^+ did not follow the trend. According to authors, the permeance decreased, due to possible reduction in the zeolite pore pathway, as the cation size increased.

Bakker et al. [44] studied the temperature dependence of gas permeation through a silicalite-1 membrane. Silicalite-1 layer with a thickness of 50 to 60 μm was grown on a porous stainless-steel support where silicalite was prepared from silica, tetrapropylammoniumhydroxide, and water, and subsequently calcined at 400 °C. A maximum permselectivity, CO_2/N_2, of 2.25 was achieved through a silicalite-1 membrane at 30 °C with CO_2 permeance of 3.1 x 10^{-7} mol m^{-2} s^{-1} Pa^{-1}. Bakker et al. also compared a theoretical model to experimental results for silicalite-1 zeolite membranes. They concentrated on single-gas permeation dominated by surface diffusion at low temperature and gas-phase translational diffusion at high temperature. Diffusivity was assumed to obey the Darken equation in the case of surface diffusion and kinetic gas theory in translational diffusion. Using four adjustable parameters $E_{D,S}$, $E_{D,GT}$, λ, and $D_S^0(0)$, excellent fits of experimental data were achieved for a number of gases, including CO_2. While this model was designed specifically for silicalite-1 membranes, surface and gas translational diffusion are common to all porous membranes, allowing it to be useful for a variety of membrane types.

$$\Pi(T) = \frac{\varepsilon}{\Delta P}\left[\rho q_{sat} D_S^0(0)\frac{1}{1-\theta}\exp\left(-\frac{E_{D,S}}{RT}\right)\frac{d\theta}{dx} + \frac{\lambda}{z}\sqrt{\frac{8}{\pi MRT}}\exp\left(-\frac{E_{D,GT}}{RT}\right)\frac{dP}{dx}\right] \qquad \text{(XV)}$$

where, Π = permeance, T = temperature, ε = support porosity, ρ = density of the membrane material, q_{sat} = moles of gas adsorbed by the membrane surface at saturation, D_S^0 = limiting diffusivity, θ = fraction of the available adsorption sites occupied, $E_{D,S}$ = activation energy for surface diffusion, R = ideal gas constant, x = spatial coordinate, λ = diffusional free length, z = constriction factor, M = molecular weight of the gas, $E_{D,GT}$ = activation energy for gaseous

translational diffusion, and P = partial pressure of the diffusing gas.

Van den Broeke et al. [45, 46] studied pure gas permeation, as well as binary gas permeation through a silicalite-1 zeolite membrane. They demonstrated that the separation factor would be the same as permselectivity if both components are weakly adsorbed on silicalite-1 zeolite membrane. They also reported that the permeation of the weakly adsorbed component (N_2 or CH_4) would be reduced in a binary mixture in which the other component (CO_2) is moderately or strongly adsorbed. In this case, the separation factor and permselectivity differ considerably.

Poshusta et al. [54] have prepared silicoaluminophosphate (SAPO-34) membranes by in-situ synthesis from gels onto porous α-alumina tubes. The molecular sieve SAPO-34 is a structural analog of the natural zeolite chabazite. They explained the temperature dependence of the gas permeances with a zeolite diffusion model. According to this model, an increase in permeance with increasing temperature is due to activated diffusion of a gas-like phase in the zeolite pores. A decrease in permeance with increasing temperature is due to a decrease in the adsorbed concentration gradient. Therefore, the heat of adsorption and diffusion activation energy of a particular gas-zeolite pair determine the regime where the permeance either increases or decreases with temperature. The increase in CH_4 permeance through SAPO-34 membrane with temperature was attributed to a high activation energy of diffusion because the kinetic diameter of CH_4 (0.38 nm) is close to the zeolite pore diameter (0.45 nm). The CO_2 permeance decreased with increasing temperature because of a decrease in the adsorbed concentration gradient (Table 5). The CO_2/CH_4 mixture had the highest separation factor of 30 at room temperature and was separated by a combination of differences in diffusivity and competitive adsorption because both favored the permeation of CO_2 due to its smaller size and higher adsorption strength compared to CH_4. The H_2/CO_2 permselectivity was 1.3 at room temperature and increased slightly with increasing pressure and temperature.

Table 5. Summary of Results from SAPO-34

Ref.	Permeation Temp. (°C)	CO_2 Permeance[a] (mol m^{-2} s^{-1} Pa^{-1})	CO_2/N_2 System		CO_2/CH_4 System		CO_2/H_2 System	
			PS	SF	PS	SF[b]	PS	SF[b]
[54]	27	2.4×10^{-8}	6		19	30		
	100	1.6×10^{-8}	4		8			
	200	1×10^{-8}	2		2	3.4		
[55]	27	1.5×10^{-7}	5	16	16	36	1.8	4
	100	8×10^{-8}	4		9		1	
	200	2×10^{-8}	2	3	4	5	0.4	0.5

PS: Permselectivity, SF: Separation Factor.

[a]CO_2 permeance is from pure gas permeation experiments. [b]Feed: 49/51 mixture of CO_2 and CH_4 for ref [54] and equimolar gas mixtures for ref [55].

In another study, Poshusta et al. [55] prepared SAPO-34 membranes at slightly different conditions from their earlier study [54]. The SAPO-34 synthesis in this study was conducted at

175 °C for 24 hours, whereas the synthesis temperature was 185 °C for 20 hours in their previous study. This change reduced the SAPO-34 crystallization rate. They observed 2.5-40 times higher CO_2 permeances than previous SAPO-34 membranes, but had a similar CO_2/CH_4 separation factor. The highest CO_2/CH_4 selectivity achieved by them from SAPO-34 was 36 at 27 °C. The mixture of CO_2 and N_2 also behaved similarly to the CO_2 and CH_4 mixture through the SAPO-34 membrane. The CO_2/H_2 separation is governed by competitive adsorption below 50 °C and by differences in diffusivity at higher temperatures.

In a separate study, Poshusta et al. [56] also reported the effects of humidity on the gas permeation for SAPO-34 membranes. It was observed that the water present in the feed completely blocked the zeolite pores in the membrane and, hence, the permeation through the membrane decreased considerably. In contrast, the gas permeation increased through the non-zeolite pores in the presence of humidity. Therefore, the authors suggested that the membrane quality and the fraction of transport through non-zeolite pores could be determined by introducing humidity in the feed. It was noted that the effects of humidity on the gas permeation are reversible, but long-term exposure can permanently degrade SAPO-34 membranes.

Lovallo et al. [32] have synthesized MFI membranes on porous alumina disks and nonporous substrate using secondary growth of precursor layers. The separation factor, CO_2/CH_4, decreased with increasing permeation temperature, while the CO_2/N_2 separation factor increased first, and then decreased as temperature increased. The permeation properties for the CO_2/CH_4 mixture were independent of feed composition. The separation factor, CO_2/CH_4 was observed as high as 15 with CO_2 permeance of 4×10^{-9} mol m^{-2} s^{-1} Pa^{-1} at 120 °C. Permeation properties were attributed to both diffusion and adsorptive features of the microstructure (thickness, grain size, degree of orientation) of the molecular sieving layer of the MFI membranes. On the other hand, the CO_2 permeance increased and the N_2 permeance decreased as the concentration of CO_2 in the feed composition was raised. The CO_2/N_2 separation factor reached values up to 20 (CO_2 permeance ~1.8×10^{-8} mol m^{-2} s^{-1} Pa^{-1}) at 180 °C for the feed containing >60 percent of CO_2.

Zeolite membranes show the least variation in both selectivity and permeability of any inorganic membrane type in separations of CO_2/H_2, CO_2/CH_4, and CO_2/N_2 mixtures. These membranes have relatively high permeabilities and relatively low selectivities, as shown in Figure 2 and Figure 3. The lack of selectivity is less pronounced in CO_2/CH_4 probably because the considerable differences in shape and size of the two molecules have enabled researchers to take full advantage of the molecular sieving properties of the zeolites. The lack of any internal trend in the zeolite results (i.e. any approximate inverse relationship between selectivity and permeability), however, is indicative of the previously discussed dual transport mechanism so well known in zeolite membranes.

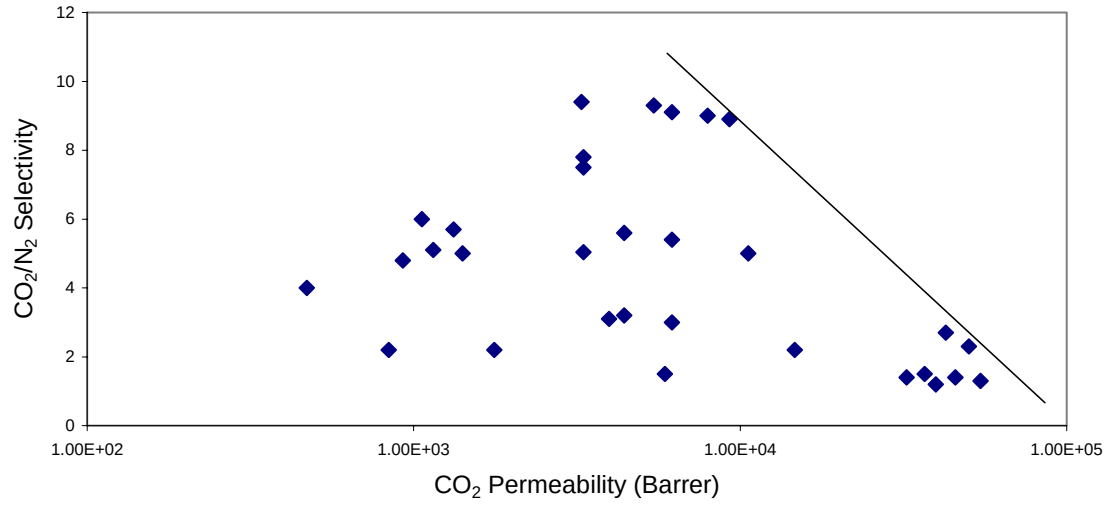

Figure 2. Literature Data for CO_2/N_2 Selectivity vs. CO_2 Permeability for Zeolite Membranes

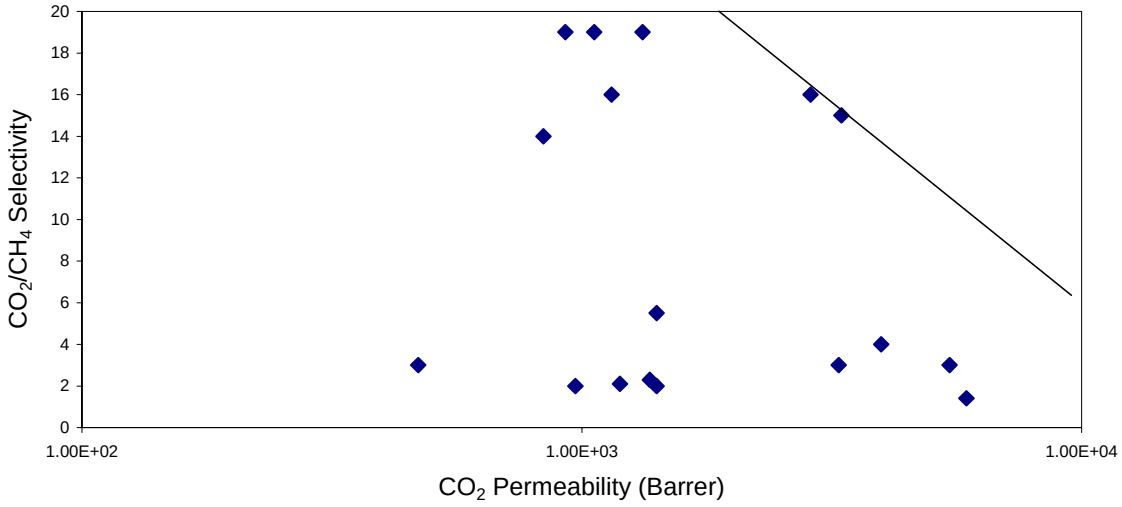

Figure 3. Literature Data for CO_2/CH_4 Selectivity vs. CO_2 Permeability for Zeolite Membranes

Carbon Membranes

Carbon membranes for gas separations are typically produced by the pyrolysis of thermosetting polymers such as polyimides, polyvinylidene chloride (PVDC), polyfurfuryl alcohol (PFA), cellulose, cellulose triacetate, polyacrylonitrile (PAN), and phenol formaldehyde [58]. The pyrolysis temperature, typically in the range of 500 to 1,000 °C, depends upon the type of precursor material and dictates the separation performance of the carbon membranes. At higher pyrolysis temperatures graphitization takes place. The pore size of carbon molecular sieve membranes (CMSM) depends upon the pyrolysis chemistry (temperature, heating rate, heating

atmosphere, etc.), as well as upon the morphology of the organic precursor [59, 60]. The porosity due to morphology is a coarse macroporosity, while microporosity depends upon the pyrolysis chemistry [59]. Pyrolysis of polymeric compounds leads to carbon material with a very narrow micropore distribution below molecular dimensions (<1 nm) [61], which makes it possible to separate gases with very similar molecular sizes. Hence, the predominant transport mechanism of most carbon membranes is molecular sieving, as its name implies. In adsorption-selective carbon membranes (ASCM), the separation takes place because of the selective surface diffusion mechanism [62]. ASCMs separate non-adsorbable or weakly adsorbable gases (He, N_2, O_2, etc.) from adsorbable gases, such as NH_3, CO_2, and SO_2. ASCMs possess slightly wider micropores (5-7 A) than those of CMSMs (3-5 A).

Generally, carbon membranes can be categorized into two types: supported membranes on a porous material (tube or flat) and unsupported carbon membranes (flat, hollow fiber, or capillary tube). Unsupported membranes are very brittle and mechanically unstable, resulting in handling problems. The permeance of carbon membranes is quite low compared to other inorganic membranes due to the large thickness of carbon membranes. The factors that determine the performance of CMSMs include [63]: the selection of the precursor polymer; the membrane preparation method; and the carbonization process.

The high cost of polyimides is a key factor that limits their utilization in the preparation of carbon membranes. The high thermal and chemical stability of CMSMs provide hope in gas separation applications, such as separation of CO_2 in flue gas emissions from power plants. The mechanical stability of CMSMs can be increased by supporting a thin carbon membrane on a porous support material, such as α-alumina, carbon etc. A review by Ismail et al. [24] gives detailed information on the latest developments associated with carbon membranes for gas separation.

Hayashi et al. [64, 65] prepared carbon membranes by coating a polyamic acid film formed from 3,3',4,4'-biphenyltetracarboxylic dianhydride (BPDA) and oxydianiline (ODA) on a porous α-alumina support tube. The polyamic acid film coated on the alumina tube was imidized in N_2 during a multi-step heating procedure up to 300 °C. The resulting membrane was then carbonized at 500 to 900 °C in air. They reported that the carbonization above 600 °C remarkably increased the permeances of CO_2 and other gases. (See Table 6.) Permeances decreased and the permselectivity increased with increasing carbonization temperatures beyond 600 °C. It was concluded that the CO_2 permeance was controlled by the size distribution of the micropores rather than the total micropore volume. The carbonized membrane pores were further modified by chemical vapor deposition (CVD) of carbon formed from the pyrolysis of propylene at 650 °C [65]. The CO_2/N_2 permselectivity of the membranes after 2 minute CVD treatment was increased from 47 to 73. Longer CVD treatment decreased CO_2 permeance due to pores narrowed with carbon deposits and hence, the permselectivity also decreased.

Table 6. Summary of Results from Different Carbon Membranes

Ref.	Precursor	Carbonization Temp (°C)[a]	Permeation Temp. (°C)	CO_2 Permeance (mol m^{-2} s^{-1} Pa^{-1})	Selectivity	
					CO_2/N_2	CO_2/CH_4
[64]	BPDA-pp'ODA	600	30	6×10^{-8}	31	80
		700	30	3×10^{-8}	55	60
		700	100	9×10^{-8}	15	16
		800	30	2×10^{-9}	29	130
[65]	BPDA-pp'ODA	700	35	2×10^{-8}	47	
		700	65	3.5×10^{-8}	35	
		CVD modified	35	8×10^{-9}	73	
[66]	BPDA-pp'ODA (oxidized)	300-700	65	4×10^{-7}	8	20
[67]	BPDA-ODA/DAT (oxidized)	500-600	35	3×10^{-8}	30	50
		0-500	35	2×10^{-9}	40	40
		500-0	35	1.2×10^{-8}	35	60
		400-700	35	3×10^{-8}	38	60
[60]	BPDA-ODA (oxidized)	300-700	35	1.5×10^{-8}	40	
		300-700	100	3.7×10^{-8}	14	
		300-700[b]	35	2.1×10^{-8}	51	
		300-700[b,c]	35	1.5×10^{-8}	50[d]	
		300-700[b]	65	3.1×10^{-8}	30[d]	
		300-700[b]	100	3.8×10^{-8}	15[d]	
[68]	COPNA	700	100	1×10^{-8}	14	
		700	30		41	

[a]For oxidized membranes, the first temperature is oxidation temperature and the second is carbonization temperature; [b]Feed was equimolar CO_2 and N_2 (sweep gas helium) binary mixture; [c]Sweep gas argon; [d]Separation factor

In another study [66], Hayashi et al. oxidized a BPDA-pp'ODA polyimide membrane in mixtures of O_2-N_2 at 300 °C or in CO_2 at 800 to 900 °C. Membrane oxidation causes the pore size distribution to broaden, resulting in increased permeances of CO_2 and other gases, with decreased permselectivity of CO_2 in a CO_2/N_2 system. (See Table 6.) However, excessive oxidation fractured the carbon membranes. The BPDA-pp'ODA polyimide based membranes carbonized at 700 °C were also exposed to air at 100 °C for one month to evaluate the stability of carbon membranes in an oxidative environment. The permeances decreased, while permselectivity increased during the initial stage of exposure, but were largely restored by a post-heat-treatment at 600 °C for 1 to 4 hours. It was suggested that the carbon molecular sieve membranes are stable at 100 °C for a prolonged period under an environment which contains only a low level of oxidants.

Yamamoto et al. [67] formed a BPDA-ODA/DAT (DAT is 2,4-diaminotoluene, contains a

methyl group) copolyimide membrane on a porous α-alumina support tube. The molar composition of 4,4'-ODA and 2,4-DAT as the diamine in copolyimide was fixed at 1:4. The methyl groups decompose during the post-treatment under an oxidative atmosphere resulting in expanded micropores. The permeation properties of the resulting carbon membranes were dependent on the precursor composition, carbonization temperature, and oxidation conditions. Permeances of the BPDA-ODA/DAT carbon membrane were much lower than those of BPDA-ODA carbon membranes; however, the performance of the BPDA-ODA/DAT membrane was greatly improved by treating it in air at temperatures up to 400 °C for 1 hour, followed by carbonization in N_2 at temperatures up to 700 °C. It was concluded that optimization of the treatment was more important than changes in the diamine portion of the copolyimide.

Kusakabe et al. [60] coated a BPDA-pp'ODA polyimide film on the outer surface of a porous α-alumina support tube. They obtained a carbon molecular sieve membrane by carbonizing the coated film at an optimized temperature of 700 °C, and then by oxidizing with either a N_2-O_2 mixture or pure O_2 at 100 to 300 °C for 3 hours (Table 6). They found that the permeances of CO_2 and other gases increased after the oxidation without damaging the permselectivities of the membrane. It was concluded that the oxidation at 300 °C for 3 hours significantly increased the micropore volume, and that the pore size distribution was not broadened, contrary to their previous work. They reported that the CO_2/N_2 selectivity of the carbon molecular sieve membrane was 40 for single component gases at 25 °C, and that the selectivity increased to 51 for an equimolar mixture of CO_2 and N_2. It was suggested that the carbon membrane has slit-like pores, the shorter width of which could be 0.4-0.5 nm. Thus, molecules could pass one another by moving to the longer width of the slit, but CO_2 molecules cannot be concentrated on the pore wall because of the small slit width. Thus the CO_2/N_2 selectivity would not be expected to greatly increase for a mixed feed. This mechanism is different from that of Y-type zeolite [38] and silica membranes [14].

For Y-type zeolite membranes, CO_2 molecules are adsorbed on the zeolite surface and then transported into the pore *via* a surface diffusion mechanism. The pore size of Y-type zeolite membranes is 0.7-0.8 nm, and CO_2 molecules are concentrated on the surface of the pore. The concentration of N_2 molecules inside the pore is lower than on the outside, and CO_2 molecules (which migrate along the pore wall), outrun N_2 molecules (which are located in the core region of the pore). The Y-type zeolite membrane showed a CO_2/N_2 selectivity of 3 at a permeation temperature of 30 °C, when the permeances were determined using pure gases. When a mixture of CO_2 and N_2 was fed, however, the separation factor increased to 80. The type of carrier gases on the permeate side had no effect on permeances. In the pore of the silica membranes, molecules are not able to pass one another. The CO_2/N_2 selectivity for a mixed feed is then determined by the slowest–moving species and is lower than for pure gases.

In another study [68], Kusakabe et al. formed a condensed polynuclear aromatic (COPNA) resin film on the outer surface of a porous α-alumina support tube and produced a pinhole-free membrane by carbonization at a temperature range of 400 to 1,000 °C. COPNA resins were synthesized from polycyclic aromatic compounds (PCA) (pyrene and phenanthrene) and 1,4-benzenedimethanol (BDM) with a BDM/PCA ratio of 1.25 giving molecular sieving carbon membranes. COPNA-based membranes contain both mesopores and micropores, while carbonized BPDA-ODA polyimide membranes possess only micropores. The mesopores of

COPNA membranes do not penetrate through the total thickness of the membrane and serve as channels connected by the micropores, which separate gases by the molecular sieving mechanism. They obtained similar permselectivities for CO_2/N_2 from COPNA-based carbon membranes and carbonized BPDA-ODA polyimide membranes despite the different pore structures of each, and, therefore, concluded that the micropores are responsible for the permselectivities of the carbonized membranes. (See Table 6.)

Fuertes et al. [61] prepared flat, asymmetric carbon membranes by casting a solution of polyamic acid (BPDA-pPDA) in N-methylpyrrolidone (NMP) upon a macroporous support and by subsequent imidization at 380 °C and carbonization at 550 °C. They emphasized that by using the phase inversion during the preparation stage, an almost defect-free carbon membrane can be obtained in only one casting step. It was observed that the CO_2/N_2 or CO_2/CH_4 permselectivity decreased with increasing temperature, while the CO_2 permeance was unchanged. (See Table 7.) Their explanation for this phenomenon was that the CO_2 transport through the membrane results from a combination of transport in the gas phase (molecular sieving) and surface diffusion of the adsorbed molecules across the micropores. The decreased CO_2 adsorption with increasing temperature was compensated by an increase in gas diffusivity, and hence CO_2 permeance was unchanged. Furthermore [69], they also prepared symmetric carbon molecular sieve membranes from the same method and the same raw material by using the multicoating step. They reported that the performance of these membranes was better than the asymmetric carbon membranes prepared in a single casting step. (See Table 7.)

Table 7. Summary of Results from Different Carbon Membranes

Ref.	Precursor	Carbonization Temp. (°C)[a]	Permeation Temp. (°C)	CO_2 Permeance (mol m^{-2} s^{-1} Pa^{-1})	Selectivity	
					CO_2/N_2	CO_2/CH_4
[61]	BDPA-pPDA	550	25	4×10^{-9}	19	37
			100	4×10^{-9}	9	13
			150	4×10^{-9}	6	7
[69]	BDPA-pPDA	550	150	2×10^{-8}	1.8	1.5
		550 (2)	25	2.7×10^{-9}	3.9	
			180	6.6×10^{-9}	4.5	
		550 (3)	25	4.2×10^{-10}	21	
			50	8.1×10^{-10}	22	27
			150	1.4×10^{-9}	9	17
[70]	Polyetherimide	800	25	1×10^{-10}	15	25
			150	4×10^{-10}	9	20
[71]	Phenolic resin	700	25	2×10^{-9}	18	87
			50	2.9×10^{-9}	17	64
		700[b]	25	2×10^{-9}	45[d]	
			50	2.9×10^{-9}	32[d]	

Ref.	Precursor	Carbonization Temp. (°C)[a]	Permeation Temp. (°C)	CO_2 Permeance (mol m^{-2} s^{-1} Pa^{-1})	Selectivity	
					CO_2/N_2	CO_2/CH_4
			150		9[d]	
		700[c]	25	2.5×10^{-9}		163[d]
			50	3.3×10^{-9}		104[d]
			150			25[d]
[72]	Phenolic resin	700	25	46 B[e]	37	85
		700	150	163 B	6	11
		700 (3)	25	16 B	40	116
		700 (3)	150	29 B	8	15
		700[c]	25	400 B		150[d]
[73]	PVDC-PVC	700	25	6×10^{-9}	18	69
			75	9×10^{-9}	13	45
			150	8×10^{-9}	7	16
		500	150	1.5×10^{-9}	8	13
		600	150	6×10^{-9}	10	15
		700[f]	25	9×10^{-10}	28	71
[63]	Matrimid® in NMP	475	25	2.7×10^{-9}	15	33
		650	25	2.4×10^{-9}	4	8
		650[g]	25	3.1×10^{-9}	22[d]	
		650[c]	25	3.7×10^{-9}		23[d]
			100	3.7×10^{-9}		11[d]
	Allotherm® in NMP		150	3.1×10^{-9}		6[d]
		550	25	1.5×10^{-8}	9	16

[a]Number of coating is in parenthesis, otherwise one coating; CO_2-CH_4 mixture (10:90 mol/mol); [b]Feed: (15% CO_2 + 85% N_2) binary gas mixture; [c]Feed: (10% CO_2 + 90% CH_4) binary gas mixture; [d]Separation factor; [e]B: Permeability in Barrer; [f]Membrane was oxidized at 200 °C prior to carbonization; [g]Feed: (20% CO_2 + 80% N_2) binary gas mixture

In a different study [70], Fuertes et al. observed that only the molecular sieving mechanism contributes in the transport of CO_2 across the carbon molecular sieve membranes, which were prepared by taking polyetherimide as a precursor upon a porous carbon support (Table 7). They chose polyetherimide because it is an inexpensive and commercially available material, compared to others used as precursors for carbon membranes.

Centeno et al. [71] prepared a carbon membrane by coating a phenolic resin (Novolak type) on a macroporous carbon disk-shaped support and subsequent carbonization under vacuum of the polymeric film. An almost defect-free carbon membrane was obtained in a single casting step. The separation factor of CO_2/N_2 or CO_2/CH_4 from a feed mixture (85 percent N_2 + 15 percent CO_2 or 10 percent CO_2 + 90 percent CH_4) was higher than those calculated from the ratio of permeances of pure gases. (See Table 7.) It was suggested that the presence of CO_2 in the

mixture restricted N_2 diffusion through the micropores of the membrane. The separation factor for CO_2/N_2 or CO_2/CH_4 decreased with increasing temperature, while remaining unchanged with pressure. They also studied phenolic resin-based carbon membranes supported on a porous alumina tube [72]. They showed that the gas permeability significantly decreased, while the permselectivity did not change much with the number of coats (shown in Table 7) and, hence, claimed to obtain a defect-free carbon membrane in a single casting step.

Fuertes et al. [63] also developed a method for preparing supported molecular sieve carbon membranes from commercially-available polyimides (Allotherm® 610-16 and Matrimid® 5218) in a single casting step. Allotherm® (BASF), a 16.5 percent solution of polyamic acid in NMP was used as a precursor of Kapton® polyimide, since Kapton® is insoluble in any solvent. Matrimid® (Ciba specialty Chemicals Co.) is a thermoplastic solid polyimide based on a proprietary diamine, 5(6)-amino-1-(4'-aminophenyl)-1,3-trimethylindane. Macroporous carbon disks were used as supports for the membranes. Carbonization of polymeric membranes was carried out at the temperature range of 475 to 700 °C. A similar trend was observed from the carbon membranes derived from the commercially available polyimides (shown in Table 7) and from the phenolic resins (discussed above).

More recently, Centeno et al. [73] also produced composite carbon membranes by single casting of poly(vinylidene chloride-co-vinyl chloride, or PVDC-PVC) on a macroporous carbon support, followed by pyrolysis at 500 to 1,000 °C under vacuum. The resulting carbon membrane (0.8 μm thickness) was almost defect free and allowed the separation of gases based on their molecular sizes. They performed an oxidative pretreatment of polymeric membrane to obtain a more amorphous carbon and expected to improve the permeation properties by changing the structure. It was reported that the pretreatment in air at 200 °C for 6 hours improved the CO_2/N_2 permselectivity of the carbon membrane, but lower CO_2 permeance was observed. (See Table 7.) Finally, they recommended the CMSM obtained at a temperature of 700 °C for better balance between the permeance and selectivity.

Kusuki et al. [74] prepared asymmetric carbon membranes by pyrolyzing an asymmetric polyimide hollow fiber membrane at temperatures ranging from 600 to 1000 °C in N_2. The polyimide hollow fiber membrane was formed from BPDA and an aromatic diamine, such as ODA. It was observed from scanning electron microscopy (SEM) studies that the top thin layers of the carbon fibers were composed of dense aggregation of nodules having diameter of about 50 nm. The asymmetric carbon membranes pyrolyzed at 850 °C showed lower permeability than the membrane pyrolyzed at 700 °C, but had higher permselectivities for the CO_2/CH_4 system (shown in Table 8).

Table 8. Summary of Results from Asymmetric Carbon Membranes Prepared from Polyimide Hollow Fiber Membrane

Carbonization Temp. (°C)	Permeation Temp. (°C)	CO_2 Permeance (mol m^{-2} s^{-1} Pa^{-1})	Permselectivity	
			(CO_2/N_2)	(CO_2/CH_4)
270	50	2.6×10^{-8}	36	27
	75	3.3×10^{-8}	20	17
	120	4.0×10^{-8}	10	10
700	50	4.0×10^{-8}	17	30
	75	6.7×10^{-8}	17	25
	120	1.0×10^{-7}	14	21
850	50	1.8×10^{-9}	18	37
	75	3.0×10^{-9}	15	45
	120	5.0×10^{-9}	13	48

Suda et al. [75] found that the microstructure (pore size, pore volume, etc.), and hence the permeation properties, of the carbon molecular sieve membranes prepared by pyrolysis of Kapton polyimide can be tailored by controlling pyrolysis conditions (pyrolysis temperature, heating rate, and pyrolysis atmosphere). They observed that the CO_2 permeability decreased whereas the permselectivity, CO_2/N_2, increased when the pore volume and pore size decreased as pyrolysis temperatures increased. Pore size distribution also became sharper at higher pyrolysis temperatures. They reported that the heating rate influenced the permeation properties to a lesser extent, whereas the pyrolysis environment did not appreciably affect the properties. The pyrolysis proceeds very slowly by decreasing the heating rate, which results in the smaller pores and, hence, lower permeabilities for larger molecules. It was suggested that the longer pyrolysis time might also contribute to the pore size reduction due to a sintering effect. It was also suggested that the gases permeate through both the cross-linked voids of the amorphous region and the interlayer spacing of the graphite-like microcrystals. The excellent permselectivities from the CMSMs were attributed to the molecular sieving effect that comes mainly from the dependence of diffusivity of penetrants on the size of the micropore. (See Table 9 below.) The higher permeabilities of CO_2 and H_2 molecules compared to that of the smaller helium molecule were ascribed to the larger sorptivities of CO_2 and H_2.

Table 9. Summary of Results from CMSM (Kapton) Membranes

Pyrolysis Temp. (°C)	Pyrolysis Condition[a]	CO_2 Permeability[b] (Barrer)	Selectivity	
			CO_2/N_2	H_2/CO_2
600	10, vac	1820	22.2	0.9
800	10, vac	128	42.2	5.2
1000	10, vac	4.15	101	14.3
950	13.3, Ar	3.54	82.7	15.0
950	4.5, Ar	2.51	87.7	16.5
950	1.33, Ar	0.50	122	39.0

[a]Heating rate(°C/min) , heating medium; [b]Permeation temperature 25 °C.

Supported nanoporous carbon membranes (SNPCM) were prepared by Shiflett et al. [76] as a thin film supported on porous stainless steel by ultrasonic deposition of polyfurfuryl alcohol (PFA). The ultrasonic deposition technique provided mechanical robustness to SNPCM, even below the critical thickness for crack formation. Carbon dioxide permselectivities, with respect to N_2 and CH_4 from SNPCM-43 membrane, were 1.4 and 45, respectively, with a CO_2 permeance of 1.87×10^{-10} mol m^{-2} s^{-1} Pa^{-1}. SNPCM-43 was obtained by pyrolyzing the first three coatings of PFA at 150 °C, followed by pyrolyzing at 450 °C, with a final finish coat applied and pyrolyzed at 450 °C.

Wang et al. [77] used a different technique, vapor deposition polymerization (VDP), to prepare supported carbon membranes using a PFA thin layer. The VDP technique can provide great control of film depositions inside the pores of supports. They used two different support tubes: γ-Al_2O_3/α-Al_2O_3, and glass/α-Al_2O_3 prepared in their lab [78]. Membranes were prepared by two cycles of VDP, and two carbonization cycles at 600 °C. The CO_2/CH_4 separation factor was lower than the CO_2/CH_4 permselectivity by a factor of 3, as shown in Table 10 below. It was concluded that the low CO_2 permeance of the VDP membranes was due to deeper penetration of gaseous furfuryl alcohol into the support during VDP, or due to a different pore structure of the carbon.

Table 10. Summary of Results from Supported Carbon Membranes from PFA by VDP

Permeation Temp. (°C)	Support	CO_2 Permeance (mol m^{-2} s^{-1} Pa^{-1})	Selectivity	
			(CO_2/N_2)	(CO_2/CH_4)
25	γ-Al_2O_3/α-Al_2O_3	5.8×10^{-9}	79	92
150	γ-Al_2O_3/α-Al_2O_3	3.3×10^{-8}	9	15
25	Glass/α-Al_2O_3	2.7×10^{-9}	40	82
150	Glass/α-Al_2O_3	3.0×10^{-9}	11	17
25[a]	γ-Al_2O_3/α-Al_2O_3	2.3×10^{-9}		27[b]
25[a]	Glass/α-Al_2O_3	1.1×10^{-9}		25[b]

[a]Feed: 85% CO_2 and 15% CH_4; [b]Separation factor

Tanihara et al. [79] prepared asymmetric carbon hollow fiber membranes by pyrolysis of asymmetric polyimide hollow fiber membranes at 700 °C. It was observed that the permeation properties of the carbon membranes did not depend on the feed pressure and were stable over time. The CO_2 permeance from the membrane was 3.4×10^{-8} mol m^{-2} s^{-1} Pa^{-1} at 50 °C with the CO_2/CH_4 permselectivity of about 30.

Ogawa et al. [80] developed carbonized hollow fiber membranes for CO_2/CH_4 separation by the phase inversion of polyamic acid solution, imidization, and carbonization. They also studied the effect of gelation conditions (time, temperature, and pH of coagulation), on the permeation properties of the resulting membrane. Polyamic acid solution was prepared by dissolving 4,4'-diaminodiphenyl ether in N,N-dimethylacetamide, and then adding pyromellitic dianhydride to the solution. They reported that the micropore volume was independent of the gelation time and, hence, gelation time was not a predominant factor controlling the permeation properties of the hollow fiber membrane. The CO_2/CH_4 and CO_2/N_2 permselectivities were highest when the polyamic acid solution was gelated for 1 hour, as shown in Table 11. The CO_2/CH_4 and CO_2/N_2 permselectivities were maintained at approximately 60 and 30, respectively, in further gelation. The micropore volume increased as gelation temperature increased and pH decreased. High permeance of CO_2 and high CO_2/N_2 and CO_2/CH_4 permselectivities through the carbon membrane were achieved at these gelation conditions: time 6 hours, temperature 2 °C, and pH 9.4. It was found that the CO_2 transport was enhanced by an adsorption effect, while transport of CH_4 and N_2 was restricted by a molecular sieving effect in the carbonized membrane.

Table 11. Effects of Gelation Conditions on Permeation of Carbon Hollow Fiber Membranes

Gelation Conditions			Permeation Temp. (°C)	CO_2 Permeance (mol m^{-2} s^{-1} Pa^{-1})	Permselectivity	
Time (hr)	pH	Temp. (°C)			(CO_2/N_2)	(CO_2/CH_4)
1	6.5	2	25	9×10^{-9}	45	100
6	6.5	2	25	5×10^{-9}	25	50
10	6.5	2	25	1×10^{-8}	33	66
6	6.5	25	25	7×10^{-8}	18	12
6	6.5	39	25	1.6×10^{-8}	12	17
6	3	2	25	2×10^{-8}	28	13
6	9.4	2	25	7×10^{-9}	230	23
6	11	2	25	7×10^{-11}	5	2

In another study [81], Ogawa et al. investigated the separation of CO_2/CH_4 mixtures and the effect of membrane micropore diameter on the permeation properties. Three different pore size membranes for the CO_2/CH_4 separation were studied: Membrane A (> 0.50 nm), Membrane B (0.43-0.50 nm), and Membrane C (<0.43 nm). As Table 12 shows, the permeances of CO_2 and CH_4 through Membranes A and C were independent of the composition of the feed gas. For Membrane B, the CH_4 permeance decreased with the increase in CO_2 content in the feed gas that resulted in the increase in the CO_2/CH_4 separation factor. It was concluded that the CO_2/CH_4 separation factor for Membrane B increased due to the hindrance of CH_4 permeation by CO_2 molecules adsorbed inside the micropores of the membrane.

Table 12. Separation of CO_2/CH_4 through Carbonized Membrane Prepared by Gel Modification

Membrane	Pure Gas Permeation		Mixed Gas Permeation		
	CO_2 Permeance (mol m^{-2} s^{-1} Pa^{-1})	P. S. (CO_2/CH_4)	Feed Gas CO_2:CH_4	CO_2 Permeance (mol m^{-2} s^{-1} Pa^{-1})	S. F. (CO_2/CH_4)
A	3.16×10^{-8}	42	15:85	3.13×10^{-8}	51
B	1.3×10^{-9}	181	15:85	1.36×10^{-9}	265
			65:35	1.01×10^{-9}	310
C	4.84×10^{-11}	5	15:85	4.05×10^{-11}	4

Permeation temperature 25 °C; Gelation conditions: time 6hr, temp 2 °C, and pH 9.4.

P.S. = Permselectivity, S.F. = Separation Factor

It is obvious from the above discussion that carbon membranes have a great potential to perform gas separations efficiently, particularly when the gas molecules to be separated are of similar sizes. Carbon membranes, illustrated in Figure 4 and Figure 5, show the greatest variation in

selectivity and permeability of any of the types of inorganic membrane for the separation of CO_2 from H_2, N_2, and CH_4. The expected inverse relationship of selectivity to permeability is present across the range of literature results primarily from the abundance of work on CMSMs. The result is that these membranes have the highest demonstrated selectivities in most separations, but the permeability limitations associated with them are unlikely to be overcome. Also, high production costs of carbon membranes along with expensive modules have prevented their intended commercial scale use. A significant amount of research is required in order to find more economical precursors for carbon membrane production, while improving their permeation properties at elevated temperatures and pressures in the presence of complex feeds.

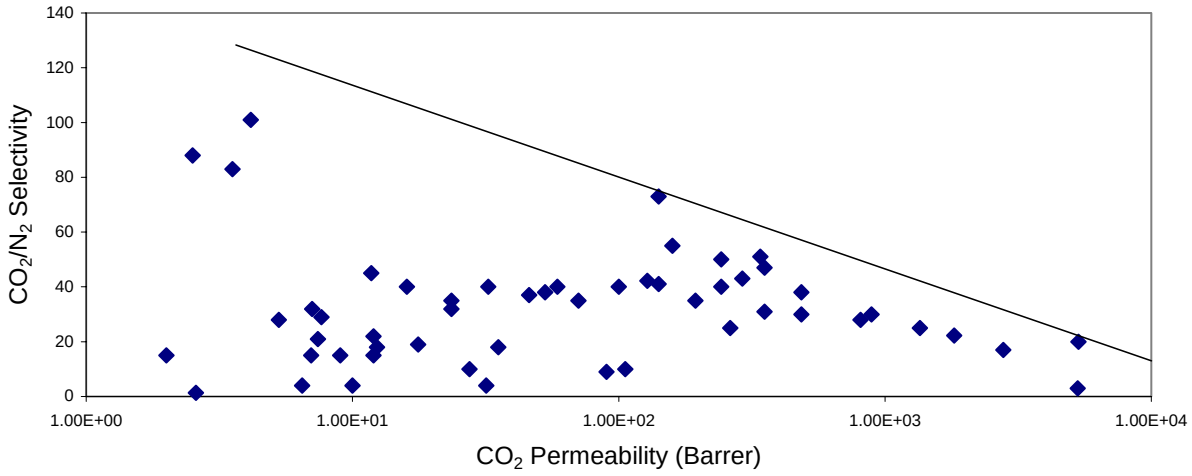

Figure 4. Literature Data for CO_2/N_2 Selectivity vs. CO_2 Permeability for Carbon Membranes

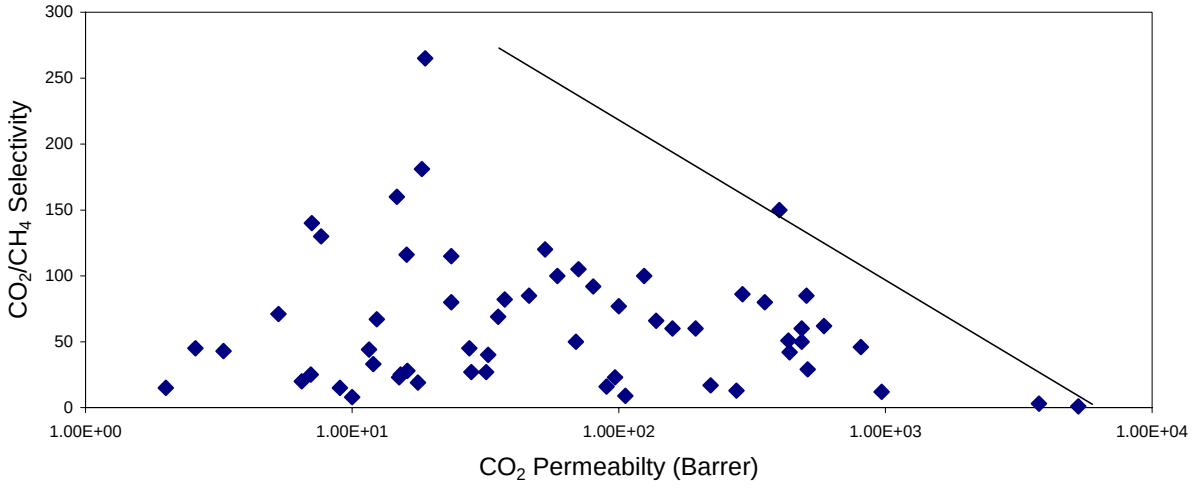

Figure 5. Literature Data for CO_2/CH_4 Selectivity vs. CO_2 Permeability for Carbon Membranes

Silica Membranes

Silica is considered a viable starting material in the fabrication of CO_2 selective membranes, primarily because of its innate stability. Unlike alumina, which tends to undergo phase transition at relatively low temperatures, or carbon, which can exhibit substantial changes in pore size in oxidizing environments [60, 66, 67, 73], silica shows exception thermal, chemical, and structural stability in both oxidizing and reducing environments. Fabrication procedures, while not as advanced as those for carbon and alumina membranes, are capable of producing defect-free silica membranes with molecular sieving pores. Though surface diffusion has been named as an important mechanism in a number of studies on silica membranes for the selective separation of CO_2, most research has only considered silica as a compliment to the molecular sieving mechanism. Research, then, has focused primarily on separation of CO_2 from N_2 and CH_4, the surface diffusion mechanism not being considered strong enough for the more difficult separation from H_2. Notable exceptions include the works of Burggraaf [82] and Morooka [83]. Both studies conclude surface diffusional control in membranes fabricated by the sol-gel method, the most common type of preparation procedure for silica membranes.

Silica is a very versatile material for gas separation membranes because its structure can be tailored by changing the preparation method and conditions. Generally, microporous silica membranes are prepared by deposition of a silica layer onto a porous support by either the sol-gel method, or chemical vapor deposition (CVD) technique, or phase separation method. The porous support provides mechanical strength to the selective top layer of silica. In the sol-gel technique [84, 85], polymeric silica sols are deposited on top of a support system consisting of about a micron thick γ-alumina over a macroporous α-alumina of desired thickness. The silica layer is then calcined at 400 to 800 °C, to end up as the separating top layer with thickness of 50 to 100 nm. The silica sols are obtained from the hydrolysis condensation reaction of alkoxysilanes, such as tetramethoxysilane (TMOS), tetraethoxysilane (TEOS), or chlorosilane.

It is technically challenging to get uniform thickness and pinhole-free silica membranes from the method described above. In the CVD technique, organic precursors in vapor phase are introduced to porous support. A uniform and almost pinhole-free top membrane layer is obtained from the CVD technique. This technique is also used to narrow down or to plug the mesopores of silica membranes [86].

In the phase separation method [8, 78], the homogeneous glass, sodium borosilicate, separates into two phases under certain time and temperature conditions: an acid soluble boric acid rich phase and an insoluble silica rich phase. Leaching of the boric acid phase in a mineral acid solution removes the acid soluble boric acid phase, leaving behind a porous insoluble silica phase. The silica pore size can be controlled by changing glass composition, annealing time, and temperature. Mesoporous silica membranes obtained from the phase separation method are not suitable for gas separations, so they find applications mostly as a support for microporous or nonporous membranes.

Uhlhorn et al. [82] formed a ~30 nm thin layer of microporous silica on top of a γ-alumina membrane using the sol-gel technique. The permeability to CO_2 strongly increased with the mean pressure of the system, while the permeability to N_2 and CH_4 remained unchanged. The transport across the silica-modified membrane is due to the surface diffusion mechanism, as

indicated by the observed pressure dependence and very small pores of the silica. Permselectivities for CO_2/N_2 and CO_2/CH_4 were as high as 15 and 10, respectively, with CO_2 permeances of about 3 x 10^{-6} mol m^{-2} s^{-1} Pa^{-1}.

De Vos et al. [87] have prepared almost defect free silica membranes by applying two sol-gel derived silica (thickness 30 nm and pore size ~5 A) layers on top of a γ-alumina layer, supported by an α-alumina support. A silica sol was prepared by acid-catalyzed hydrolysis and condensation of TEOS in ethanol. They reported that the silica membranes showed a slight increase in the permeances of gases with increasing temperature and a slight decrease for CO_2 permeance, shown in Table 13. The CO_2/CH_4 permselectivities in the silica membrane calcined at 400 °C (Si400) were very large and the H_2/CO_2 permselectivities were very large in Si600 because the membranes were so dense that CH_4 could not permeate in Si400 and CO_2 in Si600.

Table 13. Summary of Results from Different Silica Membranes

Ref.	Precursor[a]	Permeation Temp. (°C)	CO_2 Permeance (mol m^{-2} s^{-1} Pa^{-1})	Permselectivity		
				CO_2/N_2	CO_2/CH_4	H_2/CO_2
[87]	TEOS (400)	25	2.3 x 10^{-7}	23	325	2.6
		100	2.9 x 10^{-7}	15	190	4.0
		200	2.3 x 10^{-7}	8	75	7.5
		200[b]				7[d]
		200[c]			45[d]	
	(600)	100	9.4 x 10^{-9}			26
		200	6.1 x 10^{-9}			66
		300	4.6 x 10^{-9}			139
[88]	TEOS, methylated (400)	100	5.1 x 10^{-7}	1.8	1.9	4.5
		200	4.1 x 10^{-7}	1.6	1.5	5.0
		300	3.0 x 10^{-7}	1.3	1.1	6.4
[13]	Hollow fiber	25	2 x 10^{-8}	20	156	3
		150	2 x 10^{-6}	9	21	5
		25[c]			180[d]	
		150[c]			20[d]	
[90]	TEOS +MTES (550)	25	8.6 x 10^{-7}			12
		25[e]	7 x 10^{-7}			72

[a]Calcination temperature in parenthesis; [b]Equimolar feed of CO_2 and H_2; [c]Equimolar feed of CO_2 and CH_4; [d]Separation factor; [e]After surface derivatization with 1:12 TEOS monomer

In another study [88], De Vos et al. have synthesized hydrophobic silica membranes by adding methyl-tri-ethoxy-silane (MTES) to the silica sol described above. The hydroxyl groups on the silica are substituted by the methyl groups, and hence, their methylated silica membranes are 10 times more hydrophobic than the state-of-the-art silica membranes prepared by the authors in

their previous study [87]. It was suggested that the 'Knudsen-like' temperature dependence for most gases through methylated silica membranes was due to a contribution of the support resistance, not because of porosity of the membrane. (See Table 13.) They mentioned that the methylated silica membranes have larger micropores with a wider pore size distribution than the state-of-the-art silica, but the maximum pore size of the membrane was expected to be ~0.55 nm, because molecules with kinetic diameter of 0.55 nm (SF_6) hardly permeated through the methylated silica membranes. They obtained gas separation factors lower than the permselectivities due to a limitation in the maximum possible sweep flow.

Way et al. [89] used microporous hollow fiber silica membranes from PPG Industries for gas separations. They proposed that both the surface diffusion and the molecular sieving mechanism contribute to the permeation properties of the silica hollow fiber membranes, with the latter dominating the mechanism. High permselectivities were observed for CO_2/N_2 of 28 (CO_2 permeance 21 Barrer) and 30 (CO_2 permeance 53 Barrer) at 40 °C and 70 °C, respectively.

Hassan et al. [13] have studied single component and mixed gas transport using a PPG silica hollow fiber membrane, produced by the phase separation method. They observed that the molecular sieving mechanism is responsible for mass transfer through the silica hollow fiber membranes. They found that the separation factors decreased as the temperature increased, which was due to the less permeable penetrant having larger activation energy (Table 13). Large separation factors were obtained for the gas mixture as compared to those calculated from the ratio of pure gases permeances through the same membrane. It was concluded that the difference between the permselectivities and separation factors is due to a competitive adsorption effect in which the more strongly adsorbed gases saturate the surface and block the transport of the weakly interacting gases. It was also revealed using FTIR spectroscopy that the hydroxylated membrane was covered by physisorbed water at ambient conditions. Removal of the physisorbed water is expected to increase the interaction between CO_2 and the membrane surface, which would increase the surface diffusion contribution of the total flux.

Kusakabe et al. [84] formed silica membranes on a γ-alumina-coated α-alumina tube using sols prepared from the co-polymerization of TEOS and octyltriethoxysilane (C8TES), C12TES, or C18TES. The alkyltriethoxysilanes were used as the template to control the pore size of the silica membranes. The authors obtained defect-free silica membranes from C8TES and C12TES, but silica membranes prepared from C18TES contained defects and mesopores and, hence, the transport across this membrane was controlled by the Knudsen diffusion mechanism. It was concluded that the silica structure, which was formed from C18TES, might not be strong enough to withstand shrinkage during calcination. The effect of the molar ratio of water to total alkoxides, x, in the sols was also studied. High permeances and low selectivities were found for the membrane formed with x = 4. The size of micropores, before calcination, of silica membranes prepared from alkyltriethoxysilanes was found to be very close to the minimum dimension of the alkyl groups and increased slightly by increasing the size of alkyl group. The micropores in the range of 0.3 to 0.4 nm for the silica membranes were formed after calcination at 600 °C. The permselectivities for the CO_2/N_2 and CO_2/CH_4 systems increased with increasing calcination temperature of silica membranes (Table 14).

Table 14. Summary of Results from Different Silica Membranes

Ref.	Precursor[a]	Permeation Temp. (°C)	CO_2 Permeance (mol m^{-2} s^{-1} Pa^{-1})	Permselectivity		
				CO_2/N_2	CO_2/CH_4	H_2/CO_2
[84]	TEOS+ C8TES[c]	100[b]	7×10^{-8}	3.5	2.5	0.9
	(200)[c]	100	1×10^{-7}	3.0	2.0	1.3
	(600)[c]	100	2.2×10^{-7}	7.0	7.0	2.0
	(600)[d]	100	8×10^{-9}	8.0	4.5	12.0
[14]	TEOS (600)	30	3.6×10^{-10}	0.7	0.7	12
		200	3.3×10^{-10}	0.7	0.7	67
		400	3.3×10^{-10}	0.7	0.7	150
	PTES (500)	30	8×10^{-9}	5	6	1.2
		200	1×10^{-8}	6	6	6
	DPDES (500)[e]	30	8.1×10^{-8}	9	11	6
		200	3.3×10^{-8}	4	6	16
		400	1.8×10^{-8}	2	2	25
	DPDES (500)[f]	30	2.1×10^{-8}	1		
		200	1.9×10^{-8}	0.9		
	DPDES (500)[e, g]	30	1.4×10^{-8}	1.4[h]		
		200	1.5×10^{-8}	1.2[h]		
	DPDES (500)[f, g]	30	2.3×10^{-8}	1.1[h]		
		200	2.1×10^{-8}	1.0[h]		

[a]Calcination temperature in parenthesis; [b]No calcination; [c]Gel formation temperature 80 °C; [d]Gel formation temperature 60 °C; [e]Sweep gas: argon; [f]Sweep gas: helium; [g]Feed: 10% CO_2 and 90% N_2; [h]Separation factor

Sea et al. [14] used the CVD technique to deposit the amorphous silica in mesopores of a γ-alumina film coated on a porous α-alumina tube. They used TEOS, phenyltriethoxysilane (PTES) or diphenyldiethoxysilane (DPDES) as the silicon source. Carbonaceous material that remained in the resulting membranes was removed by subsequent calcination at 500 to 750 °C. The TEOS-derived membranes consisted of abundant sub-micropores (~0.3 nm) and a smaller number of Knudsen pores (~5 nm) and, hence, CO_2 and larger molecules only permeated through the Knudsen pores which were left unplugged. The DPDES-derived membranes consisted of abundant sub-micropores, few micropores (~0.5 nm), and almost negligible Knudsen pores and, thus, CO_2 permeance was controlled by the surface diffusion mechanism. The authors reported that the membrane prepared with PTES had properties intermediate between the membranes prepared from TEOS and DPDES. (See Table 14.) The use of PTES and DPDES was, therefore, effective in controlling the micropore size. The permeance of CO_2 in the DPDES-derived membrane was affected by adsorption and decreased with increasing temperature, otherwise permeances were not significantly dependent on the permeation temperature. Contrary to results from other studies of inorganic membranes [38-40, 54, 55], the CO_2/N_2 selectivity was

decreased when the binary CO_2-N_2 mixture was fed because CO_2 and N_2 permeate through micropores in which CO_2 and N_2 are barely able to pass one another. When helium, which is permeable in abundant sub-micropores, was used as the sweep gas instead of Ar, the surface diffusion of CO_2 in micropores was retarded because helium molecules frequently collided with CO_2 adsorption sites, and, as a result, the CO_2/N_2 selectivity decreased.

Raman et al. [90] deposited a hybrid organic-inorganic sol, prepared by co-polymerization of TEOS and methyltriethoxysilane (MTES) on a porous alumina support. The calcined silica membrane was further modified by derivatization of the pore surfaces with monomeric TEOS to allow monolayer by monolayer "fine tuning" of pore size. Subsequent derivatization of the pore surfaces significantly increased the CO_2/CH_4 separation factor with only a slight decrease in CO_2 permeance. (See Table 13.) The CO_2/CH_4 permselectivity of the fine-tuned membranes was 72 with the CO_2 permeance of about 7×10^{-7} mol m^{-2} s^{-1} Pa^{-1}.

Tsai et al. [91] formed dual-layer microporous silica membranes using a sol-gel dip-coating process. They deposited a surfactant-templated silica (STS) intermediate layer on the top of the γ-alumina support to improve its surface finish, and to prevent the subsequently deposited sol from penetrating into the support. The resulting membranes were dip-coated under clean room conditions to avoid dust contamination and vacuum-calcined at 300 °C for 6 hours to promote further pore shrinkage, and to enhance surface hydrophobicity. The source of the silica sol was TEOS and surfactants used in the STS layer were C6-surfactant (triethylhexylammonium bromide) and C16-surfactant (cetyltrimethylammonium bromide). The dual layer asymmetric membranes possess a gradual change of pore size from 50 A (γ-alumina support layer) to 10 to 12 A (STS intermediate layer), and then to 3 to 4 A (300 A thick microporous top layer). They achieved a high CO_2 permeance (1.1×10^{-7} mol m^{-2} s^{-1} Pa^{-1}) along with a high CO_2/CH_4 separation factor of over 300 at 26 °C from the dual-layer silica membrane for a separation of an equimolar CO_2/CH_4 gas mixture. They reported shrinkage of larger pores upon further calcination at 450 °C in air for 1 hour. The resulting membrane provided 92 percent mol H_2 purity with 50 times reduction of CO from a simulated reformate mixture (33.98% N_2, 15.00% CO_2, 0.997% CO, and 50.023% H_2) for application in fuel cells. The same membrane also gave CO_2/CH_4 and CO_2/N_2 permselectivities of 240 and 60, respectively, along with CO_2 permeance of around 2×10^{-8} mol m^{-2} s^{-1} Pa^{-1} at 80 °C.

Okubo et al. [92-94] prepared surface-modified membranes by introducing TEOS vapor into the pores of the porous glass and then decomposing it on the pore walls at 200 °C. The CO_2/N_2 permselectivity from the modified membrane at 60 °C was just 1.6 with CO_2 permeance of 8×10^{-10} mol m^{-2} s^{-1} Pa^{-1} [93].

McCarley et al. [95] fabricated gas separation membranes by modifying mesoporous γ-alumina with octadecyltrichlorosilane (ODS). They hypothesized, based on ellipsometry measurements and XPS analysis, that the composite membrane contained a very thin selective polymer film of ODS molecules (~10.1 nm) interconnected with the porous alumina surface. Selectivity of CO_2/N_2 was increased by 10 percent, while the CO_2/CH_4 selectivity almost doubled for the mixed gas separations, compared to the pure gas permeances. (See Table 15.) The increase in selectivity for the mixed gases was attributed to the competitive adsorption. They also found that the pure gas permeances followed an exponential relationship with the critical temperature,

which showed that the transport was controlled by preferential adsorption (since solubility of gases is an exponential function of critical temperature).

Table 15. Permeation Properties of Surface Flow Membrane

Membrane	Permeation Temperature (°C)	CO_2 Permeance (mol m^{-2} s^{-1} Pa^{-1})	Selectivity	
			(CO_2/N_2)	(CO_2/CH_4)
ODS/γ-alumina	20	2×10^{-8}	5.14	2.10
	20[a]	4×10^{-8}	5.84[c]	
	20[b]	1.4×10^{-8}		4.31[c]

[a]Feed: 51.3% CO_2 and 48.7% N_2; [b]Feed: CO_2 and CH_4 equimolar mixture; [c]Separation factor

Leger et al. [96] also used ODS derivatives to modify a 5 nm γ-alumina ceramic membrane for gas separations. ODS reacted with the surface hydroxyl groups on alumina and formed a chemically stable monolayer on an alumina membrane. They observed that the permeabilities reduced by three orders of magnitude after treating γ-alumina with ODS, because the pores of the treated membrane were partially blocked by the octadecyl aliphatic chains. All gases showed similar permeability through the ODS treated membrane (CO_2 permeance of 3.5×10^{-9} mol m^{-2} s^{-1} Pa^{-1}). The mechanism of transport in this membrane was solution-diffusion. The authors concluded that this membrane is not appropriate for separations of these gases.

Li et al. [19, 97] prepared silicon-based composite membranes by the polymerization-pyrolysis process. They polymerized dichlorodimethylsilane or trichloromethylsilane *in situ* in the pores of Vycor porous glass tube, and then pyrolyzed the polymerized sample at 300 to 530 °C for 8 hours in the presence of O_2 or N_2. They reported permselectivity (CO_2/N_2) as high as high 10, along with the permeability coefficient of CO_2 of 5,600 Barrer from this polysiloxane membrane. It was suggested that the permeability in the polysiloxane-Vycor glass membrane was governed by the activated diffusion mechanism. They also formed composite membranes by pyrolyzing polysilastylene at 460 °C, which exhibited permeation of gases by the molecular sieving mechanism.

Kusakabe et al. [83] also prepared composite membranes by a controlled pyrolysis of polycarbosilane coated on a γ-alumina-modified support tube. The permeation of CO_2 was controlled by the surface diffusion mechanism. The permeance of CO_2 and N_2 decreased with increasing permeation temperature for all membranes, except for the membrane pyrolyzed at <450 °C, in which N_2 permeance increased with increasing temperature. It was reported that pyrolysis in the presence of air created acidic sites on the membrane surface and, hence, the surface diffusion of CO_2 decreased. The permeance of gases increased with increasing pyrolysis temperature of polycarbosilane membranes, as shown in Table 16 below.

Table 16. Results from Composite Membrane by Pyrolysis of Polycarbosilane

Pyrolysis Temperature (°C)	Pyrolyzed Medium	Permeation Temperature (°C)	CO_2 Permeability (mol m^{-2} s^{-1} Pa^{-1})	Selectivity (CO_2/N_2)
350	N_2	10	4×10^{-8}	8.9
		100	2×10^{-8}	4.0
		200	1.5×10^{-8}	2.1
400	N_2	10	9×10^{-8}	18.0
450	Air	10	2.2×10^{-7}	3.1
450	N_2	10	9×10^{-7}	9.0
550	N_2	10	1.4×10^{-6}	3.7

Hyun et al. [98] modified γ-alumina composite membranes by the silane coupling technique using phenyltriethoxysilane to improve the CO_2/N_2 separation factor. The separation efficiency of the γ-alumina composite membranes modified by silane coupling was strongly dependent upon the hydroxylation tendency of the support materials. The CO_2/N_2 separation factor through the TiO_2 supported (average pore size 0.3 μm) γ-alumina membrane was found to be increased by silane coupling, in contrast to the α-alumina supported (average pore size 0.1 μm) membrane. (See Table 17.)

Table 17. Effect of Surface Modification on γ-Alumina Membranes by Silane Coupling

Membrane	Permeation Temp. (°C)	CO_2 Permeance (mol m^{-2} s^{-1} Pa^{-1})	PS (CO_2/N_2)	SF (CO_2/N_2)[a]
γ-Al_2O_3/TiO_2	25	1.7×10^{-6}	1.05	1.05
γ-Al_2O_3/α-Al_2O_3	25	1.7×10^{-6}	0.87	0.87
γ-Al_2O_3/TiO_2	25		1.8	1.4
(10wt% silane modified)	90			1.5
	120			1.3
γ-Al_2O_3/α-Al_2O_3	25			1.1
(10wt% silane modified)				
γ-Al_2O_3/TiO_2	25		1.55	1.25
(4wt% silane modified)	25			1.28[b]
	25			1.35[c]
γ-Al_2O_3/TiO_2	120[d]	7×10^{-8}	2.2	
(10wt% silane modified)	120[e]	1.5×10^{-7}	1.3	

[a]Feed: Binary mixture: 10% CO_2 and 90% N_2; [b]Feed: 20% CO_2 and 80% N_2; [c]Feed: 50% CO_2 and 50% N_2; [d]Membrane performance after 10 min; [e]Membrane performance after 300 min; PS: Permselectivity and SF: Separation Factor

The authors assumed that the difference in results from two different composite membranes were due to the silane coupling on the surface of α-alumina pores. They also found that the CO_2/N_2

separation factor increased as the amount of the phenyl radical coupled on the γ-alumina layer increased, and as the concentration of CO_2 increased in the feed of the binary mixture of CO_2 and N_2. They reported that the modified composite membrane was thermally stable up to 100 °C, and that transport across the membrane is caused by the surface diffusion mechanism. The phenyl group of the silane compound was decomposed when the membrane was used for a long time at the higher temperature.

The sol-gel techniques were applied by Asaeda et al. [99] to fabricate thin layer silica membranes on porous silica and silica-zirconia supports coated on α-alumina porous cylindrical tubes. The pore size of the silica membrane was around 0.35 nm. The CO_2 permeance increased through the silica membrane as the temperature decreased, while N_2 and CH_4 permeances increased very slightly, because CO_2 is more adsorptive on the silica surface than N_2 or CH_4. (See Table 18.) They reported that the porous silica membranes were quite stable when used in dry conditions, while a silica membrane on a silica-zirconia sublayer was even stable in humid conditions.

Table 18. Gas Permeances for Porous Silica Membranes

Membrane	Permeation Temp (°C)	CO_2 Permeance (mol m^{-2} s^{-1} Pa^{-1})	Permselectivity		
			CO_2/N_2	CO_2/CH_4	H_2/CO_2
Silica/silica/α-alumina	35	7×10^{-7}	17	80	2
	300	2×10^{-7}	6	25	6
Silica/silica-zirconia/α-alumina	35	9×10^{-7}	25	100	2
	300	3.5×10^{-7}	8	16	5

Shelekhin et al. [100] used the microporous silica hollow fibers (PPG Industries, Inc.) as membranes for gas separations. The fiber had a 22 μm inner diameter, 32 μm outer diameter, and a length of 0.135 m. The membranes from the fibers are high temperature and chemically resistant with very competitive transport properties, but the fiber is very brittle to fabricate the membrane module. Selectivity in the hollow fiber membrane was found to be a function of differences in the gas kinetic diameters, and decreased with increasing temperature, as shown in Table 19.

Table 19. Permeation of Gases in Microporous Glass Membranes

Permeation Temp. (°C)	CO_2 Permeance (mol m^{-2} s^{-1} Pa^{-1})	Permselectivity	
		(CO_2/N_2)	(CO_2/CH_4)
30	1.8×10^{-9}	34	1675
100	2.9×10^{-9}	23	780
250	3.1×10^{-9}	7	62

Silica membranes have shown a variety of permeabilities, but for the most part lack good selectivity, as shown in Figure 6 and Figure 7. The exceptions, as discussed above, are the work of Asaeda [99] and Tsai [91], which show the greatest promise for development of practical, CO_2-selective silica membranes.

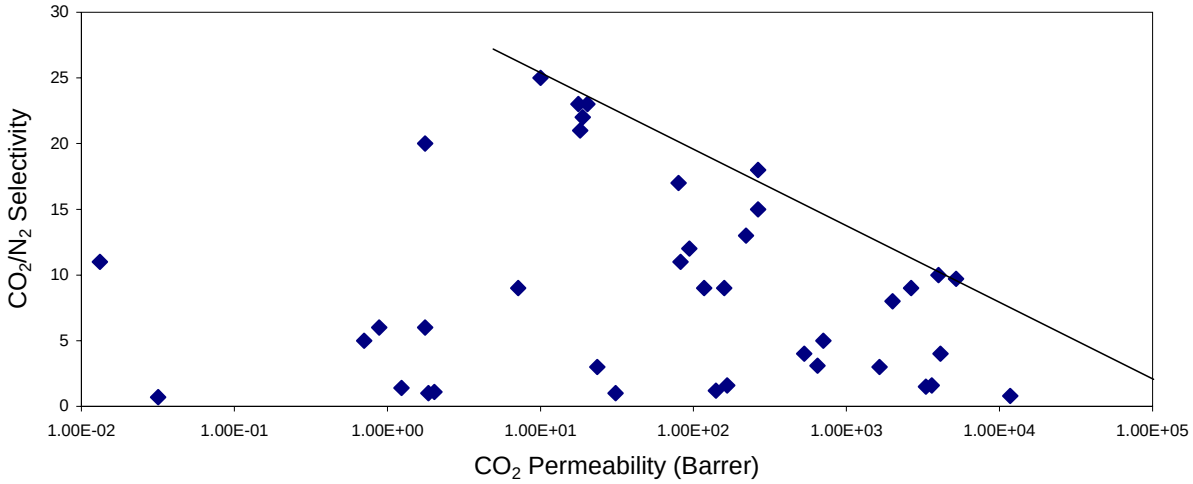

Figure 6. Literature Data for CO_2/N_2 Selectivity vs. CO_2 Permeability for Silica Membranes

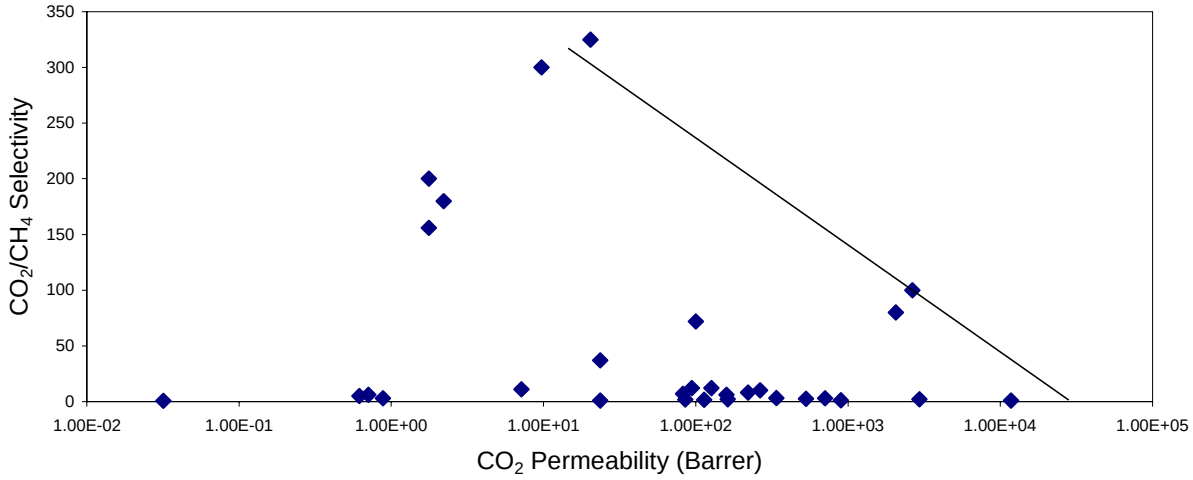

Figure 7. Literature Data for CO_2/CH_4 Selectivity vs. CO_2 Permeability for Silica Membranes

Perovskite Oxide-Type Membranes

Typically, perovskites are of the form ABO_3, where A is a lanthanide element, B is a transition metal, and O is oxygen. The A component and/or the B component may be doped with other materials to enhance the stability and performance of perovskite oxide-type materials. These ion-conductive perovskite-type oxide membranes have been extensively studied for O_2 separations at elevated temperatures. The stability of perovskite type materials at very high temperatures should attract membranologists attention towards CO_2 selective membranes at elevated temperatures.

Kusakabe et al. [101] prepared α-alumina supported $BaTiO_3$ membranes from hydrolysis of $Ba(iso\text{-}OC_3H_7)_2$, and $Ti(iso\text{-}OC_3H_7)_4$ and calcination at 600 °C in N_2, and were hoping to enhance surface diffusion of CO_2 through $BaTiO_3$-impregnated membrane. They observed that the separation factors of CO_2/N_2 were about 1.1 to 1.2, exceeding Knudsen limit of 0.8 for the CO_2/N_2 system, in the temperature range of 100 to 500 °C. These low values of separation factors through $BaTiO_3$-impregnated membranes were caused by the presence of pinholes in the membrane layer.

Hydrotalcite Membranes

Hydrotalcite (HT) compounds consist of layers containing octahedrally coordinated bivalent cations (e.g., Mg^{2+}, Ni^{2+}, Co^{+2}, Zn^{2+}, Cu^{2+}) and trivalent cations (e.g., Al^{3+}, Fe^{3+}, Cr^{3+}), as well as interlayer anions (e.g., CO_3^{2-}, SO_4^{2-}, NO_3^-, Cl^-, OH^-, $[Fe(CN)_6]^{4-}$) and water [102, 103]. Hydrotalcites show a spinel phase ($MgAl_2O_4$) in addition to γ-Al_2O_3 phase and MgO phase. After calcination at higher temperatures, these compounds lose interlayer anions and water to form mixed oxides that can be used as solid base catalysts (e.g., Mg-Al-O) as well as catalyst supports [103, 104]. Mixed oxides, Mg-Al-O, have also been shown to have high surface area and good stability toward heat treatment, making them viable candidates for ceramic membrane

materials.

Mixed oxides, or HTs, should be explored as membrane material to take advantage of the acid-base interaction between acidic CO_2 and the basic sites on HTs, or on mixed oxides for CO_2 separation. However, CO_2 adsorption on the HT surface might become irreversible due to stronger bonding of CO_2 to the stronger basic sites of HT and, hence, it would result in lower CO_2 permeability across the HT membrane.

Several researchers [103, 105-112] have investigated CO_2 adsorption on HTs and mixed oxides, but to our knowledge, no HT/mixed oxide membrane studies have been reported. Yong et al. [110] have investigated the adsorption of CO_2 onto HT-like compounds at elevated temperatures. They observed that the CO_2 adsorption capacity of all HTs higher than 0.30 mmol/g and up to 0.5 mol/kg at 300 °C and 1 bar. Interestingly, they mentioned that the HT layers would be destroyed, due to decarbonation above 300 °C, which would result in micropores in the decomposed HT and in increased surface area and pore volume. Therefore, the decomposition process would enhance the CO_2 adsorption capacity of a HT. It was concluded that the CO_2 adsorption capacity is mainly dependent on the microporous volume, interlayer spacing, and layer charge density of the HT-like compounds. They also reported that the presence of water vapor is favorable for the adsorption of CO_2 onto HTs at high temperature [112].

Ding et al. [107] have also studied high temperature CO_2 adsorption on a HT adsorbent under steam reforming of methane conditions. At 480 °C and in the presence of water vapor, they measured CO_2 adsorption capacity of a HT of 0.58 mol/kg, and also noticed that the capacity was not sensitive to water vapor content in the feed. A chronological decline in the reversible adsorption capacity was also noticed. They used a steam purge to regenerate the adsorbent. Hufton et al. [111] developed a proprietary potassium carbonate promoted hydrotalcite material to remove CO_2 in the steam reforming of methane for H_2 production. They reported a steady state reversible CO_2 adsorption capacity of 0.45 mol/kg at 400 °C by the material after 10 cycles of operation.

Schaper et al. [113] have shown that the calcination (>600 °C) of HT yields high surface area (> 200 m^2/g) and basic mixed oxides, which have improved stability towards heat and steam.

Horiuchi et al. [114] modified alumina by adding basic metal oxides to enhance the CO_2 adsorption at elevated temperatures. They examined several different oxides as modifiers such as oxides of rare earth metals (La, Ce, Nd, Pr), alkaline earth metals (Mg, Ca, Sr, Ba), and alkali metals (Na, K, Rb, Cs). It was observed that CO_2 was adsorbed on the modified alumina even at temperatures above 500 °C. The heat of CO_2 adsorption increased from 80 to 170 kJ mol^{-1} with decreasing electronegativity of the cation used in the modification.

Membrane reactors offer an appealing alternative to combine the water gas shift reaction (WGSR), and CO_2 or H_2 separation in a single step. The combination of reaction and separation in WGSR in IGCC systems is an attractive future option for CO_2 removal, as compared to conventional options [115]. The membrane reactor provides simultaneous removal of H_2 or CO_2 in the WGS reaction to shift the reaction equilibrium towards the complete conversion of CO.

Several researchers [115-118] have utilized the WGS membrane reactor with H_2 removal using palladium or other metallic membranes. Criscuoli et al. [116] have reported a H_2/CO_2 separation

factor of 1.46 at 325 °C from the mesoporous alumina membranes, which is significantly lower than the Knudsen value (4.7), because of the presence of viscous flow at elevated temperatures. Membranes made of HT-like materials or other basic mixed oxides might increase the CO_2 flux through such membranes due to enhanced surface diffusion and could be utilized as support material for a WGS catalyst. Copper-based binary CuO/ZnO and ternary $CuO/ZnO/Al_2O_3$ mixed oxide catalysts have been widely employed in industry for the WGS reaction and proved to be better than traditional iron-based catalysts. Copper-based catalysts operate at lower temperatures, allowing higher thermodynamic conversions. Several researchers [119-121] have employed HT-like compounds as catalysts for the WGS reaction. Gines et al. [120] found that $Cu/ZnO/Al_2O_3$ catalysts were more active than Cu/ZnO catalysts for the WGS reaction, due to the formation of the hydrotalcite structure in the ternary mixed oxides. Petrini et al. [121] and Lima et al. [119] made similar observations for the WGS reaction using HT-like compounds.

Researchers [122-124] from Air Products and Chemical Inc. have developed a sorption-enhanced reaction process (SERP) for carrying out simultaneous reaction and separation of desired products in a single unit operation. They studied different equilibrium controlled reactions using SERP such as the WGSR, the reverse WGSR, and steam reforming. The pressure swing adsorption (PSA) technique was applied to regenerate the CO_2 saturated adsorbent in situ at the reaction temperature. After adsorbent screening, K_2CO_3-promoted hydrotalcite was chosen as a CO_2 adsorbent for the reactions mentioned above. They found that the promoted hydrotalcite was stable over time and maintained an equilibrium CO_2 capacity of 0.3 to 0.45 mmol g^{-1} over nearly 6,000 cycles [123]. Adsorbent stability was tested by repeatedly exposing the hydrotalcite in the cyclic lifetime unit to reaction and regeneration conditions (i.e., 250 psig steam/CO_2 for 20 minutes followed by 5 minutes of N_2 purge at atmospheric pressure, all at 400 to 550 °C). The equilibrium CO_2 capacity was determined at 450 °C and 10 psi CO_2.

It is obvious from above discussion that certain hydrotalcites have the capability to adsorb a large amount of CO_2 at elevated temperatures while maintaining stability over time. Enhanced CO_2 adsorption capacity of HT in the presence of steam at elevated temperatures as well as their thermal stability also makes them very attractive materials for CO_2 selective membranes. It is not inconceivable that the PSA technique could be replaced by hydrotalcite membranes for the WGSR or steam reforming reaction. A membrane reactor would make this a continuous process, as well as save compression costs associated with the PSA process.

Polymeric Membranes

Two types of polymeric membranes are widely used commercially for gas separations. Glassy membranes are rigid and glass-like, and operate below their glass transition temperatures. On the other hand, rubbery membranes are flexible and soft and operate above their glass transition temperatures. Generally, polymeric membranes exhibit inverse permeability/ selectivity behavior; in other words, selectivity to different gas pairs increases as the gas permeability through it decreases [3]. Mostly, rubbery polymers show a high permeability, but a low selectivity, whereas glassy polymers exhibit a low permeability but a high selectivity. Glassy polymeric membranes dominate industrial membrane separations because of their high gas selectivities, along with good mechanical properties. There are not many rubbery polymers other than silicone polymers, particularly poly(dimethylsiloxane) (PDMS), that can be used in gas

separations. Glassy polymers such as polyacetylenes, poly[1-(trimethylsilyl)-1-propyne] (PTMSP), polyimides, polyamides, polyarylates, polycarbonates, polysulfones, cellulose acetate, poly(phenylene oxide), and cardo-type polymers are extensively studied polymeric material for gas separations. Polyimides are one of the most extensively investigated polymer materials for membranes, because most of them exhibit higher gas selectivity as well as higher gas permeability compared to many other glassy polymers [14]. They impart good mechanical properties along with higher chemical and thermal stability in resulting membranes. Structural modifications are required to enhance the permeation properties of polyimides.

Gas transport in polymeric membranes is affected by several polymer properties, such as morphology, free volume content, intersegmental chain spacing (d-spacing), orientation, cross-linking, polymer polarity, defects, thermal processing history, glass transition temperature, average molecular weight, molecular weight distribution, composition, degree of crystallization, types of crystallites, etc. The presence of crystalline domains in a polymer adds a tortuosity factor to gas diffusion and, thus, makes gas transport more complicated. The free volume present in polymers can be visualized as microvoids or holes dispersed in the polymeric matrix. The penetrant condensability can be calculated from the critical temperature, the boiling point, and the Lennard-Jones potential force constant of the penetrants. Chemical affinity can be defined as the interaction between the gas and polymeric matrix. Stronger interactions between a gas and the functional groups of a polymer result in higher solubility of that gas in the polymer. Therefore, CO_2, which has a quadrupolar moment, is highly soluble in polar polymers. Condensability also plays an important role in gas permeation through polymeric membranes. Condensability (in °K) and kinetic parameters (in A) for gases of interest are [125]: He (10.2, 2.69), H_2 (60, 2.8), CO_2 (195, 3.3), O_2 (107, 3.46), N_2 (71, 3.64), and CH_4 (149, 3.87). Hydrogen is more permeable than the smaller helium in amorphous polymeric membranes, due to its higher condensability.

Rubbery Polymeric Membranes

Merkel et al. [126] studied the permeability of PDMS and poly(1-trimethylsilyl-1-propyne) (PTMSP) for a simulated syngas feed containing 42 percent H_2, 46 percent CO, 10.5 percent CO_2, and 1.5 percent H_2S at temperatures up to 240 °C. They found that the PDMS and PTMSP membranes were more permeable to the more condensable gases, such as CO_2 and H_2S compared to H_2 at 25 °C, however, both membranes became H_2 selective at elevated temperatures. (Shown in Table 20.) Rubbery PDMS and high free volume, glassy PTMSP membranes behaved differently with increasing permeation temperature. Permeability decreased with increasing temperature for all gases except H_2 in PTMSP membranes, whereas it increased with temperature in PDMS membranes. They attributed this distinct behavior to accelerated physical aging of PTMSP membranes at high temperatures.

Table 20. Gas Permeation from a Simulated Syngas Mixture

Membrane Type	Temp.(°C)	CO_2 Permeability (Barrer)	Separation Factor		
			(CO_2/H_2)	(CO_2/CO)	(H_2S/H_2)
PDMS	25	3200	3.4	6.4	5.4
	70	3400	1.7	3.5	2.6
	120	3800	1.1	3.6	1.5
	150	4300	0.9	3.9	1.0
PTMSP	25	19000	1.6	3.7	1.8
	70	11000	1.0	2.4	1.2
	150	3400	0.6	2.3	0.8
	240	2000	0.4	1.9	0.5

Polyphosphazenes are hybrid polymers that consist of highly flexible inorganic phosphorus-nitrogen backbone with two functional groups attached to each phosphorus. The inorganic backbone provides thermal and chemical stability to the polymer. They are thermally stable up to 400 °C [125]. Orme et al. [125] investigated polyphosphazenes with three different functional groups of different hydrophilicity for the gas separation. Functional groups attached are 2-(2-methoxyethoxy)ethanol (MEE) to provide a polar hydrophilicity, 4-methoxyphenol (4MP) to provide hydrophobicity and film forming abilities, and 2-allylphenol (2AP) for cross-linking. Table 21 summarizes permeation results from different polyphosphazenes membranes with varying relative amounts of each functional group on the backbone. CO_2 permeability increased linearly with the amount of hydrophilic MEE on the polymer backbone. They attributed this behavior to strong intermolecular interaction between CO_2 and the MEE group. Other gases (H_2, N_2, and CH_4) are believed to have a very limited interaction with the polymer membrane, and transport of these gases occurred due to segmental chain motion.

Table 21. Results from Different Polyphosphazenes Membranes

No.	Composition (%)[a]			Permeability of CO_2 (Barrer)	Permselectivity		
	MEE[b]	4MP[c]	2AP[d]		CO_2/N_2	CO_2/CH_4	CO_2/H_2
1	6	75	19	9.3	31.0	6.6	2.2
2	23	72	5	38.9	21.6	10.8	2.9
3	25	59	16	81.9	29.3	11.5	4.2
4	38	46	16	107.7	27.6	7.7	4.2
5	48	48	4	115.9	14.0	7.2	4.9
6	74	24	2	226.7	22.2	11.8	7.9
7	100	0	0	250.0	62.5	22.7	10.0

[a]Percentages of sites on the backbone occupied by each functional group; [b]2-(2-methoxyethoxy)ethanol; [c]4-methoxyphenol; [d]2-allylphenol.Permeation temperature 25 °C.

Stern et al. [127] found that the permeation properties of a given permeant can be significantly improved by substitution of a suitable functional group in the polymer that will induce specific interactions with the permeant. Such interactions primarily increase the solubility of the permeant in the polymer. Polysiloxanes membranes exhibit a high permeability accompanied by a low selectivity. Ashworth et al. [128, 129] have studied the effect of a side-chain ester functionality in polysiloxane membrane on the permeation properties of CO_2, CH_4, and N_2. They reported that there was little change in the relative diffusivity of CO_2 to CH_4 (or N_2) at 35 °C with an increase in ester functionality, but the higher permselectivity of CO_2/CH_4 or CO_2/N_2 resulted from an increase in the relative solubility of CO_2 to CH_4 (or N_2).

Glassy Polymeric Membranes

Matsumoto et al. [130] synthesized two hexafluoro-substituted aromatic polyimides, 6-FDA-p-PDA and 6FDA-4,4'-ODA, for gas permeation studies. They achieved higher gas permeabilities through 6FDA polyimides, compared with PMDA polyimides, while high permselectivities of 6FDA polyimides were maintained. (See Table 22.) They suggested that a helix configuration contributes to the increase in the free volume of the polymer, due to the bulky $-C(CF_3)_2-$ group in the polymer backbone, hence, it controls the gas diffusivity.

Table 22. Summary of Results from FDA Membranes

Membrane	Permeation Temp (°C)	CO_2 Permeability (Barrer)	Permselectivity	
			(CO_2/N_2)	(CO_2/CH_4)
6FDA-p-PDA polyimide	25	35	29	70
6FDA-4,4'-ODA polyimide	25	21	42	75

Costello et al. [131] studied polypyrrolone material, hexafluorodianhydride-3,3',4,4'-tetraaminodiphenyl oxide (6FDA-TADPO), for membrane-based gas separations at elevated temperatures. They discussed the loss of permselectivities of various gas pairs with increasing temperature in terms of both solubility selectivity and diffusivity selectivity. They observed that the solubility selectivity of gas pairs with the 6FDA-TADPO membrane was almost unaffected with increasing temperature. Therefore, the loss of permselectivities entirely resulted from the loss of the diffusivity selectivity at elevated temperature. It was concluded that the diffusivities of larger molecules benefit more from increased polymer chain motion due to increasing temperature. The CO_2/CH_4 (size difference 0.5 A) permselectivity decreased more rapidly with increasing temperature than the CO_2/N_2 (size difference 0.34 A) permselectivity.

H. Kawakami et al. [132] have synthesized thermally cured aromatic polyimide membranes from 2,2'-bis(3,4-dicarboxyphenyl) hexafluoropropane dianhydride (6FDA) and 3,3'-diaminodiphenylsulfone (m-DDS) to elucidate the effect of membrane microstructure on the gas permeation properties. The 6FDA-m-DDS membranes were prepared by the solvent-casting method and then cured at 150, 200, and 250 °C. The authors observed a steep increase in the CO_2/CH_4 permselectivity with increasing the curing temperature while only a slight increase in CO_2/N_2 permselectivity. (See Table 23.) The increase in permselectivities for the 6FDA-m-DDS membrane was a result of an increase in diffusivity selectivities of gases by increasing the

curing temperature, because the solubility selectivities were independent of the curing temperature. It was concluded that the formation of charge transfer complexes in the 6FDA-m-DDS membrane with increasing curing temperature increased the packing density of the polymer chain and decreased the free volume, thereby leading to an increase in diffusivity selectivities. However, the gas permeabilities were very low through the 6FDA-m-DDS membrane.

Table 23. Effect of Polymeric Properties on Gas Permeation

Curing Temp (°C)	ρ (g/cm^3)	Free Volume	CO_2 Permeability (Barrer)	Permselectivity		Diffusion Selectivity		Solubility Selectivity	
				CO_2/N_2	CO_2/CH_4	CO_2/N_2	CO_2/CH_4	CO_2/N_2	CO_2/CH_4
150	1.469	0.156	2.2	25	42	0.82	12	30.0	33.5
200	1.480	0.150	2.0	30	72	1.03	21	30.5	34.1
250	1.484	0.148	1.5	30	116	0.90	33	31.5	35.3

Permeation temperature 25 °C.

Polyimides are very attractive materials for gas separation membranes because of their good gas separation and physical properties, such as high thermal stability, chemical resistance, mechanical strength, and low dielectric constant. However, problems associated with the swelling and plasticization of polyimides can limit its applications in the gas separation area. The polymer matrix swells upon sorption of CO_2 present in the feed, escalating the permeation of other species in the feed. Hence, the polyimide membrane loses its selectivity. Cross-linking the polyimides can solve the plasticization or swelling problem, and it can enhance the permeability properties of the polyimide membranes [133-141].

Staudt-Bickel et al. [136] synthesized uncross-linked and cross-linked polyimides to investigate the effect of the degree of cross-linking on swelling and plasticization due to CO_2. They used 6FDA as a dianhydride monomer and mPD (m-phenylene diamine) and DABA (diamino benzoic acid) as diamine monomers for the polymerization reaction. They observed reduced plasticization from a copolyimide containing a strong polar carboxylic acid (DABA) for CO_2 pressure up to 14 atm. The reduction was attributed to psuedo-cross-linking because of hydrogen bonding between the carboxylic groups. It was reported that the swelling effects caused by CO_2 could be reduced up to 35 atm CO_2 feed pressure by chemical cross-linking of the free carboxylic acid groups of the 6FDA-mPD/DABA 9:1 with ethylene glycol (EG). (See Table 24.) They also observed an increase in CO_2/CH_4 selectivity with increasing degree of cross-linking. Interestingly, CO_2 permeability was not significantly affected by cross-linking that used EG, because the reduced chain mobility created by cross-linking was compensated by additional free volume caused by the cross-links.

Table 24. Effect of Cross-Linking on the Performance of Polyimide Membranes

Membrane	CO_2 Permeability (Barrer)[d]	Permselectivity		S.F. (CO_2/CH_4)[b]	
		(CO_2/N_2)	(CO_2/CH_4)	4 atm[c]	18 atm[c]
6FDA-mPD	11.03	27	58	40	1
6FDA-mPD/DABA 9:1	6.53	26	65	45	45
6FDA-mPD/DABA 9:1 (cross-linked)	9.50	35	63	48	48
6FDA-DABA (cross-linked)	10.40	26	87	70	70

[a]Feed temperature: 35 °C and feed pressure: 3.64 atm, otherwise mentioned; [b]Feed: CO_2 and CH_4 equimolar mixture; [c]Feed Pressure; [d]Pure gas permeability. S.F. = Separation Factor

Multilayer composite membranes can be prepared in two different ways [142]: (A) by selective layer/gutter layer/support substrate, and by (B) sealing layer/selective layer/support substrate [142-145]. In the A type structure, the gutter layer, which is also permeable, serves as a channeling and adhesive medium between the selective layer and the support substrate. In the B type structure, the permeable sealing layer is applied to plug the remaining defects in the coated selective layer. Shieh et al. [143] prepared the B type multilayer composite membrane, where they had silicone rubber (SR) as the sealing material, poly(4-vinylpyridine) (P4VP) as the selective layer, and polyetherimide (PEI) hollow fibers as the support substrate. The PEI hollow fibers prepared from a PEI/PEG/ NMP (23/0/77) spinning dope and coated with 0.2 percent by weight P4VP and 3 percent by weight SR solutions gave CO_2 permeance of 2.5 x 10^{-9} mol m^{-2} s^{-1} Pa^{-1} at 25 °C with permselectivities of CO_2 /N_2 = 21, CO_2/CH_4 = 62, and H_2/CO_2 = 6. Composite hollow fiber membranes, P4VP/ PEI, exhibit a Knudsen mechanism, suggesting that a perfect thin P4VP layer did not form on the PEI hollow fibers without SR, which was the sealing layer material.

It has been extensively reported in the literature that aromatic polyimides containing –$C(CF_3)_2$– groups in their dianhydride moieties (e.g., 6FDA-based polyimides) have been identified as more gas-selective, particularly towards CO_2 relative to CH_4 and N_2, than other glassy polymers with comparable permeabilities [3]. Gas transport properties of 6FDA-based polymers are summarized in Table 25. Gas permeability properties of different polyimides, which were synthesized from the reactions of various diamines containing biphenyl, diphenyl, diphenylmethane, phenylether, diphenyl sulfone, or diphenyl sulfide with BPDA, 6FDA, or PMDA, are also discussed by Hirayama et al. [146]. They investigated the relation of gas permeabilities, diffusivities, and solubilities with the structures of various polyimide films. It was concluded that the diffusivities of amorphous polyimides do not correlate with the intersegmental spacing parameters (d-spacing and fractional free volumes), particularly for polyimides containing polar substituents.

Table 25. Summary of Results from Different Polymeric Membranes[a]

Ref.	Membrane	CO_2 Permeability (Barrer)	Permselectivity	
			CO_2/N_2	CO_2/CH_4
[223]	6FDA-1,5-NDA[b]	23	21	49
[224]	6FDA-6FpDA[c]	56	26	40
[225]	6FDA-durene	456	13	
	6FDA-durene/2,6-DAT[d](75:25)	220	14	
	6FDA-durene/2,6-DAT (50:50)	117	14	
	6FDA-durene/2,6-DAT (25:75)	67	16	
	6FDA-2,6-DAT	34	19	
[226]	6FDA-durene	456	13	16
		547[e]	15	17
		678[f]	18	20
		317[g]	15	19
[133]	6FDA-durene[h]	30	10	
[227]	6FDA-TAPA[j, k]	11[i]	33	50
	6FDA-TAPA[l]	65[i]	30	41
	6FDA-TAPA[l]	47[a]	23	
	6FDA-TAPA[m]	6.7[i]	27	61
[228]	6FDA-APPS[n]	9.1[i]	29	39
[138]	6FDA-IPDA[o]	25	21	37
	6FDA-IPDA[p]	20	20	40
[229]	6FDA-IPA[q]	9	21	45
	6FDA-TBI[r]	43	17	24

[a]Feed pressure: 10 atm; temperature 35 °C; [b]poly(1,5-naphthelene-2,2'-bis(3,4-phthalic) hexafluoropropane) diimide; [c]6FDA-4,4'-(hexafluoroisopropylidene) dianiline; [d]2,6-diaminotoulene; [e]Feed pressure: 5 atm; [f]2 atm; [g]After 280 days of aging; [h]Cross-linking modification by immersing the dense films in p-xylenediamine for 30 mins; [i]Feed pressure: 1 atm; [j]6FDA-tris(4-aminophenyl)amine (TAPA); [k]amine-terminated and ethylene glycol diglycidyl ether (EDGE)-cross-linked (content of EDGE = 0.34 mmol/g of polymer); [l]amine-terminated and terephthaldehyde (TPA)-cross-linked (content of TPA = 0.25 mmol/g of polymer); [m]anhydride-terminated and 4,4'-diaminodiphenyl ether (ODA) –cross-linked (content of ODA=0.04 mmol/g of polymer); [n]6FDA-bis[4-(4-aminophenoxy)phenyl]sulfone (APPS); [o]6FDA-4,4'-isopropylidene dianiline (IPDA); [p]Cross-linked with 5% 6FDA-diacetylene by thermally annealing at 240 ℃ for 4 hr; [q]6FDA-isophthalamides (IPA); [r]6FDA-5-t-butylisophthaloyl (TBI).

Suzuki et al. [147] prepared composite hollow fiber membranes composed of a thin and dense outer-layer of BPDA-PEO/ODA polyimide and a sponge-like layer of BPDA-ODA/DABA polyimide. The 1 mm thick outer layer was responsible for the gas separations. They observed very similar results from mixed gas permeation, as well as from pure gas permeation, as shown in Table 26. The CO_2 permeance and the CO_2/N_2 permselectivity decreased 40 percent and 10 to 20 percent, respectively, in a month after the membrane preparation. It was concluded that the reduction of membrane performance was caused by densification of the inner layer at the

interface to the outer layer, which might be caused by a plasticization effect of the PEO-containing polyimide. Hence, the interface of the inner layer might become very dense and act as an additional layer. However, the membrane performance did not change much subsequent to the first month.

Table 26. Performance of the Composite Hollow Fiber Membranes for CO_2/N_2 Separation [a]

Membrane Thickness (μm)	Permeation Temp (°C)	CO_2 Permeance[b] (mol m^{-2} s^{-1} Pa^{-1})	CO_2/N_2 Separation	
			Permselectivity	Separation Factor
2.0	25	5.4×10^{-9}	73	69
	35	7.7×10^{-9}	55	53
	50	1.2×10^{-8}	37	36
	50[c]	1.9×10^{-8}	46	
1.1	25	9.7×10^{-9}	52	50
	35	1.3×10^{-8}	44	44
	50	2.0×10^{-8}	33	33
	50[c]	3.4×10^{-8}	37	
	50[d]	1.9×10^{-8}	35	
0.93	25[e]	9.7×10^{-9}	54	
	50[e]	2.2×10^{-8}	33	
	50	2.3×10^{-8}	33	29
	50[c]	4.1×10^{-8}	39	

[a]Measured at feed pressure of 2 atm by a high vacuum method in one month after membrane preparation; [b]Pure gas (CO_2) permeance is given here, mixed gas permeances are very similar to pure gas permeances; [c]Measured at feed and permeate pressure of 10 and 1 atm, respectively, in a few days after membrane preparation; [d] Measured at feed and permeate pressure of 10 and 1 atm, respectively, in one month; [e]Measured at feed pressure of 2 atm by a high vacuum method in five months after membrane preparation.

Tokuda et al. [148] developed a Cardo polyimide polymeric membrane, which gave higher CO_2/N_2 permselectivities than those of other polymeric membranes. Cardo polyimides have some specific characteristics, such as high gas permeability, high heat resistivity, and a high solubility in organic solvents. Cardo polyimides, particularly those with 3,3',4,4'-benzophenonetetracarboxylic dianhydride as a monomer (PI-BT), gave highest CO_2/N_2 permselectivity. Cardo polyimide (PI-BT-COOMe), which contains CO_2-affinitive methylcarboxyl functionality, gave a CO_2/N_2 permselectivity of 52, with a CO_2 permeance of 15 Barrer at 25 °C. The CO_2/N_2 permselectivity was improved by introducing a CO_2 affinitive functional group on the Cardo constitution. Tokuda et al. also used a wet-spinning method to produce asymmetric hollow fibers with defectless inner skin layers from PI-BT-COOMe. These hollow-fiber membranes gave a maximum CO_2/N_2 permselectivity of 40, with a permeance of 1.5×10^{-4} cm^3(STP) cm^{-2} s^{-1} $cmHg^{-1}$ (~500 Barrer if membrane thickness of 35 μm was used [K. Haraya, pers. comm., 2001]) at 25 °C, and a good mechanical strength.

The term "Cardo-polymers" was proposed in 1971 by Korshak [148] to designate at least one

part of the constitutive unit, which carries a lateral ring connected to the main macromolecular backbone by a quaternary carbon atom. The presence of Cardo groups induces some specific properties to all polymers, including such groups. Thermal characteristics, glass transition temperature, and heat resistance are the characteristics of rigid macromolecules, but with significantly enhanced solubility in organic solvents and high transition temperatures.

Bos et al. [137] carried out the cross-linking of Matrimid films by a thermal treatment at 350 °C to control the CO_2-induced plasticization. They observed that the plasticizing effect accelerated the permeation of CH_4 for CO_2/CH_4 gas mixtures in the untreated membrane, whereas, CO_2 and CH_4 permeabilities remained constant for heat-treated Matrimid films at elevated feed pressures.

It has been reported [149-151] that poly(ethylene glycol) (PEG) can dissolve substantial amounts of acidic gases, and the gas diffusivity in the PEG segment may be high, since the chain is flexible. It is very difficult to obtain a thin film of PEG with mechanical and thermal stability. Therefore, highly stable membranes are obtained by blending PEG with other polymers, where the PEG segment provides high permeability coefficients and high permselectivities, and the other polymers provides robustness to the membranes. Li et al. [152] prepared poly(ethylene glycol) (PEG)/cellulose acetate (CA) blended membranes for gas permeation studies. (See Table 27.) The apparent solubility coefficients for CO_2 were decreased by blending PEG20000 (average molecular weight of 20,000). The blended membranes containing PEG showed high apparent CO_2 diffusivity coefficients, resulting in high permeability coefficients for CO_2 compare to that of the CA membrane. It was concluded that the flexible main chain of PEG20000 in the amorphous domains in the blends allowed large penetrants, CO_2, and CH_4, to diffuse easily through the blended membranes, resulting in higher permeance of CO_2 and CH_4 relative to that of N_2. Therefore, the CO_2/CH_4 permselectivities decreased by blending of PEG20000 with CA.

Table 27. Effect of PEG on Gas Permeation in its CA Blend Membranes

Membrane	Permeation Temp. (°C)	CO_2 Permeability (Barrer)	Permselectivity	
			(CO_2/N_2)	(CO_2/CH_4)
CA	30	5	30	29
	80	10	8	14
CA + 30 wt% PEG20000	30	6	32	26
	80	20	14	12
CA + 60 wt% PEG20000	50	5	27	10
	80	225	17	3

Hirayama et al. [9] prepared cross-linked polymer films having high poly(ethylene oxide) (PEO) content by photo polymerization from mono- and dimethacrylate containing PEO. The authors attributed the high CO_2/N_2 permselectivity to the high solubility selectivity due to the affinity of the PEO segment for CO_2. The CO_2 permeability increased as the fractional free volume was increased by increasing the PEO content in the cross-linked chains. The highest CO_2

permeability of 510 Barrer was obtained at 50 °C for DM69/MM9(90/10) film with a CO_2/N_2 permselectivity of 36. DM69/MM9(90/10) was prepared from the mixture of poly(ethylene glycol) dimethacrylate (DM) and poly(ethylene glycol) methyl ether methacrylate (MM) in the weight ratio of 90/10, where 69 or 9 is an average number of repeating units of ethyleneoxide. The permselectivity CO_2/N_2 was unchanged for different polymer films and stayed around 65 and 35 at 25 °C and 50 °C, respectively. The authors observed a non-linearity in the Arrhenius type plots for the CO_2 permeability. They attributed this abnormal behavior to the films with much longer blocks of PEO, which were partially crystallized at low temperatures, resulting in a large decrease in CO_2 permeability. It was also reported that the introduction of phenylene rings to the polymer chain decreased CO_2 permeability and CO_2/N_2 permselectivity, because of both reductions in the segmental motion and in the affinity of PEO for CO_2.

Kim et al. [153] prepared pore-filled membranes using polyacrylonitrile membrane as a support and methoxy poly(ethylene glycol) acrylate (MePEGA) as a filling material by UV-irradiated photografting. They reported high CO_2/N_2 permselectivity (32.5) with very low CO_2 permeability (5.65×10^{-4} Barrer) from this pore-filled membrane at a temperature of 30 °C. They attributed the high CO_2 permselectivity of the membrane to the high solubility selectivity due to the affinity of CO_2 to the PEO content of the membrane.

M. Kawakami et al. [154] also reported cellulose nitrate/PEG blend membranes having up to 50 percent by weight of PEG. These membranes showed CO_2 permselectivities of 29 to 38, with CO_2 permeabilities of 1.4-8.2 Barrer. The permeability and CO_2 permselectivity of cellulose nitrate/PEG blended membranes increase appreciably with increasing PEG fraction. The significant increase in CO_2 permeability was attributed to the increments to both diffusivity and solubility of CO_2. It has been interpreted that an increase in diffusivity results from the spreading effect of the PEG plasticizer on the polymer chain.

Okamoto et al. [155, 156] investigated gas permeation properties of poly(ether imide) segmented copolymer films prepared from polyether-diamine, comonomer diamine, and acid anhydride. They reported that the poly(ether imide) segmented copolymers have microphase-separated structures consisting of microdomains of rubbery polyether segments (for the gas permeation) and of glassy polyimide segments (for the mechanical properties and film forming ability). The copolymer films having PEO content of about 70 percent by wt displayed high CO_2 permeance (140 Barrer) with a CO_2/N_2 permselectivity of 70 at 25 °C. The PEO containing polyimide membranes have also been reported to exhibit both high permeability of CO_2 (75 Barrer) and high separation factor of CO_2/N_2 (=65) at 25 °C for a CO_2-N_2 mixture containing 18 percent CO_2. They attributed the high permselectivity to the high solubility selectivity resulting from the affinity of CO_2 to PEO segments.

Lehermeier et al. [157] introduced a new polymeric membrane material, poly(lactic acid) (PLA), which is being produced from a renewable feedstock (corn) rather than fossil resources. At 30 °C, CO_2 permeability in PLA was 10.2 Barrer with CO_2/N_2 and CO_2/N_2 permselectivities of 8 and 11, respectively. The separation factor for a CO_2/N_2 mixture was similar to CO_2/N_2 permselectivity. The authors suggested that more studies of PLA as a membrane material are needed to explore its permeation properties in detail.

Recently, several attempts have also been made to predict gas permeability and permselectivity

in polymeric materials [158-160]. Park et al. [160] used a modified free volume based group contribution method for predicting the permeability of six common gases (He, H_2, O_2, N_2, CH_4, and CO_2) in glassy polymers. The method predicts the polymer density and uses a modified estimate of a free volume specific to each gas. The various empirical group contribution factors in the model were deduced from a database of specific volume and permeability for over one hundred glassy polymers. Robeson et al. [158] also used a group contribution theory to predict permeability and permselectivity of aromatic polymers chosen from the classes of polysulfones, polycarbonates, polyarylates, poly(aryl ketones), and poly(aryl ethers). They did not follow the fractional free volume approach described by Park et al. [160], but instead utilized two other variables: the molar volume and the permeability contribution of each subunit. Unfortunately, their study was only limited to the O_2/N_2 and He/N_2 gas pairs. Alentiev et al. [161] also used the group contribution method for prediction of gas permeation parameters (permeability and diffusion coefficients) of glassy polymers. They deduced the group contributions from a database, including about 120 polyimides prepared from nine different dianhydrides, and about 70 diamines.

Most polymer membranes with high permselectivity have disappointingly low fluxes. This is illustrated in Figure 8 and Figure 9, which show an upper bound in the relationships between the CO_2/N_2 and CO_2/CH_4 selectivities, respectively, and the permeability of CO_2 for various glassy and rubbery polymers. This indicates that although the polymer is efficient at separating molecules, diffusion through the membrane is slow, resulting in little economic benefit.

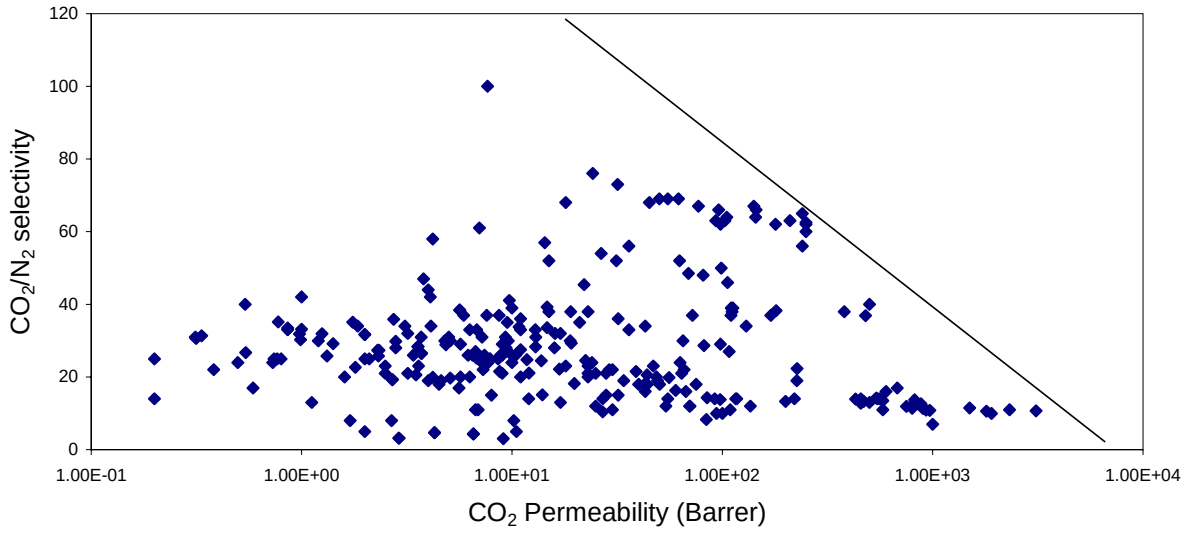

Figure 8. Literature Data for CO_2/N_2 Selectivity vs. CO_2 Permeability for Polymeric Membranes

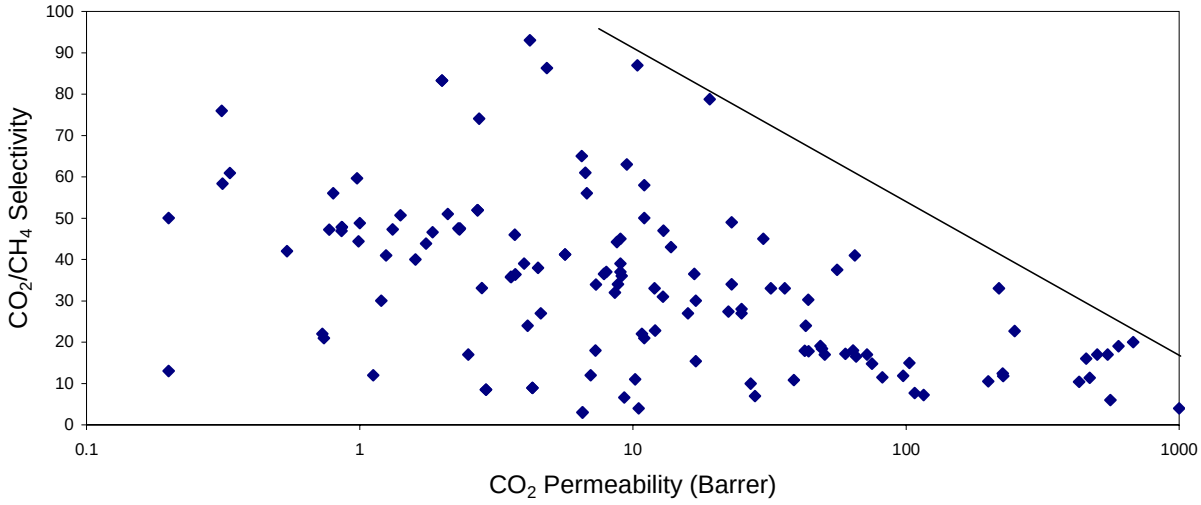

Figure 9. Literature Data for CO_2/CH_4 Selectivity vs. CO_2 Permeability for Polymeric Membranes

Hybrid Membranes

Nonporous polymeric membranes give high selectivity but poor permeability. On the other hand, porous inorganic membranes give high permeability but poor selectivity. For better results, both selectivity and permeability in a membrane should be balanced. There have been several studies that attempted to introduce organic affinities for the particular gas on inorganic membrane surface. The introduction of organic functional groups sometimes contributes to the modification of the molecular structure of the material, which results in favorable selectivity or permeability. Membrane microstructure can be controlled by either the degree of cross-linking, or the interstitial space occupied by the organic functional groups in the composite material.

Hybrid materials in which polymers and ceramics are dispersed at a molecular level have been investigated as gas separation membranes. A combination of the sol-gel reaction and polymerization is used to synthesize the hybrid material [162]. Resulting hybrid materials present the advantages of each material; for example, the flexibility and selectivity of polymers and thermal stability of ceramics. Among these hybrid materials, polyimide-silica materials have received the most attention for the gas permeation studies. Composite organic-inorganic membranes have become an expanding field of research as the introduction of organic molecules can improve the characteristics of a matrix.

Okui et al. [162] prepared porous hybrid membranes from monoalkyltrimethoxysilane using the sol-gel technique. All these hybrid membranes were formed on porous α-alumina supports. They introduced some functional groups, such as methyl, propyl, 3-chloropropyl, octadecyl, 3,3,3-trifluoropropyl, and phenyl, to study the effect of CO_2 affinity to these functional groups on the permeability properties of the resulting materials. They found that the phenyl group has stronger affinity with CO_2 than others do and, hence, the higher CO_2/N_2 permselectivity of 6 was achieved from the hybrid membrane containing a phenyl group. They also reported that these

functional groups were stable at higher temperatures. The phenyl group remained intact even at 400 °C.

Silica-polyimide hybrid membranes were also prepared on γ-alumina coated α-alumina support tubes [163]. Polyamic acid was synthesized by dehydration condensation of PMDA and ODA, and was mixed with silica sols at various ratios. After coating of the hybrid sols on a porous tube, imidization was conducted at 350 °C to form a defect-free thin silica-polyimide microcomposite membrane. The permeance of gases increased with increasing temperature and, therefore, the permeation of hybrid membranes was governed by the dissolution-diffusion mechanism through the polymeric zone in the membrane. (See Table 28.) Carbon dioxide permeance decreased somewhat with increasing permeation temperature for a hybrid membrane with the silica content of 81 percent. Surface diffusion of CO_2 through the silica zone contributed to the permeance of membranes with high silica contents, and was limited at high temperatures.

Table 28. Effect of Silica Content on the Permeation of Composite Membranes

Permeation Temp. (°C)	Silica Content (%)	CO_2 Permeability (mol m^{-2} s^{-1} Pa^{-1})	Selectivity (CO_2/N_2)
30	100	8×10^{-7}	3
	81	1.2×10^{-7}	15
	68	1.5×10^{-8}	25
	34	8×10^{-9}	27
	0	1×10^{-9}	17
100	100	6×10^{-7}	1.5
	81	1.4×10^{-7}	5
	68	3×10^{-8}	15
	34	1.6×10^{-8}	13
	0	2×10^{-9}	14
300	100	3×10^{-7}	1.1
	81	8×10^{-8}	1.8
	68	3.2×10^{-8}	6.4
	34	1.8×10^{-8}	2.3
	0	7×10^{-9}	5

Joly et al. [164] also showed that the presence of silica drastically increases the gas permeation properties in the hybrid composite membranes. They prepared the polyimide-silica membranes containing 32 percent silica by adding TMOS to polyamic acid solution and subsequently imidizing at 300 °C. The results were analyzed in terms of the dual sorption model. In this model, it is assumed that the gas molecules dissolved in the polymer can be distributed in two distinct populations: (A) Henry type dissolution and (B) Langmuir type sorption. Higher permeability of CO_2 (2.8 Barrer) and CO_2/N_2 selectivities (CO_2/N_2 = 22 and CO_2/CH_4 = 14) were observed with the hybrid membrane compared to those of polyimide membrane (1.8 Barrer;

CO_2/N_2 = 18 and CO_2/CH_4 = 18). The differences in gas permeation between the hybrid and the polyimide membrane were attributed to an increase in the sorption ability associated with an increase in contribution due to Henry's type dissolution. They also conclude, based on the membrane characterization using XRD and electron micrograph, that the addition of TMOS to the polyamic acid induces the imidization rate changes and some morphological modifications in the polymer matrix along with the formation of a heterogeneous material.

In a different study Joly et al. [18] have studied the effect of the permeation temperature and silicon content on the gas transport properties of the hybrid composite membranes. They observed a considerable increase in the CO_2 permeance with an increase in the silica content due to its high solubility in the composite material. (See Table 29.) They also reported that the permeability activation energies decreased when the silica content of the hybrid membranes increased. An increase in permeabilities and in temperature were observed, while selectivities (CO_2/N_2 and CO_2/CH_4) considerably decreased at higher temperatures.

Table 29. Effect of Silica Content on the Permeation of Composite Membranes

Ref.	Permeation Temp. (°C)	Silica Content (%)	CO_2 Permeability (Barrer)	Permselectivity	
				(CO_2/N_2)	(CO_2/CH_4)
[18]	50	0	0.80	20	40
		25	1.20	30	40
		60	1.50	30	30
		72	2.03	20	26
[165]	25	0	122	71	
		10	154	72	
		19	205	75	
		27	277	79	
	85	19	507	44	

The organic-inorganic hybrid membranes of poly(amide-6-b-ethylene oxide) (PEBAX) and silica were prepared by Kim et al. [165] via in situ polymerization of TEOS using the sol-gel process to perform their gas transport investigation. The PEBAX copolymer consisted of two distinct regions, the impermeable crystalline polyamide phase, and the permeable amorphous polyethylene phase [166]. A high permeability and a high selectivity were observed from the PEBAX copolymer for polarizable/nonpolar gas pairs [166]. Using the wide-angle x-ray diffraction (WXAD) technique, the authors showed that the crystallinity of the polyamide phase was significantly reduced by the introduction of silica particles [165]. They reported that the hybrid membranes exhibited higher gas permeability coefficients and permselectivities than the PEBAX alone, particularly at elevated temperatures. (See Table 29.) The gas permeabilities and permselectivities increased with the silica content of the hybrid membranes. It was concluded that the high permeability and permselectivity increases of the hybrid membranes arose from the strong interaction between CO_2 molecules and the residual hydroxyl groups on the silica domain,

additional sorption sites in polyamide block of PEBAX, and the organic/inorganic interface.

Hybrid composite gas-separation membranes have been prepared by Smaihi et al. [167] using a microporous polyacrylonitrile substrate and a thin organic-inorganic sol-gel layer as a permselective coating. The thin sol-gel layers were obtained from co-hydrolysis of an organoalkoxysilane - diphenyldimethoxysilane (DPMOS) or phenyltrimethoxysilane (PTMOS) - and TMOS. It was shown, based on several analytical techniques (SAXS, solid-state NMR, and DSC), that these hybrid networks were homogeneous at the molecular level. CO_2 permeation was increased in the DPMOS-TMOS membrane with increasing organoalkoxide molar ratio (DPMOS or PTMOS/(DPMOS or PTMOS+TMOS)), while it was decreased in the PTMOS-TMOS membrane. (See Table 30.) The increase in CO_2 permeation in DPMOS-TMOS was proportional to the phenyl group concentration of the membrane material. They attributed the decrease in CO_2 or N_2 permeation in PTMOS-TMOS membranes to the increase in connectivity of the network with the molar composition in these membranes. The connectivity of DPMOS-TMOS membranes remained the same with the composition, while it increased in PTMOS-TMOS membranes. The transport of CO_2 through these hybrid membranes was due to the surface diffusion mechanism. They observed the highest permselectivity of CO_2/N_2 with PTMOS-TMOS (molar composition 81 percent) and attributed this high selectivity to the enhanced chemical affinity between CO_2 and the membrane structure, due to an increased content of phenyl groups in the material.

Table 30. Permeation through Composite Membranes as a Function of the Organoalkoxide Molar Proportion

Membrane	Organoalkoxide Molar Composition (%)	CO_2 Permeance (mol m^{-2} s^{-1} Pa^{-1})	Selectivity (CO_2/N_2)
PTMOS/TMOS	54	6×10^{-6}	4
	63	4×10^{-6}	4
	72	3×10^{-6}	6
	81	2×10^{-6}	14
DPMOS-TMOS	27	6.6×10^{-6}	2
	36	10×10^{-6}	2.5
	54	13×10^{-6}	2.5

Permeation temperature 25 °C.

Smaihi et al. [168] have prepared homogeneous hybrid polyimide-siloxane copolymers containing different silica proportions by polycondensation, imidization, and the sol-gel process composed of PMDA, aminoalkoxysilane, and TMOS. They used two coupling agents, aminoalkoxysilane to provide bonding between the imide portion and the silica inorganic portion – aminopropyltrimethoxysilane (APrTMOS), and aminopropylmethyldiethoxysilane (APrMDEOS). Using ^{29}Si-NMR studies they observed that in APrMDEOS samples, siloxane networks are more connected than those of APrTMOS. IR studies of the hybrid material revealed that the presence of methyl side-groups linked to the silicon of APrMDEOS precursors inhibit the formation of OH free or OH linked bonds in the material. They obtained similar

activation energy values for samples having the same silica content. Therefore, the nature of coupling agent does not affect the gas transport mechanism. The modification of the polymeric network by including methyl-side groups in the material enhanced the permeability for APrMDEOS samples. The permeability of CO_2 decreased with increasing siloxane content, particularly, in APrMDEOS materials. (See Table 31.)

Table 31. Permeation Results from APrTMOS and APrMDEOS Samples of Various Compositions

Sample[b]	CO_2 Permeability (Barrer)			Selectivity (CO_2/N_2)			Selectivity (H_2/CO_2)	
	50 °C[a]	90 °C	190 °C	50 °C	90 °C	190 °C	90 °C	190 °C
APrTMOS-0	1.9	3	6.2	0.4	0.6	1.3	6.0	7.3
APrMDEOS-0	11.6	18.2	41	4.6	4.8	5.3	3.5	4.0
APrTMOS-4	1.3	2.1	3.4	0.7	1.2	1.9	7.4	9.1
APrMDEOS-4	9.4	14.7	21	6.0	6.4	4.7	3.5	6.0
APrTMOS-8	3.7	1.6	1.8	0.5	0.9	1.4	6.8	11.8
APrMDEOS-8	7	11	14	1.8	2.7	3.7	5.2	8.3

[a]Calculated using values of activation energy given in the paper; [b]Sample named as follows: 'precursor name-x', where x represents the molar ratio of TMOS/amic acid.

Marand and her research group [169-171] studied the relationship of alkoxysilane type, their loading, and the morphology of the composite on permselectivity of hybrid poyimide-silica membranes for several gases including CO_2, N_2, and CH_4. Hybrid membranes were based on FDA-6FpDA and 6FDA-6FpDA-DABA poyimides and various alkoxysilanes, such as phenyltrimethoxysilane (PTMOS), methyltrimethoxysilane (MTMOS), tetramethylorthosilicate (TMOS), and tetraethylorthosilicate (TEOS). These hybrid membranes were also annealed at 400 °C to drive the sol-gel reactions to a greater extent. In general, the annealing process increased gas permeation of the hybrid membranes by about 200 to 500 percent, while the permselectivity slightly decreased, as shown in Table 32. They attributed the increase in gas permeation to changes in the free volume distribution and enhanced local segment mobility of the chain ends resulting from the removal of sol-gel condensation and polymer degradation byproducts.

Table 32. Effect of Annealing and Loading of Alkoxysilane on the Gas Permeation Properties of Hybrid Membranes[1, 2]

Alkoxysilane Type	Silane Loading (wt%)	CO_2 Permeability (Barrer)	Permselectivity	
			(CO_2/N_2)	(CO_2/CH_4)
-	0	34.0	17	34
-[3]	0	70.8	16	30
TMOS	22.5	30.9	18	41
TMOS[3]	22.5	47.6	15	37
MTMOS	22.5	44.0	17	35
MTMOS[3]	22.5	110.0	16	29
PTMOS	22.5	30.7	16	34
PTMOS[3]	22.5	90.9	16	26
PTMOS	15.0	32.3	18	35
PTMOS[3]	22.5	91.8	16	28

[1]Permeation temperature 35 °C and pressure 4 atm (abs); [2]Polymer type: 6FDA-6FpDA-DABA-12.5; [3]Hybrid membrane was subjected to annealing at 400 °C.

Leger et al. [172] grafted polydimethylsiloxane (PDMS) onto a 5 nm porous γ-alumina membrane by thermal decomposition of silicone oil. They noted that the membrane is chemically and thermally stable up to 300 °C, and observed that the gas permeabilities were smaller in the modified membranes by 4 to 5 orders of magnitude. It was concluded that the treated membrane was no longer porous, and the transport of gas molecules across the treated membrane are caused by a solution/diffusion mechanism, as in a dense membrane. The hybrid membrane showed decent permselectivity for CO_2/N_2 of 10.2 with a very low CO_2 permeance (9 x 10^{-10} mol m^{-2} s^{-1} Pa^{-1}) at 20 °C, while it gave a very low permselectivity for CO_2/CH_4 of 0.6. They reported that the PDMS-modified membrane showed a high flux, compared to a dense PDMS polymeric membrane.

Plasma polymerized fluorinated monomeric (PPFM) films from C_4F_8, CHF_3, and CF_3CH_2F were coated on mesoporous silica substrates by Doucoure et al. [173] to obtain membranes for gas separations. The degree of cross-linking in different plasma polymers observed from FTIR spectra and XPS analysis was in this order: $CF_3CH_2F > CHF_3 > C_4F_8$. They observed that the plasma-treated silica membranes did not obey a solution/diffusion mechanism like polymeric membranes, but the gas transport in these membranes occurred via a molecular sieving mechanism. Plasma polymers from CHF_3 displayed the best permselectivity because the degree of cross-linking is suitable to give a substantial molecular sieving mechanism between CO_2 and N_2. Permeances of CO_2 (and permselectivity CO_2/N_2) from the PPFM for C_4F_8, CHF_3, and CF_3CH_2F were 1.6 x 10^{-7} (1.2), 1.4 x 10^{-7} (1.6), and 2.8 x 10^{-8} mol m^{-2} s^{-1} Pa^{-1} (1.0), respectively.

Soufyani et al. [174] found that the aging time (t_{ag}) of the initial solution is an important parameter for the elaboration of efficient silica membranes. A thin film of a hybrid material

prepared from TiO_2-SiO_2 and silicone (PDMS) using the sol-gel technique was formed on the surface of α-alumina. As suggested by the authors, the film thickness was reduced at higher aging time and, hence, the ceramic support became progressively impregnated. At t_{ag} of 3 hours, the film thickness of about 4 μm was estimated, whereas no more film depositing was confirmed at t_{ag} > 24 hours by SEM analysis—only an upper layer of homogeneous spheres of about 1.0 to1.5 μm in diameter. It was concluded that the best membranes in terms of permeability and selectivity were obtained at the aging time of about 48 hours, as shown in Table 33.

Table 33. Gas Separation from Silicone Modified Silica Membranes

Membrane	Permeation Temp. (C)	CO_2 Permeance (mol m^{-2} s^{-1} Pa^{-1})	Permselectivity	
			(CO_2/N_2)	(CO_2/CH_4)
Ti-silica/α-alumina	25 (Δp=1 atm)	1×10^{-6}	0.8	1
Silicone/α-alumina	25 (Δp=1 atm)	7×10^{-9}	11	7
Ti-silica-silicone/α-alumina	25 (t_{ag}=3 hr, Δp=4 atm)	6×10^{-8}	4.8	3
	25 (t_{ag}=3 hr, Δp=1 atm)	4.5×10^{-8}	4.1	2.4
	25 (t_{ag}=48 hr, Δp=1 atm)	2×10^{-9}	2.5	1
	25 (t_{ag}=48 hr, Δp=4 atm)	8×10^{-9}	12.1	12

Hu et al. [175] fabricated nano-composite membranes based on a fluorinated poly(amide-imide) (FPAI) and TiO_2, using the sol-gel technique. An aromatic poly(amide-imide) was chosen as the polymer matrix material because it provides superior mechanical properties associated with polyamides and high thermal stability, solvent resistance, and better permeability properties. The nano-composite membrane has a more rigid or denser structure than the corresponding pure 6FPAI membrane. The authors observed a specific interaction between the polar CO_2 molecules and the residual OH groups on the TiO_2 domain of the nano-composite membrane. Higher selectivities for CO_2/N_2 and CO_2/CH_4 system were observed even from the composite membrane containing very low concentration of the TiO_2. (See Table 34.) Based on these results, the authors were very hopeful for higher selectivities from the higher TiO_2 content composite membranes, if fabricated.

Table 34. Summary of Results from Different Poly(Amide-Imide)/TiO_2 Membranes

Membrane	Permeation Temp. (°C)	CO_2 Permeability (Barrer)	Permselectivity	
			(CO_2/N_2)	(CO_2/CH_4)
6FPAI	35	52.7	23	29
	55	55.8	17	21
	75	63.9	15	18
6FPAI/TiO_2 (7.3%)	35	44.7	25	34
	55	48.7	19	24
	75	50	15	17

Moadebb et al. [176] showed how the gas transport properties of thin films of polymers improved in the presence of silica particles. They formed thin films of six high performance polymers on silica impregnated Anapore™ alumina substrates. Six polymers studied in the composite membranes were: poly(hexafluorodianhydride isopropylidenedianiline) (6FDA-IPDA), poly(6FDA methylenedianiline) (6FDA-MDA), poly(6FDA 4,4'hexafluoro diamine) (6FDA-6FpDA), poly(6FDA 3,3'-hexafluoro diamine) (6FDA-6FmDA), tetramethyl hexafluoropolysulfone (TMHFPSF), and bisphenol-A polycarbonate (PC). As shown in Table 35, CO_2/N_2 permselectivities increased as much as in the presence of silica particles—173 percent for 6FDA-MDA composite membrane. However, the CO_2/CH_4 system did not follow any trend. They stated that the presence of silica particles might enhance the overall CO_2 permeation rate by surface diffusion. The increase or decrease in CO_2/CH_4 selectivity depended on the relative contribution of surface diffusion to the overall transport of CO_2 and CH_4. It was concluded that simultaneous increases in permeance and permselectivity were due to disruption of the polymeric chain packing in the presence of the silica particles. The authors were unsure about the practical application of these composite membranes because they are limited to a small temperature range, and the long-term gas separation behavior is unknown.

Table 35. Permeation Properties of Various Composite Membranes

Membrane Type	Wt of Silica (g)	Wt of Polymer (g)	Flux, CO_2[a]	PS (CO_2/N_2)	% Difference[b]	PS (CO_2/CH_4)	% Difference[c]
6FDA-IPDA	0.0103	0.0017	128	38	68		
	0.0144	0.0022	181	54	30		
	0.0081	0.0012	141	42	56		
	0.0010	0.0010	223	70	143		
6FDA-MDA	0.0030	0.0017	153	58	145	83	85
	0.0028	0.0005	167	65	173	81	80
6FDA-6FpDA	0.0030	0.0016	462	38	108	39	-3
	0.0031	0.0012	747	27	47	32	-19
	0.0021	0.0011	660	29	59	30	-26
	0.0011	0.0009	760	33	77	23	-42
6FDA-6FmDA	0.0106	0.0008	26	46	136	63	-2
TMHFPSF	0.0016	0.0882	339	31	71		
PC	0.0008	0.0014	58	37	62		

[a] 10^{-10} mol m^{-2} s^{-1} Pa^{-1}; [b,c] %Difference in selectivity = $[(PS_{composite} - PS_{dense\ film})/ PS_{dense\ film}] \times 100\%$; PS: Permselectivity

Gulsen et al. [177] synthesized mixed matrix composite membranes from polypyrrole (PPy) and polybisphenol-A-carbonate (PC) by a combined in situ polymerization and solvent evaporation method. The rationale for preparing composite membranes was to have a combination of good transport properties of conductive polymer, PPy, and good mechanical properties of insulating polymer, PC. It was found that the supporting electrolyte and its concentration were the most effective parameters for membrane performance. They obtained the best results with a membrane dried at 100 °C and cast from an initial solution of 7 percent PC containing 0.01 M para-toluene sulfonic acid as support electrolyte. Permselectivities values from these membranes were CO_2/N_2 of 5.9, CO_2/CH_4 of 3.1 while CO_2 permeability was 11.6 Barrer.

While hybrid membrane research has been considerably more limited than that on the other types of membranes discussed, interesting results have been achieved particularly in the separation of CO_2/CH_4 mixtures, Figure 10 and Figure 11. Similar results should be possible for other gas mixtures once more research has been done to perfect organic additions, which favor diffusion of CO_2 at the expense of H_2 and CH_4.

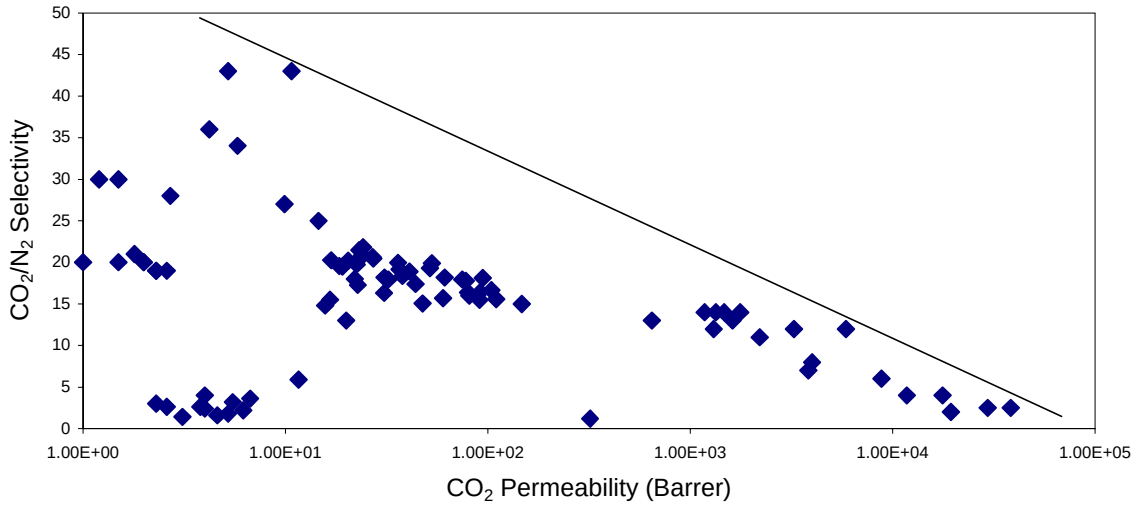

Figure 10. Literature Data for CO_2/N_2 Selectivity vs. CO_2 Permeability for Hybrid Membranes

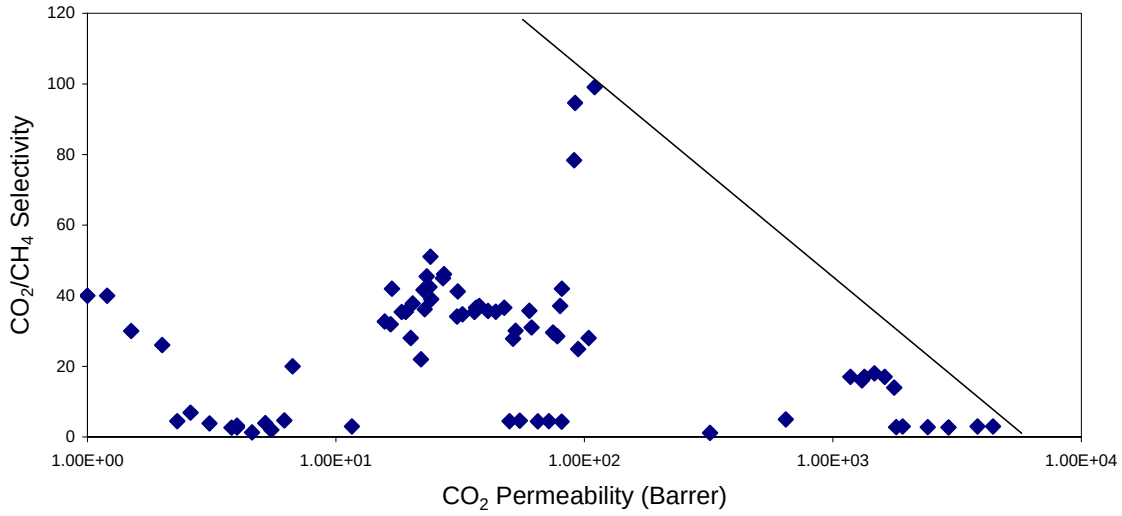

Figure 11. Literature Data for CO_2/CH_4 Selectivity vs. CO_2 Permeability for Hybrid Membranes

Mixed Matrix Membranes

Significant improvements in the performance of polymeric gas separation membranes have been witnessed in the last two decades. Despite all these efforts, polymeric membranes are not in a position above the trade-off curves between gas permeability and selectivity, as suggested by Robeson [178]. On the other hand, molecular sieving materials like zeolites and carbon molecular sieves (CMS) offer attractive transport properties, but are difficult and expensive to process as membranes [179]. Therefore, membranologists are in search of an alternate approach that can take gas separation membranes to the next level. Mixed matrix composite materials,

comprised of molecular sieving materials inserted in a polymer matrix, have the potential to provide economic as well as high-performance gas separations. The resulting mixed matrix membranes (MMM) may have the advantages of both materials: the processability of polymers and the superior gas transport properties of molecular sieves. However, their performance suffers from defects caused by poor contact at the molecular sieve/polymer interface. The molecular sieving material could be a zeolite or CMS. Figure 12 illustrates the schematic of a mixed matrix membrane. Careful matching of the intrinsic permeability and selectivity of the support matrix and the molecular sieve domain is necessary [179]. Composite organic-inorganic membranes have become an expanding field of research as the introduction of organic molecules can improve the characteristics of a matrix.

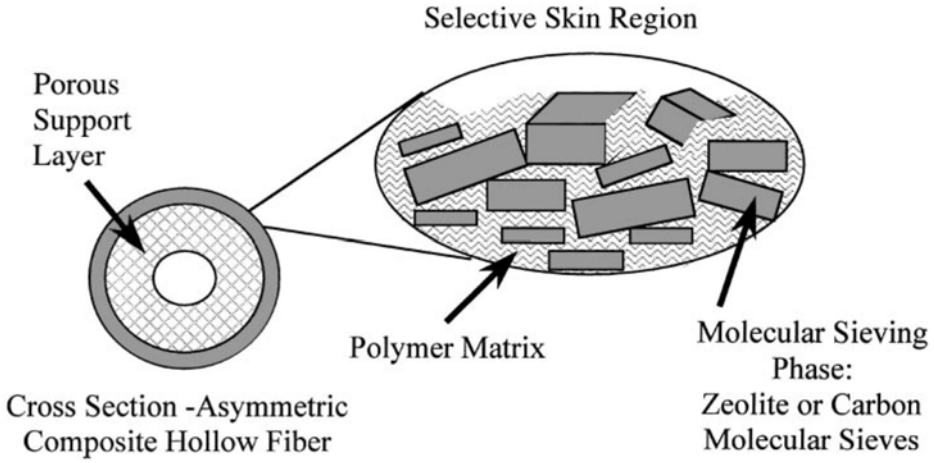

Reprinted from the Journal of Membrane Science, Vol. 175, W.J. Koros, and R. Mahajan, "Pushing the Limits on Possibilities for Large Scale Gas Separation: Which Strategies?" Page 186. Copyright 2000, with permission from Elsevier.

Figure 12. Schematic of a Mixed Matrix Membrane

Jia et al. [180] were the first to investigate zeolite-filled rubbery polymer membranes composed of PDMS, a rubbery polymer, and a hydrophobic zeolite, silicalite-1. It was concluded that the silicalite played the role of molecular sieve in the membrane by facilitating the permeation of smaller molecules but hindering the permeation of larger ones, although its pore openings were larger than the size of the permeating gases. It was suggested that the shape-selective effect was not only inherent in the equilibrium adsorption of gas molecules, but also in the kinetic adsorption and diffusion. Permeabilities of CO_2 increased, while the permeabilities of N_2 and CH_4 decreased with increased silicalite content in the composite membrane. The best permselectivities for CO_2/N_2 and CO_2/CH_4 from a composite membrane containing 70 percent silica were 17 and 9, respectively, at 30 °C with the CO_2 permeability of 3835 Barrer.

Kulprathipanja et al. [181] found that mixed matrix membranes comprised of cellulose acetate and silicalite-1 have improved characteristics as the silicalite content increases. They obtained the CO_2/H_2 separation as high as 10 from the mixed matrix membranes for an equimolar feed of CO_2 and H_2 at 25 °C.

Suer et al. [182] prepared mixed matrix membranes of polyethersulfone, a glassy polymer, and hydrophilic zeolites 13X and 4A using different membrane preparation procedures. They

observed that the permeabilities decreased up to a loading of 8 percent for zeolite 13X, and 25 percent for zeolite 4A before it increased for higher zeolite loadings. It was concluded that the channel network matures as the zeolite loading increases in the matrix, and consequently connects separate voids that provide an additional route for gas molecules. Typically, this led to an increase in the permeation of all gases with increasing zeolite content in the mixed matrix membranes. (See Table 36.) The polarity and adsorption of gases within the membrane matrix in addition to shape-selective properties of the zeolite attributed to the transport of gases across the zeolite mixed matrix membranes. CO_2 molecules have the ability to interact with the polar surface of zeolite 13X and 4A during permeation and, hence, CO_2 permeability and permselectivity increase considerably with increasing zeolite loadings in the mixed matrix membranes. The permeation properties of the membrane also depended on the type of zeolite in the matrix. This is because of different chemical interactions between polar gases wand the different zeolites as well as the macropositioning of zeolites in the matrix. It was stated that zeolite 13X crystals seemed to be more discrete, whereas zeolite 4A crystals were partly aggregated, forming wider cavities.

Table 36. Effect of Zeolite Content and Type on Mixed Matrix Membrane Performance

Zeolite Type	Zeolite Content (%)	CO_2 Permeability (Barrer)	Selectivity (CO_2/N_2)	Selectivity (H_2/CO_2)
None	0.0	2.6	19	2.5
13X	8.3	1.5	20	2.5
	16.6	1.8	21	2.6
	33.3	2.7	28	2.1
	42.0	4.2	36	1.8
	50.0	5.2	43	1.7
4A	8.3	2.3	19	2.6
	16.6	2.3	19	2.5
	33.3	2.0	20	2.4
	42.0	5.8	34	1.6
	50.0	10.7	43	1.3

Permeation temperature 25 ℃.

Duval et al. [183] studied the effect of incorporating specific adsorbents (zeolite or carbon molecular sieves) on the gas permeation properties of polymeric membranes such as PDMS, ethylene-propylene rubber (EPDM), polychloroprene (PCP) and nitrile butadiene rubber (NBR). The results showed that the introduction of silicalite-1, zeolites 13X, and KY to the polymer improved the gas permeation properties of membranes. This was attributed to both molecular sieving effects and increased CO_2 sorption capacity due to the affinity of the gas molecules for the zeolites. A maximum CO_2/CH_4 separation factor of 18 was obtained from EPDM filled zeolite KY, with the CO_2 permeance of 450 Barrer at a feed of 25 percent CO_2/ 75 percent CH_4. However, zeolite 5A's high affinity for water did not improve membrane performance, and resulted in a lower CO_2 sorption capacity. The incorporation of carbon molecular sieves was not

effective for gas separations because of the absence of interconnected channels like those found in zeolites.

In a further study [184], Duval et al. investigated the formation of non-selective interfacial voids caused by poor adhesion between the glassy polymer phase and the zeolite surface. The gas permeability increased when zeolite was added into glassy polymers, but the selectivity typically decreased or remained the same. (See Table 37.) They attributed this result to interfacial voids that drastically increased the permeability without affecting the selectivity. They investigated various methods to improve the internal membrane structure, such as surface modification of the external surface of zeolites with silane, preparation above the glass temperature, and heat treatment. However, the CO_2/CH_4 permselectivities of membranes were hardly improved to exhibit the anticipated performance increases.

Table 37. Separation from Zeolite Filled Glassy Polymer Membranes

Polymer Type	Zeolite Type, Content (wt%)	CO_2 Permeability (Barrer)	Selectivity (CO_2/CH_4)
CA[a]	-	11	41
	Silicalite-1, 25	18	40
PEI[b]	-	1.5	61
	Silicalite-1, 50	15	34
	Silicalite-1, 50[d]	9	35
	KY, 50	95	43
	KY, 50[e]	25	50
TPX[c]	-	71	7
	Silicalite-1, 25	154	9

[a]Cellulose acetate (CA); [b]Polyetherimide (PEI); [c]Poly(4-methyl-1-pentene) (TPX); [d]modified with silane; [e]heat treated at 150 °C. Permeation temperature 25 °C.

Gur [185] fabricated zeolite 13X filled polysulfone membranes by a melt extrusion process. However, no pronounced effect of the filler was observed. He concluded that the pore size of zeolite 13X was larger than the kinetic diameters of any of the gases studied. Hence, separation due to size exclusion did not take place.

Yong et al. [186] prepared Matrimid polyimide (PI) membranes filled with zeolites by introducing 2,4,6-triaminopyrimidine (TAP). They used TAP to enhance the contact of zeolite particles with polyimide chains by forming hydrogen bonding between them and, hence, obtained an interfacial void-free PI/zeolite membrane. The addition of TAP to PI/zeolite membrane increased the gas permselectivities significantly at the expense of the gas permeabilities. (See Table 38.) They observed higher gas permeabilities from a PI/zeolite 13X/TAP membrane with lower permselectivities, compared to PI/TAP membranes having the same PI/TAP ratio; they observed lower gas permeabilities but higher permselectivities with the PI/zeolite 4A/TAP membrane. It was concluded that the molecular sieving effect of zeolites took place when the kinetic diameter of the penetrant gas approached the pore size of the zeolites.

Table 38. Effect of TAP on the Permeation Properties of Zeolite-Filled PI Membranes

Membrane Type	Composition (by wt.)	CO_2 Permeability (Barrer)	Permselectivity	
			(CO_2/N_2)	(CO_2/CH_4)
PI	1	8.3	38	1
PI/TAP	1:0.21	0.2	87	84
PI/Zeolite4A	1:0.43	9.4	21	2
PI/Zeolite13X	1:0.43	33.4	25	7
PI/Zeolite4A/TAP	1:0.43:0.21	0.2	102	617
PI/Zeolite13X/TAP	1:0.43:0.21	0.6	74	133

Permeation temperature 25 ℃

Mixed matrix membrane research for gas separations has largely focused on zeolites as the dispersed phase. However, Vu et al. formed mixed matrix membranes by incorporating carbon molecular sieves (CMS) into two different glassy polymer matrices, Matrimid® 5218 and Ultem® 1000 [187, 188]. It was shown that the permselectivities (CO_2/N_2 and CO_2/CH_4) as well as CO_2 permeability significantly increased as the loading of CMS particles increased in the matrix of the membrane, shown in Table 39. The authors also identified several advantages of CMS over zeolites as possible molecular sieve entities for incorporation into mixed matrix membranes. The CMS particles have better affinity to glassy polymers, which makes the film formation easier. Also, the gas permeation properties of the CMS particles can be tailored by modifying pyrolysis procedure, which makes mixed matrix membranes containing CMS more adaptable for desired gas separations.

Table 39. Effect of Polymer Type and Content on Mixed Matrix Membrane Performance

Polymer Type	CMS Content (vol%)	CO_2 Permeability (Barrer)	Selectivity (CO_2/N_2)	Selectivity (CO_2/CH_4)
Matrimid® 5218	0	10.0	31	35
	17	10.3	36	44
	19	10.6	30	47
	33	11.5	30	48
	36	12.6	33	52
	100	44.0	27	200
Ultem® 1000	0	1.5	28	39
	16	2.5	35	43
	20	2.9	32	48
	35	4.5	33	54
	100	44.0	27	200

Permeation temperature 35 °C.

Tantekin-Ersolmaz et al. [189] reported that the permeabilities of the silicalite-PDMS mixed matrix membranes increased with increasing zeolite particle size while the CO_2/N_2 permselectivities remained unaffected. They also stated that the effect of particle size was more pronounced at the higher zeolite loading. It was concluded that the permeability of gases through mixed matrix membranes decreased with increasing particle size, due to the enhanced area and the increased number of zeolite-polymer interfaces that the gas molecules have to cross.

Much research and development is needed to more efficiently apply mixed matrix membranes to gas separations.

Facilitated Transport Membranes

Facilitated transport membranes (FTM) have received a lot of attention in gas separations because they offer higher selectivities and larger fluxes [7, 190]. Higher selectivity in FTM is achieved by incorporating a carrier agent into a membrane, which reacts reversibly with the penetrating species. In addition to the solution-diffusion mechanism of the polymeric membranes, FTMs also involve a reversible complex reaction. In FTM, the permeating species dissolves in the upstream portion of the membrane and reacts with the carrier agent to form a complex. The formed complex diffuses across the membrane, and then releases the permeants on the downstream side of the membrane, while the carrier agent is simultaneously recovered and diffuses back to the feed side.

FTMs can be divided into three general categories: fixed carrier or chained carrier membranes, solvent-swollen polymer membrane, and mobile carrier membranes or immobilized liquid membranes (ILMs) [190]. Fixed carrier membranes are solid polymer films into which reactive functional groups, or complexing agents, are incorporated. Transport in the fixed carrier membranes is limited by the absence of mobility of the complexing agents. An ILM is usually

prepared by impregnating the liquid carrier into the pores of a microporous support. The liquid (carrier agent) in ILM is held in the support pores by capillary forces. The chemical instability of the carrier agent in ILMs limits its application for gas separations. Membrane degradation might also occur by evaporation or dryout of the liquid carrier agent in the gas separation applications. Fixed carrier membranes are generally considered more stable than ILMs because there is less chance of carrier loss. There have been several efforts made to overcome this membrane leaching problem, such as the use of molten salts with very low vapor pressure, or the use of hollow-fiber contained liquid membranes. Solvent-swollen membranes are intermediate in structure and stability between ILMs and fixed carrier membranes. They can be made by swelling a polymer film in a solvent and introducing the carrier species by diffusion or by ion exchange in the case of ionomer membranes.

Guha et al. [191] prepared ILMs consisting of aqueous solutions of 20 percent diethanolamine (DEA) immobilized in 25.4 μm microporous polypropylene supports. They studied permeabilities and separation factors for the CO_2-N_2 mixture, with CO_2 partial pressure ranging from 12 to 126 cmHg at a temperature of 25 °C. The CO_2 permeabilities decreased from 4,825 to 974 Barrers as the CO_2 partial pressure increased from 12 to 126 cmHg, while resulting CO_2/N_2 separation factors also decreased from 276 to 56 over the same pressure range. For a 25.4 μm thick ILM at an intermediate CO_2 partial pressure of 22 cmHg, the CO_2 permeance was 2.9×10^{-11} mol m^{-2} s^{-1} Pa^{-1} and the CO_2/N_2 separation factor was 153. They also proposed a model for facilitated transport of CO_2 through an ILM containing aqueous DEA solution with an excellent estimate of the CO_2/N_2 separation factor over a wide range of CO_2 partial pressures.

Matsuyama et al. [192] prepared a cation-exchange membrane by grafting acrylic acid onto a microporous polyethylene membrane using a plasma-grafted polymerization technique. They used the plasma-grafted membrane with ethylenediamine as a carrier for the facilitated transport of CO_2. The membrane had a high stability as well as a high selectivity for CO_2 over N_2 at 25 °C. For 17 percent CO_2 balanced with N_2 in the feed gas, they observed a CO_2 separation factor over 1,000 along with a CO_2 permeance of 1.2×10^{-8} mol m^{-2} s^{-1} Pa^{-1}. The stability was attributable to both the hydrophillicity of the poly(acrylic acid) membrane and the retention of the carrier by electrostatic force.

Yoshikawa et al. [193, 194] synthesized polymeric membranes having a pyridine moiety or an amine moiety as a fixed carrier to take advantage of the acid-base interaction between CO_2 and the fixed carriers for CO_2 separation. They have reported CO_2/N_2 permselectivity as high as 90 with a poly{2-(N,N-dimethyl)aminoethyl methacrylate-co-acrylonitrile} membrane. However, the CO_2/N_2 permselectivity was low, about 9, with a CO_2 permeability of 26 Barrer from the poly{4-vinylpyridine-co-acrylonitrile} membrane.

Nakabayashi et al. [195] applied hydogel, prepared from a vinyl alcohol/acrylic acid-salt copolymer, on a hydrophilic PVdF porous membrane by a spin coating method, followed by heating to get cross-linkage. The cross-linked layer was immersed into a CO_2 carrier solution (2 mol/l of K_2CO_3) to form a water-swollen-gel membrane. The gel membrane was coated on a polydimethylsiloxane support. The authors discovered that K_2CO_3 had the highest permeation and separation factor and was most effective as a CO_2 carrier among several carbonate salts of alkali metals studied. They reported that the water-swollen-gel membrane was stable over 30 days. A much higher permeability and selectivity was observed after adding crown ether,

EDTA, or analogous compounds to the K_2CO_3 solution. These additives easily form complexes with potassium ions, which subsequently result in highly activated carbonate ions for CO_2 transport. The CO_2/N_2 separation factor was over 1,800 with a CO_2 permeance of ~9 x 10^{-9} mol m^{-2} s^{-1} Pa^{-1} after adding 0.07 mol/l diaza-15crown as an additive to the K_2CO_3 solution.

Matsuyama et al. [196] prepared a membrane having an amine moiety by plasma-grafting of 2-(N,N-dimethyl)aminoethyl methacrylate (DAMA) onto a microporous polyethylene substrate. They conducted permeability studies for CO_2 and O_2 in both dry and wet membranes. The wet membrane was prepared by soaking the membrane in water overnight. The membrane thickness increased with the increase in the degree of grafting, and was also higher for the wet membrane. In the dry membranes, the facilitated transport of CO_2 was caused by the weak acid-base interaction between CO_2 and amine moiety. It was suggested that CO_2 does not directly interact with the amine moiety in the wet membrane, but the CO_2 hydration reaction occurs in the membrane solution to produce free HCO_3^-. Hence, CO_2 is transported in the form of HCO_3^- and, therefore, the water-containing membrane is not strictly a fixed carrier membrane, but acts as a fixed reaction site membrane. They reported the separation factor of CO_2/N_2 as high as 130 (CO_2 permeance = 1.7 x 10^{-9} mol m^{-2} s^{-1} Pa^{-1}) for the wet membrane at the CO_2 partial pressure of 0.047 atm. The separation factor, CO_2/N_2, decreased with increasing permeation temperature from 25 °C to 50 °C as the CO_2 permeation increased slightly compared to N_2 permeation.

In a different study, Matsuyama et al. [197] studied facilitated transport of CO_2 through a thin solution-cast perfluorosulfonic acid ionomer membrane. Ethylenediamine (EDA) immobilized in the ionomer membrane by electrostatic forces was used as a CO_2 carrier. They observed a much higher CO_2 permeance from the cast membrane with the membrane thickness of 22 μm (1 x 10^{-8} mol m^{-2} s^{-1} Pa^{-1}) than the commercial Nafion® membrane with the thickness of 186 μm (2.7 x 10^{-9} mol m^{-2} s^{-1} Pa^{-1}). However, the CO_2/N_2 separation factor was lower in the cast membrane (~225 compared to ~475 in Nafion). The carbon dioxide-carrier complex is much larger than a N_2 molecule. The pore size of the cast membrane decreases with increasing annealing temperature and, hence, results in a lower permeability and selectivity of CO_2. The N_2 permeability was almost constant, while CO_2 permeability increased with increasing membrane thickness. It was concluded that the facilitated transport in the cast membrane was limited by the chemical reaction of the complex formation. A higher selectivity was observed with the larger thickness.

Chakma [198] has reported the separation of CO_2 and SO_2 from flue gas streams by liquid membranes. His membrane set-up consisted of an immobilized polyethyleneglycol (PEG 400) membrane in series with another immobilized diethanolamine (DEA)/PEG 400 membrane. Because of its high solubility in PEG, SO_2 was preferentially separated in PEG 400 membrane with a maximum separation factor, SO_2/N_2, of 140. Unlike DEA's reversible reaction with CO_2, its reaction with SO_2 forms a stable complex under the operating conditions, and the stable complex also hinders the passage of free SO_2 across the membrane. Therefore, CO_2 was separated by DEA/PEG 400 membrane with a CO_2/N_2 separation factor of 240.

As discussed earlier, the low stability of ILMs due to the ILM drying limits its intended use for gas separations. Low-volatility and hygroscopic liquids such as poly(ethylene glycol) (PEG) were used as the component in the ILM fluid to alleviate the drying problem. Chen et al. [199-201] performed separation of CO_2 from a humid mixture of CO_2-N_2 through ILMs containing

immobilized solutions of sodium carbonate/sodium glycinate-glycerol in porous and hydrophilic hollow fiber supports. They carried out separations from gas mixtures containing very low CO_2 concentrations, particularly for space-walk applications. Nevertheless, their work is theoretically important for the CO_2 separations and should be able to provide a further foundation for better understanding and development of ILMs. Sodium carbonate or sodium glycinate was used as a CO_2 carrier and glycol as the ILM solvent, which provided desired stability to the ILM. It was observed that the permeability of CO_2 increased with an increase in carrier concentration, while N_2 permeability decreased and, therefore, very high CO_2/N_2 selectivities were achieved at higher concentrations of the CO_2 carrier. They also observed that the ILMs were quite stable for prolonged use. It was suggested that the permeance of CO_2 could be increased by increasing CO_2 carrier solubility in the ILM liquid and by preparing ILMs with thinner hydrophilic supports. In another study by the same authors [202, 203], they used polyamidoamine (PAMAM) generation 0 dendrimers having ethylenediamine as the CO_2 carrier in porous hydrophilic polyvinyldine fluoride supported ILM. Dendrimer immobilized liquid membranes containing a high concentration of primary and tertiary amine provided a facilitated CO_2 transport and also nearly eliminated the other gases.

Palladium-Based Membranes

Dense palladium membranes have been prepared by depositing palladium or other metals ranging in thickness from a submicron to a few microns on a porous support. These Pd or metallic membranes are 100 percent selective to H_2 from an H_2 containing feed mixture because other gases do not diffuse through the metal. The permeation of H_2 through metal membranes involves the dissociative chemisorption of H_2 on the membrane surface followed by dissolution of the atomic hydrogen from the surface into the bulk of the metal [7]. This is followed by atomic diffusion of dissolved hydrogen in the membrane and desorption of hydrogen atoms as molecules. The rate-limiting step for H_2 permeation is the hydrogen diffusion through the bulk of the metal membrane. Hence, the H_2 flux through the membrane is directly proportional to the difference in the square roots of H_2 pressures between the feed and permeation sides of the membrane (Sievert's law). The H_2 permeability of the supported membrane is significantly higher than a single-layered Pd membrane. The supported membrane also has the advantage of having high mechanical strength imparted by the support. Besides Pd and its alloys, other metals such as tantalum, niobium, and vanadium also have high selectivities and, hence, are also candidates for the H_2 selective dense membranes. The high cost of precious metals, lower permeabilities, brittleness, and high susceptibility to poisoning compounds are some of the disadvantages of the precious metal membranes and have limited their intended use. Now, researchers have overcome most of those disadvantages by depositing a very thin layer of metal alloy on a porous support. Three methods [23] have generally been used to deposit thin metal films on porous supports: electroless plating, chemical vapor deposition, and physical sputtering. There is an enormous amount of literature discussing metallic membranes for H_2 separation. Although this review is primarily focused in CO_2 transport, a few relevant studies with H_2 membranes will be introduced since H_2/CO_2 separations may eventually be important in IGCC applications.

Silver, Rh, Ru, or rare earth metals are added to the Pd to reduce cracking and distortion of the Pd film due to alpha/beta phase Pd transitions [204, 205]. An optimum H_2 permeability is

obtained from a Pd-Ag alloy membrane containing 23 percent by weight Ag [204]. Keuler et al. [204] deposited the Pd-Ag films of thickness <2.2 μm on the inside of α-alumina by an electroless plating method. They reported poor H_2 permeances through unalloyed Pd-Ag membranes. In order to improve the H_2 permeance of the Pd-Ag film, a heating procedure was developed to obtain a homogeneous Pd-Ag alloy. The films were oxidized at 310 °C for 1 hour after heat treatment in Ar at 550 °C for 10 to15 hours and then reduced in H_2 to obtain an optimal H_2 permeance and selectivity. The permeances of those membranes at 410 °C were observed up to 6.5 x 10^{-6} mol m^{-2} s^{-1} Pa^{-1}, with the H_2/N_2 permselectivity of 400.

McCool et al. [206] prepared submicron thick Pd-Ag films by a sputter deposition process on mesoporous γ-alumina from a target composed of 75 percent Pd and 25 percent Ag. They reported H_2 permeances through these membranes in the range of 3 x 10^{-8} to 1 x 10^{-7} mol m^{-2} s^{-1} Pa^{-1} along with H_2/He selectivities in the range of 4 to 4,000, depending mainly on Ag concentration and microstructure of the Pd-Ag films. It was concluded, based on theoretical and experimental data, that the deposition power and target equilibrium are the most important variables affecting membrane composition.

Future power plants could be based on IGCC-type power generation, where palladium-based membranes can play an important role by combining the water-gas shift reaction (WGSR) with H_2 separation. A membrane reactor can drive equilibrium-limited reactions towards completion by removing a product as it forms. The result is a more compact design, plus greater conversion. These types of membrane reactors are reviewed excellently by several researchers [118, 205, 207-213].

Researchers [116, 214] have carried out the WGSR in a membrane reactor using a Pd/Ag or Pd membrane. The metallic layer of the membrane was thick enough to avoid any defects of the surface and to make sure to get an infinite H_2 selectivity, compared to other gases. Porous ceramic support was used to separate the Pd or Pd/Ag membrane from the catalyst bed of the membrane reactor. The authors conducted experiments by using N_2 as a sweep gas in co-current and counter-current modes in the temperature range 330 to 350 °C and in the feed flow range of 3.05 x 10^{-5} to 7.1 x 10^{-5} mol s^{-1}. They obtained a complete separation of H_2 from other gases along with almost complete WGSR conversion from the Pd/Ag or Pd membrane.

Damle et al. [215] have also developed a membrane reactor process for H_2 production by fuel reforming. They prepared a 2 to 3 μm thick Pd-Ag alloy films on tubular alumina support using electroless plating technique. The observed hydrogen permeances ranged from 1 to 5 x 10^{-6} mol m^{-2} s^{-1} Pa^{-1} with the H_2/N_2 selectivity (separation factor) range of 150 to 10,000 at 500 to 600 °C.

Noble metal membrane reactors have been extensively studied for hydrogenation and dehydrogenation reactions. High conversions along with good H_2 selectivity were reported from these metal membranes. However, several researchers also confined their work on the development of H_2 selective ceramic membranes. Prabhu et al. [216] nicely summarized the work conducted in the area of H_2 selective ceramic membranes. They noticed that the silica modified membranes suffer from loss of permeability (as much as 50 percent or greater in the first 12 hours) on exposure to moisture due to densification. The densification phenomenon was attributed to the formation of Si-O-Si bonds from Si-OH groups, which results in closure of pore channels. They developed a silica-modified membrane by the high temperature CVD of TEOS

on Vycor glass. The membrane (Nanosil membrane) exhibited a high H_2 selectivity over a prolonged period under hydrothermal conditions (10 percent H_2O at 600 °C and 1 bar) while maintaining a steady performance. The H_2 permeance was 1.8 x 10^{-8} mol m^{-2} s^{-1} Pa^{-1} at 600 °C with H_2/CH_4, H_2/CO, and H_2/CO_2 separation factors of 27,000, 87,000, and 8,200, respectively. The membrane was also employed in a catalytic reactor for the transformation of greenhouse gases, $CH_4 + CO_2 \Leftrightarrow 2CO + 2H_2$, using a 1 percent Rh/Al_2O_3 catalyst. They observed higher conversions from the membrane reactor compared to the packed-bed reactor at the same conditions as a result of simultaneous reaction and H_2 removal.

Future Directions

A significant amount of work has been devoted to gas separation membranes over the last 10 to 15 years. A number of the microporous inorganic membranes discussed in this paper show good permeation properties for CO_2 over N_2 and CH_4 at low temperatures, but lose CO_2 selectivity at elevated temperatures due to surface diffusion-based transport mechanism through the membrane. These membranes also suffer from stability problems at the desired operating conditions, and/or economic feasibility issues. While development of current techniques continues to move these membranes closer to commercial application, it is also interesting to consider innovative materials that could lead to new generations of membranes for CO_2 separation.

Certain characteristics are indicative of a good prospective membrane material. The material should be capable of a significant degree of CO_2 adsorption, but must not allow penetration of CO_2 into the bulk, which could lead to physical and chemical modification of the material. This adsorption should be reversible, since irreversible adsorption could only result in the reduction of membrane permeability. The membrane should not have much sorption capacity for other gases, such as N_2, CH_4, and H_2. Resistance to poisoning by other possible contaminant gases, such as H_2O, SO_X, NO_X, and H_2S, is necessary to produce a membrane, that can maintain performance for extended periods. Inexpensive fabrication techniques should be available that can produce defect-free membranes in a variety of configurations from the material. Stability at elevated temperatures is also required. The selective membrane thickness is a crucial parameter, because thicker membranes directly result in higher material cost and lower membrane flux. Lower flux means lower membrane productivity and, hence, higher operating costs.

One purpose of this review is to assess prospective materials, based on these properties and encourage fabrications and study of membranes based on these new materials. The following classes of materials stand out among the many prospects for CO_2 selective membranes in flue gas or fuel gas applications: hybrid material, mixed matrix-type material, hydrotalcite-type materials, and perovskite-type material. The rationale behind selecting these materials is detailed in the following sections.

Hybrid Membranes

Modified inorganic membranes retain the rigidity and pore morphology of the ceramic material, while the organic component alters the ceramic membrane functionality. It is a well known fact that CO_2 permeation increases when there is a chemical affinity with some molecular groups in

the membrane [167]. This has been observed for the fluorogroup [127], phenyl group [167], and carbonyl group in esters and ketones [128, 129]. As noted in the discussion of hybrid membranes, there have been numerous attempts to take advantage of these chemical affinities in order to prepare membranes with high CO_2 selectivity and permeability.

Takaba et al. [217] and Mizukami et al. [218] have investigated separation of CO_2 from CO_2/N_2 mixtures using inorganic membranes by molecular dynamics (MD) simulation and computer graphics (CG) methods. It was shown that CO_2 permeation can occur by surface diffusion and capillary condensation when the CO_2 affinity for the membrane wall is high. Separation of CO_2 and N_2 could be achieved if the N_2 affinity is weaker than that of CO_2. However, they mentioned that the optimal range of the CO_2 affinity is required to achieve good separation, because too strong affinity prevents surface diffusion. They also observed using MD simulation and CG images that CO_2 molecules were adsorbed on the site II sodium cation in the NaY-type zeolite membrane.

The exceptional CO_2 permselectivities of fluorine-containing polyimides, as well as their stability at higher temperatures and in harsh environments, make them highly attractive for gas separation membranes. However, their high cost has prevented their intended use in gas separation processes. A composite membrane comprising of a thin polyimide film coated on a strong and stable porous support would be an idealistic membrane for economical and favorable gas separations.

Problems in this research area have generally taken one of two forms. In the production of membranes using sol gel techniques designed to leave a particular organic group in the membrane structure, low coverage or over-coordination of the organic group has resulted in a lower than desired surface affinity. When previously fabricated inorganic membranes have been modified by organic reagents, such as silanes, mass transfer into the pore and the reactivity of those reagents have resulted in very thin “polymer-like” membranes covering the surface to varying thicknesses, depending upon the silane used. These techniques hold considerable potential, but research will be required to further develop the fabrication techniques required to produce membranes with monolayer coverages of a particular organic group inside the pores.

Mixed Matrix Membranes

Many inorganic membranes are stable at high temperatures, but the competitive adsorption process does not work well at high temperatures. Molecular sieving membranes have a greater potential than competitive adsorption at high temperatures, but tailored micropores are required to separate light gases with smaller size differences.

Zeolites, carbon molecular sieves (CMS), and many polymeric materials offer attractive transport properties, but are difficult and expensive to process [179]. Mixed matrix composite (MMC) materials, comprised of molecular sieving materials embedded in a polymer matrix, have potential to provide economical, high performance gas separation membranes if defects at the molecular sieve/polymer interface can be eliminated. The molecular sieving material could be zeolite or CMS. Additionally, careful matching of the intrinsic permeability and selectivity of the support matrix and the molecular sieve domains is necessary. Composite organic-inorganic membranes have become an expanding field of research as the introduction of organic molecules

can improve the characteristics of a matrix.

Hydrotalcite-Type Materials

Inorganic membranes have a great potential for gas separation at elevated temperatures in oxidative atmosphere where polymeric membranes are not resistant. Mesoporous ceramic materials are still very attractive for CO_2 selective membranes at elevated temperatures, although researchers report very low CO_2 selectivity through mesoporous ceramic membranes at higher temperatures. First, these are very thermally stable materials. Second, they might be available commercially at very low cost. Third, the flux is higher with mesoporous membranes, compared to microporous or dense membranes. As mentioned earlier, transport across mesoporous membranes is governed by the Knudsen diffusion mechanism, and the separation efficiency ($CO_2/N_2 = 0.8$; $CO_2/CH_4 = 0.6$) according to that mechanism would be unacceptable for all practical purposes. In order to improve the separation efficiency of mesoporous membranes, the transport through the membrane should be facilitated by the surface diffusion mechanism. Therefore, materials like HT, or HTs modified with basic metal oxides could be considered excellent candidate membrane materials because of their higher CO_2 adsorption capacity at elevated temperatures, while maintaining thermal stability.

Perovskite-Type Material

The adsorption of CO_2 was also investigated with perovskite-type oxides ($LaMO_3$, where M = Co, Cr, Mn, Fe) at elevated temperatures up to 400 °C [219, 220]. Physical adsorption of CO_2 on $LaCoO_3$ took place up to 100 °C, and chemisorption occurred at 350 to 400 °C. It was also shown that perovskite-type material $BaTiO_3$ adsorbed 100 to 150 mmol/kg at 500 °C [101]. The CO_2/N_2 separation factor through the $BaTiO_3$ membrane was slightly higher than Knudsen diffusion (discussed above). To our knowledge, no other perovskite-type oxide membrane studies for CO_2 separation have been reported so far in the open literature. Their stability at elevated temperatures, low susceptibility to poisoning by sulfur and other compounds [219], and their higher CO_2 adsorption capacity at higher temperatures make the perovskite-type oxides attractive membrane materials for CO_2 separation. The gas transport properties of membranes made of perovskite-type oxides must be explored in detail.

Others

Toshiba Corporation recently announced two new ceramic materials, which have high CO_2 absorption capacity [221, 222]. They claimed that one of their ceramic materials, lithium zirconate, is able to absorb 400 times its own volume of CO_2, ten times more than any other existing CO_2 absorbent. Recently, Toshiba also introduced another ceramic material, lithium silicate, which absorbs 30 times faster than lithium zirconate. They reported that 1 g of lithium silicate absorbs 62 mg of CO_2/min, while lithium zirconate absorbs 1.8 mg CO_2/min in a 20 percent CO_2 gaseous environment at 500 °C. Silicon, the main material of lithium silicate, costs only 15 percent of the price of zirconium and is 70 percent lighter in weight. The use of these novel ceramic materials as a membrane is yet to be established. However, their high CO_2 absorbing capacity and stability at elevated temperatures, coupled with their reasonable cost,

should be stimulating enough for membranologists to explore them as promising membrane materials for CO_2 separation at higher temperatures.

Membranes will have additional gas separation applications in separation technology if they can be manufactured easily and inexpensively [76]. Several other issues still need to be addressed include: further improvements in the membrane flux by reducing the thickness of the membrane without sacrificing gas separation; automating the fabrication process to increase coating uniformity and to reduce the cost of manufacturing; and increasing the membrane area by fabricating larger supported nanoporous carbon membranes (SNPCMs) in bundles with multiple tubes. It has been reported that economical separation is attained if permeability and permselectivity of CO_2 over N_2 exceed 100 Barrer and 70, respectively [9].

Conclusions

As the concentration of atmospheric CO_2 rises, it is incumbent upon the scientific community to find the means to control it while there is still the opportunity to avert potentially harmful climate change. Research continues into alternative energy sources, but it is unlikely these will be sufficiently developed to meet the world's energy requirements in the foreseeable future. As we wait for these technologies to come of age, the capture and sequestration of CO_2 produced in the utilization of fossil fuels is a viable alternative.

Research and development with conventional and advanced techniques for capturing or separating CO_2 from large point sources is progressing. Membrane technology is just one of a number of technologies being investigated to fill this role. The primary difficulty in the implementation of gas separation membranes in other industries has been the relatively undeveloped state of the technology compared to more conventional tools. Since no conventional technology in its current state can solely fill the requirements of CO_2 removal, the opportunity exists for gas separation membranes to mature along side the competing technologies, and for the first time demonstrate their full potential.

The goals of this review have been to examine previous studies of various CO_2 selective membranes and to promote further work in the area. The examination summarizes advances reported in the literature with respect to CO_2-selective membranes, their stability, the effect of operational parameters on their performance, the relationship of their structure to their permeation properties, and their observed transport mechanisms. An attempt is also made to predict the future direction for CO_2-selective membrane research. Finally, future research directions for CO_2 selective membranes are projected. Hybrid organic-inorganic membranes have become an expanding field of research as the introduction of organic molecules can improve the characteristics of a matrix. Hydrotalcite-type materials, perovskite-type oxides, and certain lithium compounds are also suggested as candidate materials for high temperature CO_2 selective membranes.

References

1. U.S. Department of Energy, *Carbon Sequestration Research and Development*, DOE/SC/FE-1. 1999.
2. White, C.M., B.R. Strazisar, E.J. Granite, J.S. Hoffman, and H.W. Pennline. "Separation and Capture of CO_2 From Large Stationary Sources and Sequestration in Geological Formations—Coalbeds and Deep Saline Aquifers." *J. Air & Waste Manage. Assoc*, Vol. 53, (2003). pp.645-715.
3. Stern, S.A. "Polymers for Gas Separations: The Next Decade," *J. Membrane Sci.*, 94 (1994). pp. 1-65.
4. Caro, J., M. Noack, P. Kolsch, and R. Schafer. "Zeolite Membranes – State of Their Development and Perspective," *Microp. Mesop. Mater*., 38 (2000). pp. 3-24.
5. Koros, W.J., and G.K. Fleming. "Membrane-Based Gas Separation," *J. Membrane Sci*., 83 (1993). pp. 1-80.
6. Pandey, P., and R.S. Chauhan. "Membranes for Gas Separation," *Prog. Polym. Sci*., 26 (2001). pp. 853-893.
7. Hsieh, H.P. "Membrane and Membrane Processes," in *Inorganic Membranes for Separation and Reaction*. Elsevier: Amsterdam., (1996). pp. 1-13.
8. Burggraaf, A.J., and K. Keizer, "Synthesis of Inorganic Membranes," in *Inorganic Membranes: Synthesis, Characteristics, and Applications*, R.R. Bhave ed. Van Nostrand Reinhold: New York. (1991). pp. 10-63.
9. Hirayama, Y., Y. Kase, N. Tanihara, Y. Sumiyama, Y. Kusuki, and K. Haraya. "Permeation Properties of CO_2 and N_2 of Poly(ethylene oxide)-Containing and Cross-linked Polymer Films." *J. Membrane Sci*., 160 (1999). pp. 87-99.
10. Bondi, A. "Free Volumes and Free Rotation in Simple Liquids and Liquid Saturated Hydrocarbons." *J. Phys. Chem*., 58 (1954). pp. 929-939.
11. Uhlhorn, R.J.R., K. Keizer, and A.J. Burggraaf. "Gas and Surface Diffusion in Modified γ-Alumina Systems." *J. Membrane Sci*., 46 (1989). pp. 225-241.
12. de Lange, R.S.A., K. Keizer, and A.J. Burggraaf. "Analysis and Theory of Gas Transport in Microporous Sol-Gel Derived Ceramic Membranes." *J. Membrane Sci.*, 104 (1995). pp. 81-100.
13. Hassan, M.H.. J.D. Way, P.M. Thoen, and A.C. Dillon. "Single Component and Mixed Gas Transport in a Silica Hollow Fiber Membrane." *J. Membrane Sci*., 104 (1995). pp. 27-42.
14. Sea, B.-K., K. Kusakabe, and S. Morooka. "Pore Size Control and Gas Permeation Kinetics of Silica Membranes by Pyrolysis of Phenyl-Substituted Ethoxysilanes with Cross-Flow through a Porous Support Wall." *J. Membrane Sci*., 130 (1997). pp. 41-52.
15. Rao, M.B., and S. Sircar. "Nanoporous Carbon Membranes for Separation of Gas Mixtures by Selective Surface Flow." *J. Membrane Sci*., 85 (1993). pp. 253-264.

16. Rao, M.B., and S. Sircar. "Performance and Pore Characterization of Nanoporous Carbon Membranes for Gas Separation." *J. Membrane Sci*., 110 (1996). pp. 109-118.

17. Uhlhorn, R.J.R., K. Keizer, and A.J. Burggraaf. "Gas Transport and Separation with Ceramic Membranes, Part I: Multilayer Diffusion and Capillary Condensation," *J. Membrane Sci*., 66 (1992). pp. 259-269.

18. Joly, C., M. Samaihi, L. Porcar, and R.D. Noble. "Polyimide-Silica Composite Materials: How Does Silica Influence Their Microstructure and Gas Permeation Properties." *Chem. Mater*., 11 (1999). pp. 2,331-2,338.

19. Li, D. and S.-T., Hwang. "Preparation and Characterization of Silicon Based Inorganic Membrane for Gas Separation." *J. Membrane Sci*., 59 (1991). pp. 331-352.

20. Kedem, O. "The Role of Coupling in Pervaporation." *J. Membrane Sci*., 47 (1989).

21. Chen, C., B. Han, J. Li, T. Shang, J. Zou, and W. Jiang. "A New Model on the Diffusion of Small Molecule Penetrants in Dense Polymer Membranes." *J. Membrane Sci*., 187 (2001). pp. 109-118.

22. Braker, W. and A.L. Mossman (eds.). *Matheson Gas Data Book. 5th Ed.* McGraw Hill: NY. (1971). pp. 91, 345, 411.

23. Lin, Y.S. "Microporous and Dense Inorganic Membranes: Current Status and Prospective." *Sep. Purif. Tech*. 25. (2001). pp. 34-55.

24. Ismail, A.F. and L.I.B. David. "A Review on the Latest Development of Carbon Membranes for Gas Separation." *J. Membrane Sci*., 193 (2001). pp. 1-18.

25. Strathmann, H. "Membrane Separation Processes: Current Relevance and Future Opportunities." *AIChE J*., 47(5) (2001). pp. 1,077-1,087.

26. Pandey, P., and R.S. Chauhan. "Membranes for Gas Separation." *Prog. Polym. Sci*., 26 (2001). pp. 853-893.

27. Ismail, A.F. and W. Lorna. "Penetrant-Induced Plasticization Phenomenon in Glassy Polymers for Gas Separation Membrane." *Sep. Purif. Tech*., 27 (2002). pp. 173-194.

28. Coronas, J. and J. Santamaria. "Separation Using Zeolite Membranes." *Sep. Purif. Methods*, 28(2) (1999). pp. 127-177.

29. Cho, Y.-K., K. Han, and K.-H. Lee. "Separation of CO_2 by Modified γ-Alumina Membranes at High Temperature." *J. Membrane Sci*., 104 (1995). pp. 219-230.

30. Kusakabe, K., S. Yoneshige, A. Murata, and S. Morooka. "Morphology and Gas Permeance of ZSM-5 Type Zeolite Membrane Formed on a Porous α-Alumina Support Tube." *J. Membrane Sci*., 116 (1996). pp. 39-46.

31. Aoki, K., V.A. Tuan, J.L. Falconer, and R.D. Noble. "Gas Permeation Properties of Ion-Exchanged ZSM-5 Zeolite Membranes." *Microp. Mesop. Mater*., 39 (2000). pp. 485-492.

32. Lovallo, M.C., A. Gouzinis, and M. Tsapatsis. "Synthesis and Characterization of Oriented MFI Membranes Prepared by Secondary Growth." *AIChE J*., 44(8) (1998). pp. 1,903-

1,913.

33. Bernal, M. P., E. Piera, J. Coronas, M. Menendez, and J. Santamaria. "Mordenite and ZSM-5 Hydrophilic Tubular Membranes for the Separation of Gas Phase Mixtures." *Catal. Today*, 56 (2000). pp. 221-227.

34. Coronas, J., R.D. Noble, and J.L. Falconer. "Separation of C_4 and C_6 Isomers in ZSM-5 Tubular Membranes." *Ind. Eng. Chem. Res*., 37 (1998). pp. 166-176.

35. Lai, R. and G.R. Gavalas. "Surface Seeding in ZSM-5 Membrane Preparation." *Ind. Eng. Chem. Res*., 37 (1998). pp. 4,275-4,283.

36. Gump, C.J., R.D. Noble, and J.L. Falconer. "Separation of Hexane Isomers Through Nonzeolite Pores in ZSM-5 Zeolite Membranes." *Ind. Eng. Chem. Res*., 38 (1999). pp. 2,775-2,781.

37. Tuan, V.A., J.L. Falconer, and R.D. Noble. "Alkali-Free ZSM-5 Membranes: Preparation Conditions and Separation Performance." *Ind. Eng. Chem. Res*., 38 (1999). pp. 3,635-3,646.

38. Kusakabe, K., T. Kuroda, A. Murata, and S. Morooka. "Formation of a Y-Type Zeolite Membrane on a Porous α-Alumina Tube for Gas Separation." *Ind. Eng. Chem. Res*., 36 (1997). pp. 649-655.

39. Kusakabe, K., T. Kuroda, and S. Morooka. "Separation of Carbon Dioxide from Nitrogen Using Ion-Exchanged Faujasite-Type Zeolite Membranes Formed on Porous Support Tubes." *J. Membrane Sci*., 148 (1998). pp. 13-23.

40. Hasegawa, Y., K. Watanabe, K. Kusakabe, and S. Morooka. "The Separation of CO_2 Using Y-Type Zeolite Membranes Ion-Exchanged with Alkali Metal Cations." *Sep. and Purif. Tech*., 22-23, (2001). pp. 319-325.

41. Kusakabe, K., T. Kuroda, K. Uchino, Y. Hasegawa, and S. Morooka. "Gas Permeation Properties of Ion-Exchanged Faujasite-Type Zeolite Membranes." *AIChE J*., 45(6) (1999). pp. 1220-1226.

42. Kumakiri, I, T. Yamaguchi, and S.-I. Nakao, "Preparation of Zeolite A and Faujasite Membranes from a Clear Solution." *Ind. Eng. Chem. Res*., 38 (1999). pp. 4,682-4,688.

43. Weh, K, M. Noack, I. Sieber, and J. Caro. "Permeation of Single Gases and Gas Mixtures through Faujasite-Type Molecular Sieve Membranes." *Microp. Mesop. Mater*., 54 (2002). pp. 27-36.

44. Bakker, W.J.W., L.J.P. van den Broeke, F. Kapteijn, and J.A. Moulijn. "Temperature Dependence of One-Component Permeation through a Silicalite-1 Membrane." *AIChE J*., 43(9) (1997). pp. 2,203-2,214.

45. van den Broeke, L.J.P., W.J.W. Bakker, F. Kapteijn, and J.A. Moulijn. "Transport and Separation Properties of a Silicalite-1 Membrane-I. Operating Conditions." *Chem. Eng. Sci*., 54 (1999). pp. 245-258.

46. van den Broeke, L.J.P., F. Kapteijn, and J.A. Moulijn. "Transport and Separation Properties of a Silicalite-1 Membrane-II. Variable Separation Factors." *Chem. Eng. Sci*.,

54 (1999). pp. 259-269.

47. Funke, H.H., M.G. Kovalchick, J.L. Falconer, and R.D. Noble. "Separation of Hydrocarbon Isomer Vapors with Silicalite Zeolite Membranes." *Ind. Eng. Chem. Res*., 35 (1996). pp. 1,575-1,582.

48. Funke, H.H., A.M. Argo, J.L. Falconer, and R.D. Noble. "Separations of Cyclic, Branched, and Linear Hydrocarbon Mixtures through Silicalite Membranes." *Ind. Eng. Chem. Res*., 36 (1997). pp. 137-143.

49. Lin, X., H. Kita, and K.-I. Okamoto. "Silicalite Membrane Preparation, Characterization, and Separation Performance." *Ind. Eng. Chem. Res*., 40 (2000). pp, 4,069-4,078.

50. Nomura, M., T. Yamaguchi, and S.-I. Nakao. "Silicalite Membranes Modified by Counterdiffusion CVD Technique." *Ind. Eng. Chem. Res*., 36 (1997). pp. 4,217-4,223.

51. Aoki, K. K. Kusakabe, and S. Morooka. "Gas Permeation Properties of A-Type Zeolite Formed on Porous Substrate by Hydrothermal Synthesis." *J. Membrane Sci*., 141 (1998). pp. 197-205.

52. Aoki, K. K. Kusakabe, and S. Morooka. "Separation of Gases with an A-Type Zeolite Membrane." *Ind. Eng. Chem. Res*., 39 (2000). pp. 2,245-2,251.

53. Dong, J., and Y.S. Lin. "In Situ Synthesis of P-Type Zeolite Membranes on Porous α-Alumina Supports." *Ind. Eng. Chem. Res*., 37 (1998). pp. 2,404-2,409.

54. Poshusta, J.C., V.A. Tuan, J.L. Falconer, and R.D. Noble. "Synthesis and Permeation Properties of SAPO-34 Tubular Membranes." *Ind. Eng. Chem. Res*., 37 (1998). pp. 3,924-3,929.

55. Poshusta, J.C., V.A. Tuan, E.A. Pape, R.D. Noble, and J.L. Falconer. "Separation of Light Gas Mixtures Using SAPO-34 Membranes." *AIChE J*., 46(4) (2000). pp. 779-789.

56. Poshusta, J.C., R.D. Noble, and J.L. Falconer. "Characterization of SAPO-34 Membranes by Water Adsorption." *J. Membrane Sci*., 186 (2001). pp. 25-40.

57. Keizer, K., A.J. Burggraaf, Z.A.E.P. Vroon, and H. Verwiej. "Two Component Permeation through Thin Zeolite MFI Membranes." *J. Membrane Sci*., 147 (1998). pp. 159-172.

58. Koresh, J.E., and A. Soffer. "Study of Molecular Sieve Carbons. Part I. Pore Structure, Gradual Pore Opening, and Mechanism of Molecular Sieving." *J. Chem. Soc. Faraday Trans*. I, 76 (1980). pp. 2,457-2,471.

59. Koresh, J.E., and A. Sofer. "Molecular Sieve Carbon Permselective Membrane. Part I. Presentation of a New Device for Gas Mixture Separation," *Sep. Sci. Tech*., 18(8) (1983). pp. 723-734.

60. Kusakabe, K., M. Yamamoto, and S. Morooka. "Gas Permeation and Micropore Structure of Carbon Molecular Sieving Membranes Modified by Oxidation." *J. Membrane. Sci*., 149 (1998). pp. 59-67.

61. Fuertes, A.B., and T.A. Centeno. "Preparation of Supported Asymmetric Carbon Molecular Sieve Membranes." *J. Membrane Sci*., 144 (1998). pp.105-111.

62. Fuertes, A.B. "Adsorption-Selective Carbon Membrane for Gas Separation." *J. Membrane Sci*., 177 (2000). pp. 9-16.

63. Fuertes, A.B., D.M. Nevskaia, and T.A. Centeno. "Carbon Composite Membranes from Matrimid® and Kapton® Polyimides for Gas Separation." *Microp. Mesop. Mater*., 33 (1999). pp. 115-125.

64. Hayashi, J.-I., M. Yamamoto, K. Kusakabe, and S. Morooka. "Simultaneous Improvement of Permeance and Permselectivity of 3,3',4,4'-Biphenyltetracarboxylic Dianhydride-4,4'-Oxydianiline Polyimide Membrane by Carbonization." *Ind. Eng. Chem. Res*., 34 (1995). pp. 4,364-4,370.

65. Hayashi, J.-I., H. Mizuta, M. Yamamoto, K. Kusakabe, and S. Morooka. "Pore Size Control of Carbonized BPDA-pp'ODA Polyimide Membrane by Chemical Vapor Deposition of Carbon." *J. Membrane Sci*., 124 (1997). pp. 243-251.

66. Hayashi, J.-I., M. Yamamoto, K. Kusakabe, and S. Morooka. "Effect of Oxidation on Gas Permeation of Carbon Molecular Sieving Membranes Based on BPDA-pp'ODA Polyimide." *Ind. Eng. Chem. Res*., 36 (1997). pp. 2,134-2,140.

67. Yamamoto, M., K. Kusakabe, J.-I. Hayashi, and S. Morooka. "Carbon Molecular Sieve Membrane Formed by Oxidative Carbonization of a Copolyimide Film Coated on a Porous Support Tube." *J. Membrane Sci*., 133 (1997). pp. 195-205.

68. Kusakabe, K., S. Gohgi, and S. Morooka. "Carbon Molecular Sieving Membranes Derived from Condensed Polynuclear Aromatic (COPNA) Resins for Gas Separations." *Ind. Eng. Chem. Res*., 37 (1998). pp. 4262-4266.

69. Fuertes, A.B., and T.A. Centeno. "Preparation of Supported Carbon Molecular Sieve Membranes." *Carbon*, 37 (1999). pp. 679-684.

70. Fuertes, A.B., and T.A. Centeno. "Carbon Molecular Sieve Membranes from Polyetherimide." *Microp. Mesop. Mater*., 26 (1998). pp. 23-26.

71. Centeno, T.A., and A.B. Fuertes. "Supported Carbon Molecular Sieve Membranes Based on a Phenolic Resin." *J. Membrane Sci*., 160 (1999). pp. 201-211.

72. Centeno, T.A., and A.B. Fuertes. "Carbon Molecular Sieve Membranes Derived from a Phenolic Resin Supported on Porous Ceramic Tubes." *Sep. Purif. Tech*., 25 (2001). pp. 379-384.

73. Centeno, T.A., and A.B. Fuertes. "Carbon Molecular Sieve Gas Separation Membranes Based on Poly(Vinylidene Chloride-co-Vinyl Chloride)." *Carbon*, 38 (2000). pp. 1067-1073.

74. Kusuki, Y., H. Shimazaki, N. Tanihara, S. Nakanishi, and T. Yoshinaga. "Gas Permeation Properties and Characterization of Asymmetric Carbon Membranes Prepared by Pyrolyzing Asymmetric Polyimide Hollow Fiber Membrane." *J. Membrane Sci*., 134 (1997). pp. 245-253.

75. Suda, H. and K. Haraya. "Gas Permeation through Micropores of Carbon Molecular Sieve Membranes Derived from Kapton Polyimide." *J. Phys. Chem. B*, 101 (1997). pp. 3,988-

3,994.

76. Shiflett, M.B. and H.C. Foley. "On the Preparation of Supported Carbon Membranes." *J. Membrane Sci*. 179. (2000). pp. 275-282.

77. Wang, H., L. Zhang, and G.R. Gavalas. "Preparation of Supported Carbon Membranes from Furfuryl Alcohol by Vapor Deposition Polymerization." *J. Membrane Sci*., 177 (2000). pp. 25-31.

78. Wang, H., and G.R. Gavalas. "Mesoporous Glass Films Supported on α-Al_2O_3." *J. Membrane Sci*., 176 (2000). pp. 75-85.

79. Tanihara, N., H. Shimazaki, Y. Hirayama, S. Nakanishi, T. Yoshinaga, and Y. Kusuki. "Gas Permeation Properties Asymmetric Carbon Hollow Fiber Membranes Prepared from Asymmetric Polyimide Hollow Fiber." *J.* Membrane *Sci*., 160 (1999). pp. 179-186.

80. Ogawa, M. and Y. Nakano. "Gas Permeation through Carbonized Hollow Fiber Membranes Prepared by Gel Modification of Polyamic Acid." *J. Membrane Sci.*, 162 (1999). pp. 189-198.

81. Ogawa, M. and Y. Nakano. "Separation of CO_2/CH_4 Mixture through Carbonized Membrane Prepared by Gel Modification." *J. Membrane Sci.*, 173 (2000). pp. 123-132.

82. Uhlhorn, R.J.R., M.H.B.J. Huis In't Veld, K. Keizer, and A.J. Burggraaf. "High Permselectivities of Microporous Silica-Modified γ-Alumina Membranes." *J. Mater. Sci. Lett*., 8 (1989). pp. 1,135-1,138.

83. Kusakabe, K., Z.Y. Li, H. Maeda, and S. Morooka. "Preparation of Supported Composite Membrane by Pyrolysis of Polycarbosilane for Gas Separation at High Temperature." *J. Membrane Sci*., 103 (1995). pp. 175-180.

84. Kusakabe, K., S. Sakamoto, T. Saie, and S. Morooka. "Pore Structure of Silica Membranes Formed by a Sol-Gel Technique Using Tetraethoxysilane and Alkyltriethoxysilanes." *Sep. Purif. Tech*., 16 (1999). pp. 139-146.

85. Munoz-Aguado, M.J. and M. Gregorkiewitz. "Preparation of Silica-Based Microporous Inorganic Gas Separation Membranes." *J. Membrane Sci*., 111 (1996). pp. 7-18.

86. Cooper, C.A. and Y.S. Lin. "Microstructural and Gas Separation Properties of CVD Modified Mesoporous γ-Alumina Membranes." *J. Membrane Sci.*, 195 (2002). pp. 35-50.

87. de Vos, R.M. and H. Verweij. "Improved Performance of Silica Membranes for Gas Separation." *J. Membrane Sci*., 143 (1998). pp. 37-51.

88. de Vos, R.M., W.F. Maier, and H. Verweij. "Hydrophobic Silica Membranes for Gas Separation." *J. Membrane Sci*. 158. (1999). pp. 277-288.

89. Way, J.D. and D.L. Roberts. "Hollow Fiber Inorganic Membranes for Gas Separations." *Sep. Sci. Tech*., 27(1) (1992). pp. 29-41.

90. Raman, N.K. and C.J. Brinker. "Organic "Template" Approach to Molecular Sieving Silica

Membranes." *J. Membrane Sci*., 105 (1995). pp. 273-279.

91. Tsai, C.-Y., S.-Y. Tam, Y. Lu, and C.J. Brinker. "Dual-Layer Asymmetric Microporous Silica Membranes." *J. Membrane Sci*., 169 (2000). pp. 255-268.

92. Okubo, T. and H. Inoue. "Improvement of Surface Transport Property by Surface Modification." *AIChE J.*, 34(6) (1988). pp. 1,031-1,033.

93. Okubo, T. and H. Inoue. "Single Gas Permeation through Porous Glass Modified with Tetraethoxysilane." *AIChE J*., 35(5) (1989). pp. 845-848.

94. Okubo, T. and H. Inoue. "Introduction of Specific Gas Selectivity to Porous Glass Membranes by Treatment with Tetraethoxysilane." *J. Membrane Sci*., 42 (1989). pp. 109-117.

95. McCarley, K.C., and J.D. Way. "Development of a Model Surface Flow Membrane by Modification of Porous γ-Alumina with Octadecyltrichlorosilane." *Sep. Purif. Tech*., 25 (2001). pp. 195-210.

96. Leger, C., H.D.L. Lira, and R. Paterson. "Preparation and Properties of Surface Modified Ceramic Membranes. Part III. Gas Permeation of 5 nm Alumina Membranes Modified by Trichloro-Octdecylsilane." *J. Membrane Sci*., 120 (1996). pp. 187-195.

97. Li, D. and S.-T. Hwang. "Gas Separation by Silicon Based Inorganic Membrane at High Temperature." *J. Membrane Sci*., 66 (1992). pp. 119-127.

98. Hyun, S.H., S.Y. Jo, and B.S. Kang. "Surface Modification of γ-Alumina Membranes by Silane Coupling for CO_2 Separation." *J. Membrane Sci*., 120 (1996). pp. 197-206.

99. Asaeda, M. and S. Yamasaki. "Separation of Inorganic/Organic Gas Mixtures by Porous Silica Membranes." *Sep. Purif. Tech*., 25 (2001). pp. 151-159.

100. Shelekhin, A.B., A.G. Dixon, and Y.H. Ma. "Adsorption, Permeation, and Diffusion of Gases in Microporous Membranes. II. Permeation of Gases in Microporous Glass Membranes." *J. Membrane Sci*., 75 (1992). pp. 233-244.

101. Kusakabe, K., K. Ichiki, and S. Morooka. "Separation of CO_2 with $BaTiO_3$ Membrane Prepared by the Sol-Gel Method." *J. Membrane Sci*., 95 (1994). pp. 171-177.

102. Shekhawat, D. "Catalytic Upgrading of Succinates to Itaconic Acid." Ph.D. Thesis. Michigan State University. (2000).

103. Shen, J., J.M. Kobe, Y. Chen, and J.A. Dumesic. "Synthesis and Surface Acid/Base Properties of Magnesium-Aluminum Mixed Oxides Obtained from Hydrotalcites." *Langmuir*, 10 (1994). pp. 3,902-3,908.

104. Corma, A., V. Fornes, R.M. Martin-Aranda, and F. Key. "Determination of Base Properties of Hydrotalcites: Condensation of Benzaldehyde with Ethyl Acetoacetate." *J. Catal*., 134 (1992). pp. 58-65.

105. Tsuji, M., G. Mao, T. Yoshida, and Y. Tamaura. "Hydrotalcites with an Extended Al^{3+} - Substitution: Synthesis, Simultaneous TGA-DTA-MS Study, and their CO_2 Adsorption Behaviors." *J. Mater. Res*., 8(5) (1993). pp. 1137-1142.

106. Miyata, S., and T. Hirose. "Adsorption of N_2, O_2, CO_2, and H_2 on Hydrotalcite-Like System: Mg^{2+}-Al^{3+}-$(Fe(CN)_6)_{4-}$", *Clays & Clay Minerals*, 26(6) (1978). pp. 441-447.

107. Ding, Y. and E. Alpay. "Equilibria and Kinetics of CO_2 Adsorption on Hydrotalcite Adsorbent.: *Chem. Eng. Sci*., 55 (2000). pp. 3,461-3,474.

108. McKenzie, A.L., C.T. Fishel, and R.J. Davis. "Investigation of the Surface Structure and Basic Properties of Calcined Hydrotalcites." *J. Catal*., 138 (1992). pp. 547-561.

109. Prinetto, F., G. Ghiotti, R. Durand, and D. Tichit. "Investigation of Acid-Base Properties of Catalysts Obtained from Layered Double Hydroxides." *J. Phys. Chem. B*, 104 (2000). pp. 11,117-11,126.

110. Yong, Z., V. Mata, and A.E. Rodrigues. "Adsorption of Carbon Dioxide onto Hydrotalcite-Like Compounds (HTLCs) at High Temperatures." *Ind. Eng. Chem. Res*., 40 (2001). pp. 204-209.

111. Hufton, J.R., S. Mayorga, and S. Sircar. "Sorption-Enhanced Reaction Process for Hydrogen Production." *AIChE J*., 45(2) (1999). pp. 248-256.

112. Yong, Z., V. Mata, and A.E. Rodrigues. "Adsorption of Carbon Dioxide at High Temperature – A Review." *Sep. Purif. Tech*., 26 (2002). pp. 195-205.

113. Schaper, H., J.J. Berg-Slot, and W.H.J. Stork. "Stabilized Magnesia: A Novel Catalyst (Support) Material." *Appl. Catal*., 54 (1989). pp. 79-90.

114. Horiuchi, T., H. Hidaka, T. Fukui, Y. Kubo, M. Horio, K. Suzuki, and T. Mori. "Effect of Added Basic Metal Oxides on CO_2 Adsorption on Alumina at Elevated Temperatures." *Appl. Catal. A: Gen*., 167 (1998). pp. 195-202.

115. Bracht, M., P.T. Alderliesten, R. Kloster, R. Pruschek, G. Haupt, E. Xue, J.R.H. Ross, M.K. Koukou, and N. Papayannakos. "Water Gas Shift Membrane Reactor for CO_2 Control in IGCC Systems: Techno-Economic Feasibility Study." *Energy Convers. Mgmt*., 38 (1997). pp. S159-S164.

116. Criscuoli, A., A. Basile, and E. Drioli. "An Analysis of the Performance of Membrane Reactors for the Water-Gas Shift Reaction Using Gas Feed Mixtures." *Catal. Today*, 56 (2000). pp. 53-64.

117. Basile, A., G. Chiappetta, S. Tosti, and V. Violante. "Experimentation and Simulation of Both Pd and Pd/Ag for a Water Gas Shift Membrane Reactor." *Sep. Purif. Tech*., 25 (2001). pp. 549-571.

118. Kikuchi, E. "Palladium/Ceramic Membranes for Selective Hydrogen Permeation and their Application to Membrane Reactor." *Catal. Today*, 25 (1995). pp.333-337.

119. Lima, A.A.G., M. Nele, E.L. Moreno, and H.M.C. Andrade. "Composition Effects on the Activity of Cu-ZnO-Al2O3 Based Catalysts for the Water Gas Shift Reaction: A Statistical Approach." *Appl. Cat. A: Gen*., 171 (1998). pp. 31-43.

120. Gines, M.J.L, A. Amadeo, M. Laborde, and C.R. Apesteguia. "Activity and Structure-Sensitivity of the Water-Gas Shift Reaction Over Cu-Zn-Al Mixed Oxide Catalysts." *Appl. Cat. A: Gen*., 131 (1995). pp. 283-296.

121. Petrini, G., and F. Garbassi. "XPS Study on the Low-Temperature CO Shift Reaction Catalyst. II. The Effects of the Addition of Alumina and Reaction Conditions." *J. Catal.*, 90 (1984). pp. 113-118.

122. Carvill, B.T., J.R. Hufton, M. Anand, and S. Sircar. "Sorption-Enhanced Reaction Process." *AIChE J.*, 42(10) (1996). pp. 2,765-2,772.

123. Hufton, J., W. Waldron, S. Weigel, M. Rao, S. Nataraj, and S. Sircar. "Sorption-Enhanced Reaction Process (SERP) for the Production of Hydrogen." *Proceedings of the 2000 U.S. DOE Hydrogen Program Review*. (2000).

124. Nataraj, S., B.T. Carvill, J.R. Hufton, S.G. Mayorga, T.R. Gaffney, and J.R. Brzozowski. "Process for Operating Equilibrium Controlled Reactions." U.S. Patent No. 6,315,973 Issued November 13, 2001.

125. Orme, C.J., M.K. Harrup, T.A. Luther, R.P. Lash, K.S. Houston, D.H. Weinkauf, and F.F. Stewart. "Characterization of Gas Transport in Selected Rubbery Amorphous Polyphosphazene Membranes." *J. Membrane Sci.*, 186 (2001). pp. 249-256.

126. Merkel, T.C., R.P. Gupta, B.S. Turk, and B.D. Freeman. "Mixed-Gas Permeation of Syngas Components in Poly(Dimethylsiloxane) and Poly(1-Trimethylsilyl-1-Propyne) at Elevated Temperatures." *J. Membrane Sci.*, 191 (2001). pp. 85-94.

127. Stern, S.A., V.M. Shah, and B.J. Hardy. "Structure-Permeability Relationships in Silicone Polymers." *J. Poly. Sci.: Part B: Poly. Phy.*, 25 (1987). pp. 1,263-1,298.

128. Ashworth, A.J., B.J. Brisdon, R. England, B.S.R. Reddy, and I. Zafar. "The Permselectivity of Polyorganosiloxanes Containing Ester Functionalities." *J. Membrane Sci.*, 56 (1991). pp. 217-228.

129. Ashworth, A.J., B.J. Brisdon, R. England, A.G.W. Hodson, and A.R. Watts. "The Permeability of Carbon Dioxide and Methane in Poly(Organosiloxane) Membranes Containing Mono- and Di-Ester Functionalities." *J. Membrane Sci.*, 101 (1995). pp. 109-115.

130. Matsumoto, K., and P. Xu. "Gas Permeation Properties of Hexafluoro Aromatic Polyimides." *J. Appl. Poly. Sci.*, 47 (1993). pp. 1,961-1,972.

131. Costello, L.M., D.R.B. Walker, and W.J. Koros. "Analysis of a Thermally Stable Polypyrrolone for High Temperature Membrane-Based Gas Separations." *J. Membrane Sci.*, 90 (1994). pp. 117-130.

132. Kawakami, H., M. Mikawa, and S. Nagaoka. "Gas Transport Properties in Thermally Cured Aromatic Polyimide Membranes." *J. Membrane Sci.*, 118 (1996). pp. 223-230.

133. Liu, Y., R. Wang, and T.-S. Chung. "Chemical Cross-Linking Modification of Polyimide Membranes for Gas Separation." *J. Membrane Sci.*, 189 (2001). pp. 231-239.

134. Fang, J., H. Kita, and K.-I. Okamoto. "Gas Permeation Properties of Hyperbranched Polyimide Membranes." *J. Membrane Sci.*, 182 (2001). pp. 254-256.

135. Hays, R.A. "Polyimide Gas Separation Membranes." U.S. Patent No. 4,717,393 Issued on January 5, 1988.

136. Staudt-Bickel, C and W.J. Koros. "Improvement of CO_2/CH_4 Separation Characteristics of Polyimides by Chemical Crosslinking." *J. Membrane Sci*., 155 (1999). pp. 145-154.

137. Bos, A., I.G.M. Punt, M. Wessling, and H. Strathmann. "Plasticization-Resistant Glassy Polyimide Membranes for CO_2/CH_4 Separations." *Sep. Purif. Tech*., 14 (1998). pp. 27-39.

138. Rezac, M.E., E.T. Sorensen, and H.W. Beckham. "Transport Properties of Crosslinkable Polyimide Blends." *J. Membrane Sci*., 136 (1997). pp. 249-259.

139. Wright, C.T. and D.R. Paul. "Feasibility of Thermal Crosslinking of Polyarylate Gas-Separation Membranes Using Benzocyclobutene-Based Monomers." *J. Membrane Sci.*, 129 (1997). pp. 47-53.

140. Wright, C.T. and D.R. Paul. "Gas Sorption and Transport in UV-Irradiated Polyarylate Copolymers Based on Tetramethyl Bisphenol-A and Dihydroxybenzophenone." *J. Membrane Sci*., 124 (1997). pp. 161-174.

141. Wind, J.D., C. Staudt-Bickel, D.R. Paul, and W.J. Koros. "The Effects of Crosslinking Chemistry on CO_2 Plasticization of Poyimide Gas Separation Membranes." *Ind. Eng. Chem. Res*., 41 (2002). pp. 6,139-6,148.

142. Shieh, J.-J. and T.S. Chung. "Cellulose Nitrate-Based Multilayer Composite Membranes for Gas Separation." *J. Membrane Sci*., 166 (2000). pp. 259-269.

143. Shieh, J.-J., T.-S. Chung, R. Wang, M.P. Srinivasan, and D.R. Paul. "Gas Separation Performance of Poly(4-Vinylpyridine)/Polyetherimide Composite Hollow Fibers." *J. Membrane Sci*., 182 (2001). pp. 111-123.

144. Chung, T.-S., J.-J. Shieh, W.W.Y. Liu, M.P. Srinivasan, and D.R. Paul. "Fabrication of Multilayer Composite Hollow Fiber Membranes for Gas Separation." *J. Membrane Sci*., 152 (2001). pp. 211-225.

145. Shieh, J.-J., T.-S. Chung, and D.R. Paul. "Study on Multi-Layer Composite Hollow Fiber Membranes for Gas Separation." *Chem. Eng. Sci*., 54 (1999). pp. 675-684.

146. Hirayama, Y., T. Yoshinaga, Y. Kusuki, K. Ninomiya, T. Sakakibara, and T. Tamari. "Relation of Gas Permeability with Structure of Aromatic Polyimide I." *J. Membrane Sci*., 111 (1996). pp. 169-182.

147. Suzuki, H., K. Tanaka, H. Kita, K. Okamoto, H. Hoshino, T. Yoshinaga, and Y. Kusuki. "Preparation of Composite Hollow Fiber Membranes of Poly(ethylene oxide)-Containing Polyimide and Their CO_2/N_2 Separation Properties." *J. Membrane Sci*., 146 (1998). pp. 31-37.

148. Tokuda, Y., E. Fujisawa, N. Okabayashi, N. Matsumiya, K. Takagi, H. Mano, K. Haraya, and M. Sato. "Development of Hollow Fiber Membranes for CO_2 Separation." *Energy Convers. Mgmt*., 38 (1997). pp. S111-S116.

149. Matsumoto, K., P. Xu, and T. Nishikimi. "Gas Permeation of Aromatic Polyimides. I. Relationship Between Gas Permeabilities and Dielectric Constants." *J. Membrane Sci*., 81 (1993). pp. 15-22.

150. Matsumoto, K., and P. Xu. "Gas Permeation of Aromatic Polyimides. II. Influence of Chemical Structure." *J. Membrane Sci*., 81 (1993). 23.

151. Kuehne, D.L., and S.K. Friedlander. "Selective Transport of Sulfur Dioxide through Polymer Membranes." *Ind. Eng. Chem. Process Des. Dev*., 19 (1980).

152. Li, J., S. Wang, K. Nagai, T. Nakagawa, and A.W-H Mau. "Effect of Polyethyleneglycol (PEG) on Gas Permeabilities and Permselectivities in its Cellulose Acetate (CA) Blend Membranes." *J. Membrane Sci*., 138 (1998). pp. 143-152.

153. Kim, J.H., S.Y. Ha, S.Y. Nam, J.W. Rhim, K.H. Baek, and Y.M. Lee. "Selective Permeation of CO_2 through Pore-Filled Polyacrylonitrile Membrane with Poly(Ethylene Glycol)." *J. Membrane Sci*., 186 (2001). 97-107.

154. Kawakami, M., H. Iwanaga, Y. Hara, M. Iwamoto, and S. Kagawa. "Gas Permeabilities of Cellulose Nitrate/Poly(Ethylene Glycol) Blend Membranes." *J. Appl. Poly. Sci*., 27 (1982). pp. 2,387-2,393.

155. Okamoto, K., N. Umeo, S. Okamyo, K. Tanaka, and H. Kita. "Selective Permeation of Carbon Dioxide Over Nitrogen through Polyethylene-Containing Polyimide Membranes." *Chem. Lett*., (1993). pp. 225-228.

156. Okamoto, K., M. Fujii, S. Okamyo, H. Suzuki, K. Tanaka, and H. Kita. "Gas Permeation Properties of Poly(Ether Imide) Segmented Copolymers." *Macromolecules*, 28 (1995). pp. 6,950-6,956.

157. Lehermeier, H.L., J.R. Dorgan, and J.D. Way. "Gas Permeation Properties of Poly(Lactic Acid)." *J. Membrane Sci*., 190 (2001). pp. 243-251.

158. Robeson, L.M., C.D. Smith, and M. Langsam. "A Group Contribution Approach to Predict Permeability and Permselectivity of Aromatic Polymers." *J. Membrane Sci*., 132 (1997). pp. 33-54.

159. Alentiev, A.Y., and Y.P. Yampolskii. "Free Volume Model and Tradeoff Relations of Gas Permeability and Selectivity in Glassy Polymers. *J. Membrane Sci*., 165 (2000). pp. 201-216.

160. Park, J.Y. and D.R. Paul. "Correlation and Prediction of Gas Permeability in Glassy Polymer Membrane Materials via a Modified Free Volume Based Group Contribution Method." *J. Membrane Sci*., 125 (1997). pp. 23-39.

161. Alentiev, A.Y., K.A. Loza, and Y.P. Yampolskii. "Development of the Methods for Prediction of Gas Permeation Parameters of Glassy Polymers: Polyimides as Alternating Co-Polymers." *J. Membrane Sci*., 167 (2000). pp. 91-106.

162. Okui, T., Y. Saito, T. Okubo, and M. Sadakata. "Gas Permeation of Porous Organic/Inorganic Hybrid Membranes." *J. Sol-Gel Sci. Tech*., 5 (1995). pp. 127-134.

163. Kusakabe, K., K. Ichiki, J.-i. Hayashi, H. Maeda, and S. Morooka. "Preparation and Characterization of Silica-Polyimide Composite Membrane Coated on Porous Tubes for CO_2 Separation." *J. Membrane Sci*., 115 (1996). pp. 65-75.

164. Joly, C., S. Goizet, J.C. Schrotter, J. Sanchez, and M. Escoubes. " Sol-Gel Polyimide-Silica

Composite Membrane: Gas Transport Properties. ” *J. Membrane Sci.*, 130 (1997). 63-74.

165. Kim, J.H., and Y.M. Lee. “Gas Permeation Properties of Poly(Amide-6-b-Ethylene Oxide)-Silica Hybrid Membranes.” *J. Membrane Sci*., 193 (2001). pp. 209-225.

166. Kim, J.H., S.Y. Ha, and Y.M. Lee. “Gas Permeation of Poly(Amide-6-b-Ethylene Oxide) Copolymer.” *J. Membrane Sci*., 190 (2001). pp. 179-193.

167. Smaihi, M., T. Jermoumi, J. Marignan, and R.D. Noble. “Organic-Inorganic Gas Separation Membranes: Preparation and Characterization.” *J. Membrane Sci*., 116 (1996). pp. 211-220.

168. Smaihi, M., J.-C. Schrotter, C. Lesimple, I. Prevost, and C. Guizard. “Gas Separation Properties of Hybrid Imide-Siloxane Copolymers with Various Silica Contents.” *J. Membrane Sci*., 161 (1999). pp. 157-170.

169. Cornelius, C., C. Hibshman, and E. Marand. “Hybrid Organic-Inorganic Membranes.” *Sep. Purif. Tech*., 25 (2001). pp. 181-193.

170. Cornelius, C.J. and E. Marand. “Hybrid Silica-Polyimide Composite Membranes: Gas Transport Properties.” *J. Membrane Sci*., 202 (2002). pp. 97-118.

171. Hibshman, C., C.J. Cornelius, and E. Marand. “The Gas Separation Effects of Annealing Polyimide-Organosilicate Hybrid Membranes.” *J. Membrane Sci*., 211 (2003). pp. 25-40.

172. Leger, C., H.D.L. Lira, and R. Paterson. “Preparation and Properties of Surface Modified Ceramic Membranes. Part II. Gas and Liquid Permeabilities of 5 nm Alumina Membranes Modified by a Monolayer of Bound Polydimethylsiloxane (PDMS) Silicone Oil.” *J. Membrane Sci*., 120 (1996). pp. 135-146.

173. Doucoure, A., C. Guizard, J. Durand, R. Berjoan, and L. Cot. “Plasma Polymerization of Fluorinated Monomers on Mesoporous Silica Membranes and Application to Gas Permeation.” *J. Membrane Sci*., 117 (1996). pp. 143-150.

174. Soufyani, M., T. Jei, D. Bourret, A. Sivade, and A. Larbot. “Silicone Modified Silica Membrane. Application to the Gas Separation.” *Sep. Purif., Tech*., 25 (2001). pp. 451-457.

175. Hu, Q., E. Marand, S. Dhingra, D. Fritsch, J. Wen, and G. Wilkes. “Poly(Amide-Imide)/TiO2 Nano-Composite Gas Separation Membranes: Fabrication and Characterization.” *J. Membrane Sci*., 135 (1997). pp. 65-79.

176. Moaddeb, M., and W.J. Koros. “Gas Transport Properties of Thin Polymeric Membranes in the Presence of Silicon Dioxide Particles.” *J. Membrane Sci*., 125 (1997). pp. 143-163.

177. Gulsen, D., H. Hacarloglu, L. Toppare, and L. Yilmaz. “Effect of Preparation Parameters on the Performance of Conductive Composite Gas Separation Membranes. *J. Membrane Sci*., 182 (2001). pp. 29-39.

178. Robeson, L.M. “Correlation of Separation Factor Versus Permeability for Polymeric Membranes.” *J. Membrane Sci.*, 62 (1991). pp. 165-185.

179. Zimmerman, C.M., A. Singh, and W.J. Koros. "Tailoring Mixed Matrix Composite Membranes for Gas Separations. *J. Membrane Sci*., 137 (1997). pp. 145-154.

180. Jia, M., K.-V. Peinemann, and R.-D. Behling. "Molecular Sieving Effects of Zeolite-Filled Silicone Rubber Membranes in Gas Permeation. *J. Membrane Sci*., 57 (1991). pp. 289-296.

181. Kulprathipanja, S., R.W. Neuzil, and N.N. Li. "Separation of Fluids by Means of Mixed Matrix Membranes." U.S. Patent No. 4,740,219. Issued April 26,1988.

182. Suer, M.G., N. Bac, and L. Yilmaz. "Gas Permeation Characteristics of Polymer-Zeolite Mixed Matrix Membranes." *J. Membrane Sci*., 91 (1994). pp. 77-86.

183. Duval, J.-M., B. Folkers, M.H.V. Mulder, G. Desgrandchamps, and C.A. Smolders. "Adsorbent Filled Membranes for Gas Separation. Part 1. Improvement of the Gas Separation Properties of Polymeric Membranes by Incorporation of Microporous Adsorbents." *J. Membrane Sci*., 80 (1993). pp. 189-198.

184. Duval, J.-M., A.J.B. Kemperman, B. Folkers, M.H.V. Mulder, G. Desgrandchamps, and C.A. Smolders. "Separation of Zeolite Filled Glassy Polymer Membranes." *J. Appl. Poly. Sci*., 54 (1994). pp. 409-418.

185. Gur, T.M. "Permselectivity of Zeolite Filled Polysulfone Gas Separation Membranes." *J. Membrane Sci*., 93 (1994). pp. 283-289.

186. Yong, H.H., H.C. Park, Y.S. Kang, J. Won, and W.N. Kim. "Zeolite-Filled Polyimide Membrane Containing 2,4,6-Triaminopyrimidine." *J. Membrane Sci*., 188 (2001). pp. 151-163.

187. Vu, D.Q., W.J. Koros, and S.J. Miller. "Mixed Matrix Membranes Using Carbon Molecular Sieves I. Preparation and Experimental Results. *J. Membrane Sci*., 211 (2003). pp. 311-334.

188. Vu, D.Q., W.J. Koros, and S.J. Miller. "Mixed Matrix Membranes Using Carbon Molecular Sieves II. Modeling Permeation Behavior. *J. Membrane Sci*., 211 (2003). pp. 335-348.

189. Tantekin-Ersolmaz, S.B., C. Atalay-Oral, M. Tatier, A. Erdem-Senatalar, B. Schoeman, and J. Sterte. "Effect of Zeolite Particle Size on the Performance of Polymer-Zeolite Mixed Matrix Membranes." *J. Membrane Sci*., 175 (2000). pp. 285-288.

190. Way, J.D. and R.D. Noble. "Facilitated Transport," in Membrane Handbook. W.S. Winston Ho and K.K. Sirkar (Eds.). Van Nostrand Reinhold: New York, (1992). pp. 833-866.

191. Guha, A.K., S. Majumdar, and K.K. Sirkar. "Facilitated Transport of CO_2 through an Immobilized Liquid Membrane of Aqueous Diethanolamine." *Ind. Eng. Chem. Res*., 29 (1990). pp. 2,093-2,100.

192. Matsuyama, H., M. Teramoto, and K. Iwai. "Development of a New Functional Cation-Exchange Membrane and Its Application to Facilitated Transport of CO_2." *J. Membrane Sci*., 93 (1994). pp. 237-244.

193. Yoshikawa, M., T. Ezaki, K. Sanui, and N. Ogata. "Selective Permeation of Carbon Dioxide through Synthetic Polymer Membranes Having Pyridine Moiety as a Fixed Carrier." *J. Appl. Poly. Sci*., 35 (1988). pp. 145-154.

194. Yoshikawa, M., K. Fujimoto, H. Kinugawa, T. Kitao, and N. Ogata. "Selective Permeation of Carbon Dioxide through Synthetic Polymer Membranes Having Amine Moiety." *Chem. Lett*., (1994). p. 243.

195. Nakabayashi, M., K. Okabe, E. Fujisawa, Y. Hirayama, S. Kazama, N. Matsumiya, K. Takagi, H. Mano, K. Haraya, and C. Kamizawa. "Carbon Dioxide Separation through Water-Swollen-Gel Membrane." *Energy Convers. Mgmt*., 36 (6-9) (1995). pp. 405-410.

196. Matsuyama, H., M. Teramoto, and H. Sakakura. "Selective Permeation of CO_2 through Poly{2-(N,N-Dimethyl) Aminoethyl Methacrylate} Membrane Prepared by Plasma-Graft Polymerization Technique." *J. Membrane Sci*., 114 (1996). pp. 193-200.

197. Matsuyama, H., K. Matsui, Y. Kitamura, T. Maki, and M. Teramoto. "Effects of Membrane Thickness and Membrane Preparation Condition on Facilitated Transport of CO_2 through Ionomer Membrane." *Sep. Purif. Tech*., 17 (1999). pp. 235-241.

198. Chakma, A. "Separation of CO_2 and SO_2 from Flue Gas Streams by Liquid Membranes." *Energy Convers. Mgmt*., 36 (6-9) (1995). pp. 405-410.

199. Chen, H., A.S. Kovvali, S. Majumdar, and K.K. Sirkar. "Selective CO_2 Separation from CO_2-N_2 Mixtures by Immobilized Carbonate-Glycerol Membranes." *Ind. Eng. Chem. Res*., 38 (1999). pp. 3,489-3,498.

200. Chen, H., A.S. Kovvali, and K.K. Sirkar. "Selective CO_2 Separation from CO_2-N_2 Mixtures by Immobilized Glycerine-Na-Glycerol Membranes." *Ind. Eng. Chem. Res*., 39 (2000). pp. 2,447-2,458.

201. Chen, H., G. Obuskovic, S. Majumdar, and K.K. Sirkar. "Immobilized Glycerol-Based Liquid Membranes in Hollow Fibers for Selective CO_2 Separation from CO_2-N_2 Mixtures." *J. Membrane Sci*., 183 (2001). pp. 75-88.

202. Kovvali, A.S., H. Chen, and K.K. Sirkar. "Dendrimer Membranes: A CO_2-Selective Molecular Gate." *J. Am. Chem. Soc*., 122 (2000). pp. 7,594-7,595.

203. Kovvali, A.S. and K.K. Sirkar. "Dendrimer Liquid Membranes: CO_2 Separation from Gas Mixture." *Ind. Eng. Chem. Res*., 40 (2001). pp. 2,502-2,511.

204. Keuler, J.N., and L. Lorenzen. "Developing a Heating Procedure to Optimize Hydrogen Permeance through Pd-Ag Membranes of Thickness Less than 2.2 μm." *J. Membrane Sci*., 195 (2002). pp. 203-213.

205. Armor, J.N. "Membrane Catalysis: Where is it Now, What Needs to be Done?" *Catal. Today*, 25 (1995). pp. 199-207.

206. McCool, B., G. Xomeritakis, and Y.S. Lin. "Composition Control and Hydrogen Permeation Characteristics of Sputter Deposited Palladium-Silver Membranes." *J. Membrane Sci*., 161 (1999). pp. 67-76.

207. Armor, J.N. "Catalysis with Permselective Inorganic Membranes." *J. Appl. Catal*., 49

(1989). pp. 1-25.

208. Armor, J.N. "Applications of Catalytic Inorganic Membrane Reactors to Refinery Products." *J. Membrane Sci*., 147 (1998). pp. 217-233.

209. Zaman, J. and A. Chakma. "Inorganic Membrane Reactors." *J. Membrane Sci*., 92 (1994). pp. 1-28.

210. Julbe, A., D. Farrusseng, and C. Guizard. "Porous Ceramic Membranes for Catalytic Reactors – Overview and New Ideas." *J. Membrane Sci*., 181 (2001). pp. 3-20.

211. Coronas, J. and J. Santamaria. "Catalytic Reactors Based on Porous Ceramic Membranes." *Catalysis Today*, 51 (1999). pp. 377-389.

212. Ross, J.R.H. and E. Xue. "Catalyst with Membranes or Catalyst Membranes?" *Catal. Today*, 25 (1995). pp. 291-301.

213. Sirkar, K.K., P.V. Shanbhag, and A.S. Kovvali. "Membrane in a Reactor: A Functional Perspective." *Ind. Eng. Chem. Res*., 38 (1999). pp. 3,715-3,737.

214. Criscuoli, A., A. Basile, E. Drioli, and O. Loiacono. "An Economic Feasibility Study for Water Gas Shift Membrane Reactor." *J. Membrane Sci*., 181 (2001). pp. 21-27.

215. Damle, A.S. and T.P. Dorchak. "Recovery of Carbon Dioxide in Advanced Fossil Energy Conversion Processes Using a Membrane Reactor." *Proceedings of the First National Conference on Carbon Sequestration*, Washington D.C. (2001).

216. Prabhu, A.K. and S.T. Oyama. "Highly Hydrogen Selective Ceramic Membranes: Application to the Transformation of Greenhouse Gases." *J. Membrane Sci*., 176 (2000). pp. 233-248.

217. Takaba, H., K. Mizukami, M. Kubo, A. Stirling, and A. Miyamoto. "The Effect of Gas Molecule Affinities on CO_2 Separation from the CO_2/N_2 Gas Mixture Using Inorganic Membranes as Investigated by Molecular Dynamics Simulation." *J. Membrane Sci*., 121 (1996). pp. 251-259.

218. Mizukami, K., H. Takaba, Y, Kobayashi, Y. Oumi, R.V. Belosludov, S. Takami, M. Kubo, and A. Miyamoto. "Molecular Dynamics Calculations of CO_2/N_2 Mixture through the NaY Type Zeolite Membrane." *J. Membrane Sci*., 188 (2001). pp. 21-28.

219. Tascon, J.M.D. and L.G. Tejuca. "Adsorption of CO_2 on the Perovskite-Type Oxide $LaCoO_3$." *J. Chem. Soc., Faraday Trans. I*, 77 (1981). 591-602.

220. Tejuca, L.G., C.H. Rochester, J.L.G. Fierro, and J.M.D. Tascon. "Infrared Spectroscopic Study of the Adsorption of Pyridine, Carbon Monoxide, and Carbon Dioxide on the Perovskite-Type Oxides $LaMO_3$." *J. Chem. Soc., Faraday Trans*. I, 80 (1984). pp. 1,089-1,099.

221. *Toshiba Corporation.* "Toshiba Continues Progress in Promising Method of CO_2 Absorption." Online Press Release. June 18, 1999.

222. *Toshiba Corporation.*. "Toshiba Group Continues Progress in Promising Method of CO_2 Absorption." Online Press Release. April 19, 2001.

223. Wang, R., S.S. Chan, Y. Liu, and T.S. Chung. "Gas Transport Properties of Poly(1,5-Naphthelene-2,2'-Bis(3,4-Phthalic) Hexafluoropropane) Diimide (6FDA-1,5-NDA) Dense Membranes." *J. Membrane Sci*., 199 (2002). pp. 191-202.

224. Wang, R., C. Cao, and T.-S. Chung. "A Critical Review on Diffusivity and the Characterization of Diffusivity of 6FDA-6FpDA Polyimide Membranes for Gas Separation." *J. Membrane Sci*., 198 (2002). pp. 259-271.

225. Liu, S.L., R. Wang, Y. Liu, M.L. Chng, and T.S. Chung. "The Physical and Gas Permeation Properties of 6FDA-Durene/2,6-Diaminotoluene Copolyimides." *Polymer*, 42 (2001). pp. 8,847-8,855.

226. Lin, W.-H., and T.-S. Chung. "Gas Permeability, Diffusivity, Solubility, and Aging Characteristics of 6FDA-Durene Polyimide Membranes." *J. Membrane Sci*., 186 (2001). pp. 183-193.

227. Fang, J., H. Kita, and K.-I. Okamoto. "Gas Permeation Properties of Hyperbranched Polyimide Membranes." *J. Membrane Sci*., 182 (2001). pp. 245-256.

228. Kawakami, H., M. Mikawa, and S. Nagaoka. "Formation of Surface Skin Layer of Asymmetric Polyimide Membranes and their Gas Transport Properties." *J. Membrane Sci*., 137 (1997). pp. 241-250.

229. Morisato, A. K. Ghosal, B.D. Freeman, R.T. Chern, J.C. Alvarez, J.G. del la Campa, A.E. Lozano, and J. de Abajo. "Gas Separation Properties of Aromatic Polyamides Containing Hexafluoroisopropylidene Groups." *J. Membrane Sci*., 104 (1995). pp. 231-241.